INTERNATIONAL ATOMIC ENERGY AGENCY
UNITED NATIONS EDUCATIONAL, SCIENTIFIC AND CULTURAL ORGANIZATION

INTERNATIONAL CENTRE FOR THEORETICAL PHYSICS
34100 TRIESTE (ITALY) - P.O.B. 586 - MIRAMARE - STRADA COSTIERA 11 - TELEPHONE: 2240-1
CABLE: CENTRATOM - TELEX 460392 - I

H4.SMR/204 - 14

WINTER COLLEGE ON

ATOMIC AND MOLECULAR PHYSICS

(9 March - 3 April 1987)

(ANALYTICAL LASER SPECTROSCOPY 1)

S/N Raios and Detection Limits
Considerations on Single Atom Detection

N. OMENETTO

Joint Research Centre
Ispra (Va), Italy

ICTP
WINTER COLLEGE ON ATOMIC AND MOLECULAR PHYSICS

TRIESTE , March 1987

"ANALYTICAL LASER SPECTROSCOPY 1"

Lecturer : N. OMENETTO

Joint Research Centre

Ispra (Va) , Italy

-14-

VII.

☆ S/N Ratios and Detection Limits

☆ Considerations on Single Atom Detection

LASERS IN ANALYTICAL SPECTROSCOPY*

Authors: **N. Omenetto**
Chemistry Division
Joint Research Center
Ispra (Varese), Italy

J. D. Winefordner
Department of Chemistry
University of Florida
Gainesville, Florida

Referee: J. I. Steinfeld
Department of Chemistry
Massachusetts Institute of Technology
Cambridge, Massachusetts

VII. SIGNAL-TO-NOISE RATIOS AND DETECTION LIMITS IN LASER SPECTROMETRY

A. General Comments

In this section, expressions (not derived but referenced) will be given for the signal-to-noise ratios for various types of laser spectrometry under limiting conditions which can be applied in certain cases. The detection limit in spectroscopy is defined as that concentration, C_{Lim} resulting in a S/N of 3.[311] Similar considerations, together with an evaluation of the minimum detectable concentration of atoms and molecules by several laser spectrometric methods, can be found in the papers by Falk[310] and Morgan.[312] Alkemade[313] has also discussed the various single atom detection techniques based on laser excitation.

B. Signal-to-Noise Expressions — Gas Phase

The expressions in this section will be taken from Winefordner et al.,[314] Tolles and Turner,[257] and Omenetto and Winefordner[2] for two-level atoms or molecules. In addition, expressions for the signal-to-noise ratios will be given only for the major

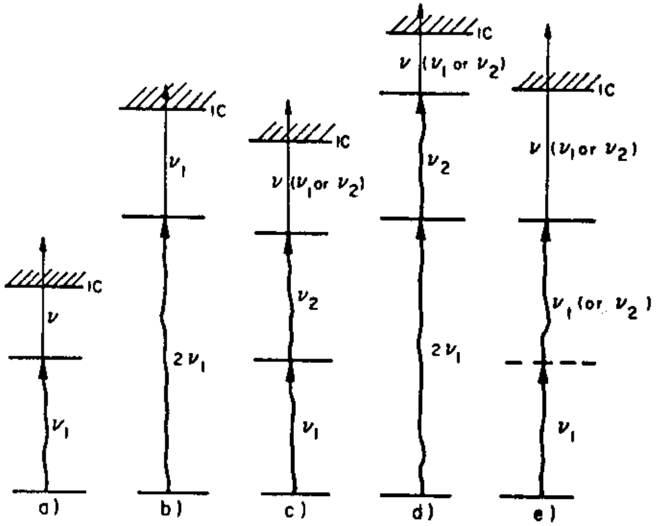

FIGURE 10. RIS detection schemes. Ionization is achieved with: (a) two photons at the same frequency ν_1; (b) one frequency doubled photon at $2\nu_1$ and one photon at ν_1; (c) two photons at frequency ν_1 or ν_2 and one photon at frequency ν_1 or ν_2; (d) one frequency doubled photon at $2\nu_1$ and two photons at ν_2 or one photon at ν_2 and one photon at ν_1; (e) one photon at frequency ν_1 or ν_2 from a state reached by a two-photon allowed transition at ν_1. (Redrawn from Hurst, G. S., Nayfeh, M. H., and Young, J. P., *Appl. Phys. Lett.*, 30, 229 (1977).)

limiting noise present in the measurements. Therefore, the detection limits in real analytical situations will be expected to be poorer than the calculated ones. Moreover, no real significance should be given to the extremely low limits calculated since the limiting noise due to the fluctuations of atoms in the probe volume[310,313] has not been considered here.

Absorption (Atomic or Molecular) Continuum Source — No Saturation — Source Shot Noise:

$$\left(\frac{S}{N}\right)_{ACS} \approx \frac{\left({}_{o}\int^{\infty}\sigma(\lambda)d\lambda\right)n_o\ell_A B_{C\lambda}(\lambda_o)K_A D_s}{\sqrt{2B_{C\lambda}(\lambda_o)\Delta\lambda_s K_A D_s}} \qquad (3)$$

Absorption (Atomic or Molecular) Line Source — No Saturation — Source Shot Noise:

$$\left(\frac{S}{N}\right)_{ALS} = \frac{\sigma_o\delta_o\, n_o\ell_A B_L K_A D_s}{\sqrt{2B_L K_A D_s}} \qquad (4)$$

Fluorescence (Atomic or Molecular) Continuum Source — No Saturation — Detector Shot Noise:

$$\left(\frac{S}{N}\right)_{FCD} = \frac{\left(\frac{1}{4\pi}\right)\left({}_{o}\int^{\infty}\sigma(\lambda)d\lambda\right)n_o\ell_F Y B_{C\lambda}(\lambda_o)K_F D_s}{\sqrt{2R_D t_o}} \qquad (5)$$

Fluorescence (Atomic or Molecular) — Continuum Source — No Saturation — Background Shot Noise:

$$\left(\frac{S}{N}\right)_{FCB} = \frac{\left(\frac{1}{4\pi}\right)\left({}_{o}\int^{\infty}\sigma(\lambda)d\lambda\right)n_o\ell_F Y B_{C\lambda}(\lambda_o)K_F D_s}{\sqrt{2B_{B\lambda}(\lambda_o)\Delta\lambda_s K_B D_B}} \qquad (6)$$

Fluorescence (Atomic or Molecular) Line Source — No Saturation — Detector Shot Noise:

$$\left(\frac{S}{N}\right)_{FLD} = \frac{\left(\frac{1}{4\pi}\right)\sigma_o\delta_o n_o\ell_F B_L Y K_F D_s}{\sqrt{2R_D t_o}} \qquad (7)$$

Fluorescence (Atomic or Molecular) Line Source — No Saturation — Background Shot Noise:

$$\left(\frac{S}{N}\right)_{FLB} = \frac{\left(\frac{1}{4\pi}\right)\sigma_o\delta_o n_o\ell_F B_L Y K_F D_s}{\sqrt{2B_{B\lambda}(\lambda_o)\Delta\lambda_s K_B D_B}} \qquad (8)$$

Spontaneous Raman Scattering — Line Source — Detector Shot Noise:

$$\left(\frac{S}{N}\right)_{SRD} = \frac{\phi_L n_o\ell_R K_R D_s\left(\frac{d\sigma_R}{d\Omega}\right)}{\sqrt{2R_D t_o}} \qquad (9)$$

Fluorescence (Atomic or Molecular) Continuum Source — Saturation — Detector Shot Noise:

$$\left(\frac{S}{N}\right)_{FCD\text{-}S} = \frac{\left(\frac{\ell_F}{4\pi}\right)n_o\left(\frac{1}{2}\right)A_{21}h\nu_o K_F' D_s\sigma_s}{\sqrt{2R_D t_o}} \qquad (10)$$

Fluorescence (Atomic or Molecular) Continuum Source — Saturation — Background Shot Noise:

$$\left(\frac{S}{N}\right)_{FCB\text{-}S} = \frac{\left(\frac{\ell_F}{4\pi}\right)n_o\left(\frac{1}{2}\right)A_{21}h\nu_o K_F' D_s\sigma_s}{\sqrt{2B_{B\lambda}(\lambda_o)\Delta\lambda_s K_B D_B}} \qquad (11)$$

Fluorescence (Atomic or Molecular) Line Source — Saturation — Detector Shot Noise:

$$\left(\frac{S}{N}\right)_{FLD\text{-}S} = \frac{\left(\frac{\ell_F}{4\pi}\right)n_o\left(\frac{1}{2}\right)\eta A_{21}h\nu_o K_F' D_s\sigma_s}{\sqrt{2R_D t_o}} \qquad (12)$$

Fluorescence (Atomic or Molecular) Line Source — Saturation — Background Shot Noise:

$$\left(\frac{S}{N}\right)_{FLB\text{-}S} = \frac{\left(\frac{\ell_F}{4\pi}\right) n_o \left(\frac{1}{2}\right) \eta A_{21} h\nu_o K_F^s D_s \alpha_s}{\sqrt{2B_{BA}(\lambda_o)\Delta\lambda_s K_B D_B}} \quad (13)$$

Fluorescence (Atomic or Molecular) Line Source — Two-Photon Excitation — Detector Shot Noise:

$$\left(\frac{S}{N}\right)_{F2P\text{-}D} \cong \frac{\left(\frac{\ell_F}{4\pi}\right)\left(\frac{E_L}{h\nu_o}\right)^2 \sigma^{(2)} \eta n_o D_s K_F''}{\sqrt{2R_D t_o}} \quad (14)$$

CARS — Detector Noise Limit:

$$\left(\frac{S}{N}\right)_{CARS\text{-}D} \cong \frac{\left(\frac{4\pi^2\omega_{as}}{c^2}\right)^2 E_p^2 \phi_s \chi'^2 \ell_R^2 K_R' D_s n_o^2 \left(\frac{d\sigma_R}{d\Omega}\right)^2}{\sqrt{2R_D t_o}} \quad (15)$$

No theoretical relationships are given for optogalvanic and optoacoustic methods, since the authors do not know of suitable S/N expressions for flames. The symbols (and units) used in the above expressions are defined below:

$\int\sigma(\lambda)d\lambda$ = integrated absorption cross section for line or band, cm^{2}nm
= $\left(\frac{\pi e^2}{mc}\right)\left(\frac{\lambda_o^2}{c}\right) f_{12}$, cm^{2}nm
m,e = mass, charge of electron, g, esu
c = speed of light, cm s^{-1}
$\frac{\pi e^2}{mc}$ = 0.027 cm^2 Hz
λ_o = peak (central) wavelength of absorption (luminescence), cm or nm
$\frac{\lambda_o^2}{c}$ = conversion factor from Hz to nm, × 10^7 nm Hz^{-1}
f_{12} = absorption oscillator strength, dimensionless
n_o = total concentration of absorbers (analyte) in the ground state, cm^{-3}
ℓ_A = absorption path length in absorption spectrometry, cm
$B_{C\lambda}(\lambda_o)$ = spectral radiance of continuum source at λ_o, J s^{-1} cm^{-2} nm^{-1} sr^{-1}
K_A = optical-detector factor for absorption spectrometry, cm^2 sr s J^{-1}
= $\Omega_{ex}(wh)_{ex}T_e\eta_d t_o\left(\frac{1}{h\nu_o}\right)$; cm^2 sr s J^{-1}
Ω_{ex} = excitation solid angle, sr
$(wh)_{ex}$ = (slit width) × (slit width) of excitation spectrometer; cm^2
η_d = photodetector efficiency (counts per photon in cathode), dimensionless
T_e = overall transmission of excitation optical system dimensionless
t_o = observation (integration, measurement, counting) time, s
$h\nu_o$ = energy of absorbed (fluorescent; scattered) photon, J
D_s = measurement duty factor for signal (fractional "on" time), dimensionless
$\Delta\lambda_s$ = spectrometer bandpass, nm
σ_o = peak absorption coefficient, cm^2
= $\left(\frac{2\sqrt{\ell n 2}}{\sqrt{\pi}}\right)\left(\frac{\pi e^2}{mc}\right)\left(\frac{\lambda_o^2}{c}\right)\frac{f_{12}}{\Delta\lambda_D}$; cm^2
$\Delta\lambda_D$ = Doppler (Gaussian) half width of peak, nm
δ_e = convolution overlap integral accounting for peak shifts and widths of line (excitation source and absorption line) or band (evaluated from Voigt integral), dimensionless
B_L = integral radiance of line source at λ_o, J s^{-1} cm^{-2} sr^{-1}
ℓ_F = fluorescence path length, cm
Y = fluorescence quantum (power) efficiency, dimensionless
K_F = optical-detector factor for fluorescence excitation and emission, cm^{2}sr^{2}s J^{-1}

= $\Omega_{ex}\Omega_{F}(wh)_{em}T_o\eta_d t_o\left(\frac{1}{h\nu_o}\right)$, cm^{2}sr^{2}s J^{-1}
Ω_F = fluorescence solid angle of collection, sr
$(wh)_{em}$ = (slit width) × (slit width) of emission monochromator observing fluorescence, cm^2
T_o = overall transmission including excitation and emission optics in fluorimetric system, dimensionless
R_d = detector dark count rate, s^{-1}
K_B = optical detector factor for background, cm^{2}sr s J^{-1}
D_B = measurement duty factor for background, dimensionless
ϕ_L = flux of line source used for Raman (spontaneous) scatter, J s^{-1}
ℓ_R = Raman interaction region, cm
K_R = optical-detector factor for Raman scatter
= $\Omega_{em}\ T_o\ \eta d\ t_o\left(\frac{1}{h\nu_o}\right)$, sr s J^{-1}
$\frac{d\sigma_R}{d\Omega}$ = differential Raman cross section, cm^2 sr^{-1}
A_{21} = Einstein coefficient of spontaneous emission, s^{-1}
K_F^s = optical-detector factor for saturated fluorescence, cm^2 sr s J^{-1}
α_s = beam expansion factor for laser source in fluorescence when near saturation conditions can be maintained after expansion, dimensionless
E_L = line source irradiance, J s^{-1} cm^{-2}
$\sigma^{(2)}$ = two-photon absorption cross section, cm^4 s
η = fraction of atoms or molecules excited with narrow line source, i.e., ratio of homogeneous to inhomogeneous half widths (Lorentztan to Doppler), dimensionless
K_F'' = optical detector factor for two-photon fluorescence, cm^2 sr s
ω_{as} = $2\pi\nu_{as}$ = angular anti-Stokes Raman scatter frequency, Hz
E_p = irradiance of CARS pump beam, J s^{-1} cm^{-2}
ϕ_s = flux of CARS Stokes beam, J s^{-1}
χ' = modified susceptibility for resonant conditions, cm^4 sr J^{-1}
χ = susceptibility = $\chi'\frac{d\sigma_R}{d\Omega}n_o$, cm^3 J^{-1}
K_R' = $T_o\eta_d t_o\left(\frac{1}{h\nu_o}\right)$, s J^{-1}

Several comments should be made about the above expressions:

1. It is assumed that the continuum source cases involve a flat source spectral distribution over the line or band in all cases.
2. It is assumed that the line source cases involve a source line considerably narrower than the absorption line or band.
3. It is assumed that the optical detector system responds in a constant manner at all measurement wavelengths.
4. It is assumed that the absorbance is low in all cases.
5. It is assumed that only *one* noise source is present for each case.
6. It is assumed that the source does not cause any reactions, temperature change, and coherency effects upon passing through the sample.
7. For the cases of molecular fluorescence, it is assumed that the fluorescence over all wavelengths is measured.
8. For the case of a condensed phase medium, the above expressions still hold except different noises may become apparent, e.g., source transmission flicker noise in absorption spectrometry and impurity fluorescence shot and flicker noises in fluorescence spectrometry.

C. Estimation of Minimum Detectable Concentration of Analytes by Absorption, Fluorescence, and Raman Scatter Methods[2,112,246,247,257,310]

Using the above expressions for S/N for each of the various methods, $n_o)_{lim}$ values,

Table 9
CALCULATED LIMITS OF DETECTION[a] IN SPECIES/CM^3 FOR ANALYTE SPECIES MEASURED BY SEVERAL METHODS

	Limit of Detection (cm^{-3}), wavelength of transition			
	300 nm, Sample temperature		600 nm, Sample temperature	
Method-source-key	300 K	2500 K	300 K	2500 K
Absorption-continuum (ACS)	3×10^7	3×10^7	6×10^7	6×10^7
Absorption-line (ALS)	2×10^4	4×10^4	5×10^3	2×10^4
Fluorescence-continuum (FCD)	1×10^3	1×10^3	2×10^2	2×10^2
Fluorescence-continuum (FCB)	6×10^5	6×10^6	2×10^5	2×10^3
Fluorescence-line (FLD)	7×10^2	2×10^3	2×10^2	5×10^2
Fluorescence-line (FLB)	4×10^4	1×10^7	2×10^3	5×10^3
Raman (SRD)	1×10^{14}	1×10^{14}	2×10^{13}	2×10^{13}
Fluorescence-continuum (FCD-S)	3×10^0	3×10^0	3×10^0	3×10^0
Fluorescence-continuum (FCB-S)	2×10^1	2×10^1	3×10^0	3×10^0
Fluorescence-line (FLD-S)	3×10^2	3×10^2	3×10^1	3×10^2
Fluorescence-line (FLB-S)	2×10^3	2×10^3	3×10^2	3×10^2
Fluorescence-line (F2P-D)	7×10^8	7×10^8	2×10^7	2×10^7
Coherent AS Raman (CARS-D)	5×10^{13}	5×10^{13}	5×10^{10}	5×10^{10}

Note: See text for expressions used and evaluation of parameters. The analyte is any hypothetical species with characteristics listed in text. Values given are "order of magnitude" estimates.

[a] Limit of detection is that concentration of species, n_o, resulting in a S/N = 3.

i.e., the limit of detection in species per cm^3, can be estimated; these values appear in Table 9. The choice of parameters used to estimate the $n_o)_{lim}$ values are discussed below

Absorption values — ($f_{12} = 1$, $\lambda_o = 300$ nm or 600 nm)

- $\int \sigma(\lambda) d\lambda = 8.1 \times 10^{-15}$ cm^{2}nm at 300 nm
  $= 3.2 \times 10^{-14}$ cm^{2}nm at 600 nm
- $\sigma_o = \dfrac{8.1 \times 10^{-15}}{\Delta\lambda_D}$ cm^{2}nm^{-1} at 600 nm
  $= \dfrac{3.2 \times 10^{-14}}{\Delta\lambda_D}$ cm^{2}nm^{-1} at 600 nm
- $h\nu_o = 6.6 \times 10^{-19}$ J at 300 nm
  $= 3.3 \times 10^{-19}$ J at 600 nm
- $\Delta\lambda_D = 7.16 \times 10^{-7} \lambda_o \dfrac{\sqrt{T}}{M}$ (assume analyte has M = 50 amu)
  $= 1.5 \times 10^{-3}$ nm at 300 nm and T = 2500 K
  $= 5.4 \times 10^{-4}$ nm at 300 nm and T = 300 K
  $= 3.1 \times 10^{-3}$ nm at 600 nm and T = 2500 K
  $= 1.1 \times 10^{-3}$ nm at 600 nm and T = 300 K
- $\delta_o \simeq 1.0$ (for a narrow line source/absorber system)
- $B_{C\lambda}$ ($\lambda_o = 300$ nm or 600 nm) $= 10^{-1}$ J s^{-1}cm^{-2}sr^{-1}nm^{-1} (for a xenon arc lamp) (also $D_1 = 0.5$)

- B_l ($\lambda_o = 300$ nm or 600 nm) $= 10^{-4}$ J s^{-1}cm^{-2}sr^{-1} (for a good electrodeless discharge) (also $D_2 = 0.5$)
- $\Delta\lambda_s = 1$ nm (for spectrometer)
- $\ell_A = 10$ cm
- $K_A = \Omega_{ex}(wh)_{ex} T_s \eta_d t_o \left(\dfrac{1}{h\nu_o}\right)$ cm^{2}sr s J^{-1}

  $= 0.02 \text{ sr} \times 0.05 \text{ cm} \times 1 \text{ cm} \times 0.5 \times 0.5 \times 10 \text{ s} \times \dfrac{1}{h\nu_o}$

  $= 2.5 \times 10^{-3} \left(\dfrac{1}{h\nu_o}\right)$ cm^{2}sr s J^{-1}
- $t_o = 10$ s

Fluorescence values — ($f_{12} = 1$, $\lambda_o = 300$ nm or 600 nm) — No Saturation

- $\int \sigma(\lambda) d\lambda$, σ_o, $h\nu_o$, δ_o, $B_{C\lambda}$, $\Delta\lambda_s$, $\Delta\lambda_D$, and B_L are assumed to be the same as for absorption measurements
- Y = 0.02 for C_2H_2/air flame (T = 2500 K)
  = 0.02 for gas cell (T = 300 K, 1 atm)
- $\ell_F = 1$ cm
- $B_{B\lambda}$ ($\lambda_o = 300$ nm) $= 10^{-6}$ J s^{-1}cm^{-2}sr^{-1}nm^{-1} (C_2H_2/air flame)
- $B_{B\lambda}$ ($\lambda_o = 600$ nm) $= 10^{-8}$ J s^{-1}cm^{-2}sr^{-1}nm^{-1} (C_2H_2/air flame)
- $B_{B\lambda}$ ($\lambda_o = 300$ nm or 600 nm) $\cong 0$ (T = 300 K)
- $D_s = 1$ for all conventional fluorescence measurements
- $R_D = 10^3$ s^{-1} (for a *good* photomultiplier detector)
- $K_F = \Omega_{ex}\Omega_{f\ell}(wh)_{em} T_o \eta_d t_o \left(\dfrac{1}{h\nu_o}\right) = 1 \text{ sr} \times 1 \text{ sr} \times 0.1 \text{ cm} \times 1 \text{ cm} \times 0.5 \times 0.5 \times$

  $10\text{s} \times \dfrac{1}{h\nu_o}$

  $= 2.5 \times 10^{-1} \left(\dfrac{1}{h\nu_o}\right)$ cm^{2}sr^{2}s J^{-1}
- $t_o = 10$ s

Fluorescence values — ($A_{21} = 10^8$ s^{-1}, $\lambda_o = 300$ nm or 600 nm) — Saturation

$h\nu_o$, $B_{B\lambda}$ ($\lambda_o = 300$ nm or 600 nm), R_D, t_o, $\Delta\lambda_s$, and K_F are assumed to be the same as for fluorescence — no saturation cases. The "continuum" (pseudo) and narrow line lasers assumed for this case have spectral radiances and irradiances, respectively, exceeding the saturation spectral radiances and irradiances for the atoms or molecules absorbing at $\lambda_o = 300$ nm and at $\lambda_o = 600$ nm. Also, $D_2 = 10^{-6}$; $D_s = 10^{-6}$ (for pulsed N_2-pumped dye laser and gated detector); $\alpha_s = 10^2$ (100-fold expansion in the above laser beam while still maintaining near saturation conditions); $\eta = 10^{-2}$ (assuming the ratio of laser line width to Doppler width is $\sim 10^{-2}$). (The choice of $A_{21} = 10^8$ s^{-1} is for convenience; it should be stressed that an $f_{12} = 1$ and $\lambda_o = 300$ nm or 600 nm transposes to an $A_{21} > 10^8$ s^{-1} in both cases.)

Raman (spontaneous) values

- $\dfrac{d\sigma_R}{d\Omega} = 10^{-30}$ cm^{2}sr^{-1} (at $\lambda_o = 600$ nm)

$= 10^{-27}$ cm^{2}sr^{-1} (at $\lambda_o = 300$ nm; near resonance enhancement)

- $\ell_R = 1$ cm
- $K_R = \Omega_{cm} T_o \eta_d t_o \left(\frac{1}{h\nu_o}\right) = 0.02$ sr ×

$$0.5 \times 0.5 \times 10 \text{ s} \times \frac{1}{h\nu_o}$$

$$= 5 \times 10^{-2} \left(\frac{1}{h\nu_o}\right) \text{sr s J}^{-1}$$

Two-photon fluorescence values

- $\sigma^{(2)} = 10^{-51}$ cm^2/photon/cm^2 s
- $\eta = 10^{-2}$ (same as for fluorescence — saturation)
- E_L ($\lambda_o = 300$ nm) $= 10^9$ J s^{-1} cm^{-2} (pulsed flashlamp dye laser doubled)
- E_L ($\lambda_o = 600$ nm) $= 10^{10}$ J s^{-1} cm^{-2} (pulsed flashlamp dye laser)
- $D_s = 10^{-6}$
- $K_F = 2.5 \times 10^{-1} \left(\frac{1}{h\nu_o}\right)$ (same as for fluorescence)
- $R_D = 10^3$ s^{-1}
- $t_o = 10$ s

CARS values — (Assume Nd-YAG doubled, $\lambda_p = 532$ nm, $\lambda_s = 607$ nm, $\lambda_{as} = 473$ nm.)

- $\omega_{as} = 2\pi\nu_{as} = 4.0 \times 10^{15}$ Hz
- $E_p = 5 \times 10^9$ J s^{-1}cm^{-1} (at $\lambda_p = 532$ nm)
- $\phi_s = 10^5$ J s^{-1} (at $\lambda_s = 607$ nm)
- $D_s = 10^{-6}$
- $R_D = 10^3$ s^{-1}
- $t_o = 10$ s
- $\frac{d\sigma_R}{d\Omega} = 10^{-30}$ cm^{2}sr^{-1} (for vibrational Q of N_2)
- $\chi' = 3 \times 10^2$ cm^{4}sr J^{-1}
- $\ell_R = 1$ cm

D. Discussion of Calculated Limits of Detection

It is apparent from the results of Table 9 that such values are rarely achieved or even approached in experimental absorption, fluorescence, and Raman spectrometry. The reasons for this are intimately related to several assumptions and choices of parameters for estimating the limits of detection. For example, we assumed initially that only shot noise was important, and furthermore, for each case, only one limiting type of shot noise was significant. In reality, more than one source of shot noise may be important, but even more important, various flicker noises may appear. In addition, the instrumental factors like K_A, K_F, K_R, and the source intensities were estimated for ideal experimental conditions, and even though better values are achievable in practice, the chosen values may be too liberal. Finally, the transition probabilities (f_{12} and A_{21}) were chosen for a very intense atomic or molecular transition.

Some simple, obvious, but worthwhile conclusions from the limits of detection in Table 9 and the signal-to-noise ratio expressions are given below:

1. For absorption, fluorescence (no saturation), fluorescence (saturation), and fluorescence (two photon), the detection limit will increase (become poorer) by 10 times if: (a) the transition probability, f_{12} or A_{21}, decreases by 10 times; and (b) the fluorescence path length is decreased by 10 times.
2. For absorption, fluorescence (no saturation) — background noise limited and fluorescence (saturation) — background noise limited, the detection limit will increase (become poorer) by 10 times if: (a) the background spectral radiance (for fluorescence, the background is from the cell; for absorption, the background is from the source itself) increases by 100 times; (b) the spectral bandwidth (for continuum background only) of the spectrometer increases by 100 times; (c) the instrumental factor K_A or K_F decreases by 100 times; and (d) the signal duty factor decreases by 10 times; (assuming the background duty factor remains the same); if the signal and background duty factors are interrelated as with a boxcar detector, then they must decrease by 100 times.
3. For fluorescence (saturation), the limits of detection do *not* vary with source intensity unless the source intensity change (decrease) results in a need to reduce the beam expansion factor to maintain near saturation conditions; if the source power can be maintained for a longer pulse width, then D_S (and D_B) can be increased, resulting in a corresponding decrease in the detection for the detector noise limit and in a square root decrease in the detection for the background noise limit; thus higher power, longer pulse width lasers (which also cost more) are nice for analysis since the beam expansion factor can be increased as well as the duty factors.
4. For spontaneous Raman scatter and detector noise limitation, the detection limit will increase (become poorer) by 10 times if: (a) the source flux is reduced by 10 times; (b) the interaction length is reduced by 10 times; (c) the differential cross section is reduced by 10 times; (d) either the instrumental factor or duty factor are reduced by 10 times; (e) the dark count rate is increased by 100 times; and (f) the observation time is reduced by 100 times.
5. For CARS and detector noise limitation, the detection limit will be increased by 10 times if: (a) the interaction region is $\sqrt{10}$ times smaller; (b) the susceptibility is $\sqrt{10}$ times smaller; (c) the probe laser irradiance is $\sqrt{10}$ times smaller; (d) the Stokes laser flux is 10 times smaller; (e) the differential cross section is $\sqrt{10}$ times smaller; (f) the dark count rate and/or observation time are 10^2 times larger and/or smaller, respectively; and (g) the instrumental factor, K_R' is 10 times smaller.
6. For molecular fluorescence (two-photon excitation), the detector noise limit is reduced by 10 times if: (a) the source intensity is decreased by $\sqrt{10}$ times; (b) the absorption cross section is reduced by 10 times; (c) the duty factor, D_s, is reduced by 10 times; (d) the instrumental factor, K_F, is reduced by 10 times; and (e) the dark count rate is increased by 100 times or the observation time is reduced by 100 times.

In Table 9, calculated detection limits in terms of species per cm^3 are listed. In the previous section, some of the reasons were given why the calculated and experimental values might differ in terms of (molecules or atoms) per cm^3. However, no mention was given of the inefficient conversion of sample species to measured species. In *condensed phase* molecular spectrometry, the conversion from analyte concentration, C, in moles per liter, to n_o in molecules per cm^3, is simply given by

$$n_o = 10^{-3}\beta_m \cdot C \cdot N_A \qquad (16)$$

where N_A is Avogadro's number (6×10^{23}) and β_m is the fraction of analyte species present in the correct form for the spectroscopic transition, e.g., β_m will depend upon pH, temperature, complexing species, etc. In *static gas phase* atomic or molecular spectrometry where the sample is vaporized by a thermal process (assuming solid or liquid material exists in the cell),

$$n_a = \frac{\beta_m \rho_s}{kT} \qquad (17)$$

where ρ_s is the saturation vapor pressure, torr, k is the Boltzmann constant (torr $K^{-1}cm^3$), and T is the temperature (in K) of the cell. In *dynamic gas phase* atomic or molecular spectrometry where the sample solution is converted to submicroscopic species via an aerosol intermediate, as in flame spectrometry,

$$n_a = \frac{\beta_m (\text{or } \beta_a) \epsilon \beta_v FCN_A \cdot 10^{-3}}{Qe_f} \qquad (18)$$

where β_v is the vaporization fraction, β_m (or β_a) is the fraction of analyte species present in the measured gaseous system as molecules or as atoms, ϵ is the fraction of solution sprayed into a chamber which is transferred as aerosol into the hot gases, F is the sample solution transport rate (cm^3s^{-1}), C is the analyte concentration (mol ℓ^{-1}), N_A is Avogadro's number, Q is the flow rate of gases at room temperature (in cm^3s^{-1}), and e_f is the gas expansion factor due to heating of the gases from room temperature to some hot gas temperatures. For a furnace system[115] where the sample is instantaneously vaporized into a cell volume, V_c, cm^3,

$$n_a = \frac{\beta_m (\text{or } \beta_a) \beta_v w N_A}{M_a V_c} \qquad (19)$$

where β_m or β_a are as above, β_v is the fraction of species introduced which appear finally in the gas phase, i.e., accounts for losses due to carbide formation, particles condensing out in the ends of the furnace, etc., w is the weight, in g, of the sample introduced, M_a is the molecular (atomic) weight of the pure material, and N_A is Avogadro's number. It is assumed in the latter case that the atomization times, t_a, are much less than the residence time, t_r, of species in the cell where $t_r = L^2/8D$, where L is the length of the furnace, and D is the analyte diffusion coefficient at the furnace temperature.

In any event, it should be pointed out that the β factors account for losses of the analyte. In condensed phase work, the β value will often be unity indicating no losses. For static gas phase work, there will also be few gas phase losses in many cases. However, in such studies, there is the obvious "loss" in going from a small amount of analyte in the solid or liquid phase to a larger volume in the gas phase. In flames, plasmas, etc., there are not only the losses due to the above named β-factors but also those due to conversion of a volume of liquid sample to a gas. For example, 1 mmol of analyte is converted to 22.4 mℓ of gas (assuming an ideal gas) at 273.1 K (~10 times or 224 mℓ of gas at 2500 K) and is further diluted by a rapidly flowing stream of hot gas which supplies the flame. For furnaces, the latter dilution is insignificant since the system is static, but the "loss" due to conversion of the analyte from the solid or liquid phase to the gas phase is important; finally, complex losses of analyte in furnaces can occur through either vaporization losses prior to the measurement, as $AsCl_3$, or *in situ* losses of analyte by forming carbides, such as ZrC_2.

It may be instructive to give the conversion factor from moles per liter to atoms per cm^3 of flame gases for a typical atomic flame spectrometric measurement. Assume an analysis is to be performed on an element Z which is present at concentration, moles per ℓ, in solution and is introduced into a flame at a liquid flow rate of 0.2 cm^3/s. Assume the nebulizer efficiency ϵ is 0.02, the efficiency of conversion of droplets to submicroscopic species, $\beta_v = 0.5$, and a total gas flow rate, Q of 200 cm^3/s with a flame temperature of ~2500 K (e_f ~ 10). This system could represent a typical C_2H_2/air flame with nebulizer burner such as is used in atomic absorption flame spectrometry. Then

$$\frac{n_a}{C} = 6 \times 10^{14} \times \beta_a \qquad (20)$$

Therefore, if element Z (M_a = 100 amu) has a concentration of 10^{-9} *M* (10^{-4} μg/mℓ or 0.1 ppb), then $n_a = 6 \times 10^5$ atomic species per cm^3, which is typical of detection limits in atomic fluorescence flame spectrometry, if the atomization efficiency (β_a) is unity.

No attempt will be made here to correlate experimental detection limits with theoretical ones, not only because of lack of space, but more importantly, lack of adequate physical parameters to evaluate the S/N ratio expressions for specific experimental systems.

E. Analytical Figures of Merit (Experimental)

In Table 10 and 11, approximate limits of detection (LOD), linear dynamic ranges (LDR), precisions (% RSD — % relative standard deviations), and minimum sample sizes for the various laser methods are listed. Also several other methods are listed for comparison purposes.

F. Experimental Limits of Detection

In Tables 2 to 5, experimental limits of detection for atoms (Tables 2 and 3) and for molecules (Tables 4 and 5) are given. The molecular detection limits are further divided according to gas phase (Table 5) and condensed phase (Table 4), and in the condensed phase according to the technique fluorimetry (Table 4) and phosphorimetry (Table 6). The gas phase atomic-spectrometric detection limits are given not only for laser excited atomic fluorescence, but also for conventional line-source excited atomic fluorescence, conventional continuum-source excited atomic fluorescence, conventional line-source atomic absorption flame spectrometry, and for atomic emission spectrometry with an inductively coupled plasma. No tables for absolute detection limits will be given for molecules because estimates can be made from the data in the tables by multiplying the concentrational detection limit by the cell volume or interaction volume; in other words, the systems used to detect small amounts of molecules are identical to those used to detect small concentrations of molecules. However, in the case of elemental analysis, furnace methods are used in atomic absorption and atomic fluorescence rather than flames, plasmas, etc., which are used for concentration measurements. Therefore, in Table 3, examples of elemental detection limits for atomic fluorescence, atomic absorption furnace, and atomic emission with the inductively coupled plasma methods are given.

It is apparent that laser methods are extremely sensitive methods capable of excellent precision, long linear dynamic ranges, and microsampling (also see Tables 10, 11). Certainly Arthur Robinson's[6] catchy title in *Science*, "Analytical Chemistry: Using Lasers to Detect Less and Less", is valid and the detection of even less is to be expected. The considerable advances since Steinfeld's excellent review[1] are also important.

ACKNOWLEDGMENTS

The authors would like to express their thanks to Dr. J. I. Steinfeld for his careful reading of the manuscript and useful comments.

Table 10
DETECTION LIMITS (LOD), LINEAR DYNAMIC RANGES (LDR), AND PRECISION (%RSD) OF MOLECULES (pg) BY SEVERAL LASER SPECTROMETRIC METHODS

Method	Practical LOD (pg)	%RSD	LDR	Estimated LOD[a] (pg)	Ref.
Laser fluorimetry	1	1—2	~10^4	10^{-3}	160
Xenon fluorimetry	1	1—2	~10^3	1	[b]
Laser phosphorimetry	10^1	1—5	~10^4	1	214
Laser fluorescence microscopy (tagging of molecule)	10^{-1}	2	?	$10^{-10}10^{-11}$	[c]
Laser Raman (spontaneous)	~10^6	2—5	~10^3	~10^1	220
Laser Raman (resonance)	~10^4	2—5	~10^3	~10^2	227, 228
Laser Raman (CARS)	~10^5	5—10	~10^2	~10^4	220
Laser Raman (inverse)	~10^5	2—5	~10^1	~10^3	243
Laser-thermal lensing	~10^5	1—5	~10	~10^3	108,109
Laser Raman microprobe	~1	?	?	~10^{-1}	264

[a] Best estimate based on detector noise limit.

[b] Guilbault, G. G., *Practical Fluorescence, Theory, Methods, and Techniques*, Marcel Dekker, New York, 1973.

[c] Kaufman, G. I., Mester, J. F., and Wasserman, D. E., *J. Histochem. Cytochem.*, 14, 260(1966).

Table 11
DETECTION LIMITS (LOD), LINEAR DYNAMIC RANGES (LDR), AND PRECISION (%RSD) OF ELEMENTS (pg) BY SEVERAL LASER SPECTROMETRIC METHODS

Method	Sample size[a]	Practical LOD (pg)	%RSD	LDR	Estimated LOD[b] (pg)
Laser exc AFS[c]	0.1—1	10^2—1	1—2	10^3—10^4	10^{-4}—10^{-2}
Conventional EDL AFS[c]	0.1—1	10^1	1—2	10^4—10^5	1
Conventional xenon AFS[c]	0.1—1	10^3	1—2	10^3—10^4	10^2
Laser Exc optogalvanic[c]	0.1—1	10^2—1	1—5	10^3—10^4	10^{-1}
Laser emission microprobe[d]	10^{-6} (10—200 μm)[e]	10^{-3}—1	5—15	10^2—10^1	10^{-1}—10^{-3}
Laser mass spectrometer[f]	10^{-10}—10^{-12} (1 μm)[e]	10^{-6}—10^{-8}	~5—10	~10^3 10^3—10^4	10^{-7}—10^{-9}
Laser atomization AA[g]		10^1—10^2	~5—15	~10^2 10^1—10^2	1—20
Ion microprobe	10^{-11} (1—5 μm)[e]	10^{-5}—10^{-7}	~25—50	10^3—10^4	10^{-7}—10^{-9}
Neutron activation	10^{-3}—1	10^{-1}—10^3	~5—10	10^3—10^4	10^{-1}—10^2

[a] Minimum sample size for analysis, cm^3.

[b] The estimates are made on the basis of the author's estimates assuming detector limited noise.

[c] Omenetto, N. and Winefordner, J. D., *Prog. Anal. At. Spectrom.*, 2, 1(1979).

[d] Treytl, W. J., Orenberg, J. B., Marich, K. W., Saffir, A. J., and Glick, D., *Anal. Chem.*, 44, 1980(1972).

[e] Diameter of crater produced.

[f] Kovalov, I. D., Makismov, G. A., Suchkov, A. I., and Larin, J. V., *J. Mass. Spect. Ion Physics*, 27, 101(1978).

[g] Vulfson, E. K., Karyakin, A. V., and Shidlovskii, A. I., *J. Anal. Chem. U.S.S.R.*, 28, 1253(1973).

REFERENCES

1. Steinfeld, J. I., *CRC Crit. Rev. Anal. Chem.*, 6, 225(1975).
2. Omenetto, N. and Winefordner, J. D., *Prog. Anal. At. Spectrosc.*, 2(1,2), (1979).
3. Omenetto, N., Ed., *Analytical Laser Spectroscopy*, John Wiley & Sons, New York, 1979.
4. Hieftje, G. M., New Applications of Lasers to Chemistry, ACS Symp. Ser. No. 85, Washington, D.C., 1978.
5. West, M. A., *Lasers in Chemistry*, Elsevier, Amsterdam, 197
6. Robinson, A. I., *Science*, 199, 1191(1978).
7. Fraser, L. M., and Winefordner, J. D., *Anal. Chem.*, 43, 1693(1971).
8. Denton, M. B. and Malmstadt, H. V., *Appl. Phys. Lett.*, 18, 485(1971).
9. Fraser, L. M. and Winefordner, J. D., *Anal. Chem.*, 44, 1444(1972).
10. Omenetto, N., Hatch, N. N., Fraser, L. M., and Winefordner, J. D., *Anal. Chem.*, 45, 195(1973).
11. Omenetto, N., Hatch, N. N., Fraser, L. M., and Winefordner, J. D., *Spectrochim. Acta*, 28B, 65(1973).
12. Omenetto, N., Hart, L. P., Benetti, P., and Winefordner, J. D., *Spectrochim. Acta*, 28B, 301(1973).
13. Omenetto, N., Benetti, P., Hart, L. P., Winefordner, J. D., and Alkemade, C. Th. J., *Spectrochim. Acta*, 28B, 289(1973).
14. Kuhl, J., Neumann, S., and Kriese, M., *Z. Naturforsch. A*, 28, 273(1972).
15. Kuhl, J. and Spitschan, H., *Opt. Commun.*, 7, 256(1973).
16. deOlivares, D. R., Ph.D. thesis, Indiana University, 1976.
17. Green, R. B., Travis, J. C., and Keller, R. A., *Anal. Chem.*, 48, 1954(1976).
18. Gelbwachs, J. A., Klein, C. F., and Wessel, J. E., *Appl. Phys. Lett.*, 30, 489(1977).
19. Smith, B. W., Blackburn, M. B., and Winefordner, J. D., *Can. J. Spectrosc.*, 22, 57(1977).
20. Daily, J. W. and Chan, C., University of California, Berkeley, unpublished work.
21. Epstein, M. S., Bayer, S., Bradshaw, J., Voigtman, E., and Winefordner, J. D., *Spectrochim. Acta*, 35B, 23:(1980).
22. Epstein, M. S., Bradshaw, J., Bayer, S., Bower, J., Voigtman, E., and Winefordner, J. D., *Appl. Spectrosc.*, 34, 372(1980).
23. Kuhl, J. and Marowsky, G., *Opt. Commun.*, 4, 125(1971).
24. Weeks, S. J., Haraguchi, H., and Winefordner, J. D., *Anal. Chem.*, 50, 360(1978).
25. Blackburn, M. B., Mermet, J. M., Boutilier, G. D., and Winefordner, J. D., *Appl. Opt.*, 18, 1804(1979).
26. Blackburn, M. B., Mermet, J. M., and Winefordner, J. D., *Spectrochim. Acta*, 34A, 847(1978).
27. Weeks, S. J., Haraguchi, H., and Winefordner, J. D., *J. Quant. Spectrosc. Radiat. Transfer*, 19, 633(1978).
28. Haraguchi, H., Weeks, S. J., and Winefordner, J. D., *Spectrochim. Acta*, 35A, 391(1979).
29. Neumann, S., and Kriese, M., *Spectrochim. Acta*, 29B, 127(1974).
30. Fairbanks, W. M., Jr., Hansch, T. W., and Schawlow, A. L., *J. Opt. Soc. Am.*, 65, 199(1975).
31. Brod, H. L. and Yeung, E. S., *Anal. Chem.*, 48, 344(1976).
32. Sharp, B. L. and Goldwasser, A., *Spectrochim. Acta*, 31B, 431(1976).
33. Mayo, S., Keller, R. A., Travis, J. C., and Green, R. B., *J. Appl. Phys.*, 47, 4012(1976).
34. Bolshov, M. A., Zybin, A. V., Zybina, L. A., Koloshnikov, V. G., and Majorov, I. A., *Spectrochim. Acta*, 31B, 493(1976).
35. Hohimer, J. P. and Hargis, P. J., Jr., *Appl. Phys. Lett.*, 30, 344(1977).
36. Epstein, M. S., Nikdel, S., Bradshaw, J., Kosinski, M., Bower, J., and Winefordner, J. D., *Anal. Chim. Acta*, 113, 22(1980).
37. Pollard, B. D., Blackburn, M. B., Nikdel, S., Massoumi, A., and Winefordner, J. D., *Appl. Spectrosc.*, 33, 5(1979).
38. Measures, R. M. and Kwong, H. S., *Appl. Opt.*, 18, 281(1979).
39. Kwong, H. S. and Measures, R. M., *Anal. Chem.*, 51, 428(1979).
40. Meng, H. C. and Kunze, H. J., *Phys. Fluids*, 22, 1082(1979).
41. Miron, E., David, R., Erez, G., Lavi, S., and Levin, L. A., *Appl. Phys. Lett.*, 35, 737(1979).
42. VanDijk, C. A. and Alkemade, C. Th. J., *J. Quant. Spectrosc. Radiat. Transfer*, 23, 445(1980).
43. Van Calcar, R. A., Van de Ven, M. J. M., Van Uitert, B. K., Biewenga, K. J., Hollander, Tj., and Alkemade, C. Th. J., *J. Quant. Spectrosc. Radiat. Transfer*, 21, 11(1979).
44. VanDijk, C. A., Zeegers, P. J. Th., and Alkemade, C. Th. J., *J. Quant. Spectrosc. Radiat. Transfer*, 21, 115(1979).
45. Omenetto, N., Epstein, M. S., Bradshaw, J. D., Horvath, J. H., and Winefordner, J. D., *J. Quant. Spectrosc. Radiat. Transfer*, 22, 287(1979).

45a. Lucht, R. P. and Laurendeau, N. M., *Combust. Flame*, 34, 215(1979).

46. Wright, J. C., *Anal. Chem.*, 49, 1690(1977).

47. **Gustafson, F. J. and Wright, J. C.,** *Anal. Chem.*, 49, 1680(1977).
48. **Johnston, M. V. and Wright, J. C.,** *Anal. Chem.*, 51, 1774(1979).
49. **Wright, J. C., Gustafson, F. J., and Porter, L. C.,** New Applications of Lasers to Chemistry, ACS Symp. Ser. No. 85, Washington, D.C., 1978.
50. **Gustafson, F. J. and Wright, J. C.,** *Anal. Chem.*, 51, 1762(1979).
51. **Schroder, H., Neusser, H. J., and Schlag, E. W.,** *Opt. Commun.*, 14, 395(1975).
52. **Keller, R. A., Zalewski, E. F., and Peterson, N. C.,** *J. Opt. Soc. Am.*, 62, 319(1972).
53. **Holt, H. K.,** *Phys. Rev.*, All, 625(1975).
54. **Horlick, G. and Codding, E. G.,** *Anal. Chem.*, 46, 133(1974).
55. **Peterson, N. C., Kurylo, M. J., Braun, W., Bass, A. M., and Keller, R. A.,** *J. Opt. Soc. Am.*, 61, 746(1971).
56. **Thrash, R. J., Von Weyssenhoff, H., and Shirk, J. S.,** *J. Chem. Phys.*, 55, 4659(1971).
57. **Atkinson, G. H., Laufer, A. H., and Kurylo, M. J.,** *J. Chem. Phys.*, 59, 350(1973).
58. **Latz, H. W., Wyles, H. F., and Green, R. B.,** *Anal. Chem.*, 45, 2405(1973).
59. **Green, R. B. and Latz, H. W.,** *Spectrosc. Lett.*, 7, 419(1974).
60. **Childs, W. J., Fred, M. S., and Goodman, L. S.,** *Appl. Opt.*, 13, 2297(1974).
61. **Werncke, W., Klein, J., Lau, A., Lenz, K., and Hunsalz, G.,** *Opt. Commun.*, 11, 159(1974).
62. **Maeda, M., Ishitzuk, F., and Miyozoe, Y.,** *Opt. Commun.*, 13, 314(1975).
63. **Konjevic, N. and Kokovic, M.,** *Spectrosc. Lett.*, 7, 615(1974).
64. **Green, J. M., Hohimer, J. P., and Tittel, F. K.,** *Opt. Commun.*, 7, 349(1973).
65. **Belikova, T. P., Sviridenkov, E. A., Suchkov, A. F., Titova, L. V., and Churilov, S. S.,** *J. Exp. Theor. Phys.*, 62, 2060(1972).
66. **Belikova, T. P., Sviridenkov, E. A., and Suchkov, A. F.,** *Quant. Electron.*, USSR, 1(1974).
67. **Belikova, T. P., Sviridenkov, E. A., and Suchkov, A. F.,** *Opt. Spectrosc. U.S.S.R.*, 37, 372(1974).
68. **Spiker, R. C. and Shirk, J. S.,** *Anal. Chem.*, 46, 572(1974).
69. **Datta, S., Anderson, R. W., and Zare, R. N.,** *J. Chem. Phys.*, 63, 5503(1973).
70. **Klein, M. B., Shank, C. V., and Dienes, A.,** *Opt. Commun.*, 7, 178(1973).
71. **Keller, R. A., and Travis, J. C.,** *Analytical Laser Spectroscopy*, Omenetto, N., Ed., John Wiley & Sons, New York, 1979.
72. **Hohimer, J. P. and Hargis, P. J.,** *Anal. Chem.*, 51, 930(1979).
73. **Antonov, E. N., Berik, E. B., and Koloshnikov, V. G.,** *J. Quant. Spectrosc. Radiat. Transfer*, 22, 45(1979).
74. **Hill, W. T., Abreu, R. A., Hansch, T. W., and Schawlow, A. L.,** *Opt. Commun.*, 37, 96(1980).
75. **Manabee, R. M. and Piepmeier, E. H.,** *Anal. Chem.*, 51, 2066(1979).
76. **Quentmeier, A., Laqua, K., and Hagenah, W. D.,** *Spectrochim. Acta*, 34B, 117(1979).
77. **Quentmeier, A., Laqua, K., and Hagenah, W. D.,** *Spectrochim. Acta*, 35B, 139(1980).
78. **Kantor, T., Bezur, L., Pungor, E., Fodor, P., Nagy-Balogh, J., and Heinez, G.,** *Spectrochim. Acta*, 34B, 341(1979).
79. **Van Deijck, W., Balke, J., and Maessen, F. J. M. J.,** *Spectrochim. Acta*, 34B, 359(1979).
80. **Ishizuka, T. and Uwanino, Y.,** *Anal. Chem.*, 52, 125(1980).
81. **Green, R. B., Keller, R. A., Luther, G. G., Schenck, P. K., and Travis, J. C.,** *Appl. Phys. Lett.*, 29, 727(1976).
82. **Green, R. B., Keller, R. A., Schenck, P. K., Travis, J. C., and Luther, G. G.,** *J. Am. Chem. Soc.*, 98, 8517(1976).
83. **Turk, G. C., Travis, J. C., DeVoe, J. R., and O'Haver, T. C.,** *Anal. Chem.*, 50, 817(1978).
84. **VanDijk, C. A.,** Ph.D. thesis, Utrecht, 1978.
85. **Travis, J. C., Schenck, P. K., Turk, G. C., and Mallard, W. G.,** *Anal. Chem.*, 51, 1516(1979).
86. **Schenck, P. K. and Smyth, K. C.,** *J. Opt. Soc. Am.*, 68, 626(1978).
87. **King, D. S. and Schenck, P. K.,** *Laser Focus*, 14, 50(1978).
88. **Smyth, K. C. and Schenck, P. K.,** *Chem. Phys. Lett.*, 55, 466(1978).
89. **Schenck, P., Mallard, W. G., Travis, J. C., and Smyth, K. C.,** *J. Chem. Phys.*, 69, 5147(1978).
90. **Bridges, W. M.,** *J. Opt. Soc. Am.*, 68, 352(1978).
91. **Johnston, T. F.,** *Laser Focus*, 14, 58(1978).
92. **Smyth, K. C., Keller, R. A., and Crim, F. F.,** *Chem. Phys. Lett.*, 55, 473(1978).
93. **Zalewski, F. F., Keller, R. A., and Engleman, R.,** *J. Chem. Phys.*, 70, 1015(1979).
94. **Smyth, K. C., Bentz, B. L., Bruhn, C. G., and Harrison, W. W.,** *J. Am. Chem. Soc.*, 101, 797(1979).
95. **Travis, J. C., Turk, G. C., and Green, R. B.,** *New Applications of Lasers to Chemistry*, Hieftje, G. M., Ed., ACS Symp. Ser. No. 85, Washington, D.C., 1978.
96. **Schenck, P. K., King, D. S., Smyth, K. C., Travis, J. C., and Turk, G. C.,** *Lasers in Chemistry*, West, M. A., Ed., Elsevier, Amsterdam, 1977.
97. **Turk, G. C., Travis, J. C., DeVoe, J. R., and O'Haver, T. C.,** *Anal. Chem.*, 51, 1890(1979).

98. **Turk, G. C., Mallard, W. G., Schenck, P. K., and Smyth, K. S.,** *Anal. Chem.*, 51, 2408(1979).
99. **Keller, R. A., Engleman, R., and Zalewski, E. F.,** *J. Opt. Soc. Am.*, 69, 738(1979).
100. **Beeman, G. J., Lessard, B. P., and Piepmeier, E. H.,** *Anal. Chem.*, 51, 1721(1979).
101. **Allen, J. E., Anderson, W. R., and Crosley, D. R.,** *Opt. Lett.*, 1, 118(1977).
102. **Allen, J. E., Anderson, W. R., Crosley, D. R., and Fansler, T. D.,** 17th Symp. Combust., Leeds, August, 1978.
103. **Anderson, W. R., Allen, J. E., Fansler, T. D., and Crosley, D. R.,** 17th Symp. Combust., Leeds, August, 1978.
104. **Howard, A. G. and Greenhalgh, D. A.,** *Anal. Chim. Acta*, 106, 361(1979).
105. **Schawlow, A. L.,** *Science*, 202, 141(1978).
106. **Letokhov, V. S., and Chebotayev, V. P.,** *Nonlinear Laser Spectroscopy*, Springer-Verlag, New York, 1977.
107. **O'Haver, T. C.,** *Anal. Chem.*, 51, 91A(1979).
108. **Dovichi, N. J. and Harris, J. M.,** *Anal. Chem.*, 51, 728(1979).
109. **Harris, J. M. and Dovichi, N. J.,** *Anal. Chem.*, 52, 695A(1980).
110. **Gelbwachs, J. A.,** *Appl. Opt.*, 15, 2654(1976).
111. **Gelbwachs, J. A., Jones, P. F., and Wessel, J. E.,** *Appl. Phys. Lett.*, 27, 40(1975).
112. **Gelbwachs, J. A. and Wessel, J. E.,** *Opt. Eng.*, 16, 197(1977).
113. **Patel, C. K. N.,** *Science*, 202, 157(1978).
114. **Measures, R. M.,** *Analytical Laser Spectroscopy*, Omenetto, N., Ed., John Wiley & Sons, New York, 1979.
115. **Hoell, J. M., Wade, W. R., and Thompson, R. T.,** Institute of Electrical and Electronics Engineers, Ann. No. 75, CH 1004-1, 10-6, 1976.
116. **Kuhl, J. and Spitschan, H.,** *Opt. Commun.*, 13, 6(1975).
117. **O'Shea, D. and Dodge, L. G.,** *Appl. Opt.*, 13, 1481(1974).
118. **Murray, E. R., Van der Laan, J. E., and Hawley, J. G.,** *Appl. Opt.*, 15, 3140(1976).
119. **Rothe, K. W., Brinkmann, U., and Walther, H.,** *Appl. Phys.*, 3, 115(1974).
120. **Rothe, K. W., Brinkmann, U., and Walther, H.,** *Appl. Phys.*, 4, 181(1974).
121. **Hennigsen, T., Garbuny, M., and Byer, R. L.,** *Appl. Phys.*, 24, 242(1974).
122. **Baumgartner, R. A., and Byer, R. L.,** *Opt. Lett.*, 2, 163(1978).
123. **Megie, G. and Menzies, R. T.,** *Appl. Opt.*, 19, 1173(1980).
124. **Fredriksson, K., Galle, B., Nystrom, K., and Svanberg, S.,** *Appl. Opt.*, 13, 2998(1979).
125. **Halpern, J. B., Jackson, W. M., and McCrory, V.,** *Appl. Opt.*, 18, 590(1979).
126. **Tonnissen, A., Wanner, J., Rothe, K. W., and Walther, H.,** *Appl. Phys.*, 18, 297(1979).
127. **Hinkley, E. D. and Kelley, P. L.,** *Science*, 171, 635(1971).
127a. **Eng, R. S., Butler, J. F., and Linden, K. J.,** *Opt. Eng.*, 19, 945(1980).
128. **Hinkley, E. D., Nill, K. W., and Blum, F. A.,** *Laser Focus*, April, 47(1976).
129. **Hinkley, E. D., Ku, R. T., Nill, K. W., and Butler, J. F.,** *Appl. Opt.*, 15, 1653(1976).
130. **Nill, K. W.,** *Laser Focus*, February, 32(1977).
131. **Wahlen, M., Eng, R. S. and Nill, K. W.,** *Appl. Opt.*, 16, 2350(1977).
132. **Nill, K. W.,** Laser Analytics, Inc., Lexington, Mass., 1978.
133. **Reid, J., Shewchun, M. J., Garside, B. K., and Ballik, E. A.,** *Appl. Opt.*, 17, 300(1978).
134. **El-Sherbiny, M., Ballik, E. A., Shewchun, J., Garside, B. K., and Reid, J.,** *Appl. Opt.*, 18, 1198(1979).
135. **Eng, R. S., Mantz, A. W., and Todd, T. R.,** *Appl. Opt.*, 18, 3438(1979).
136. **Chaney, L. W., Rickel, D. G., Russwurm, G. M., and McClenny, W. A.,** *Appl. Opt.*, 18, 3004(1979).
137. **Hanson, R. K.,** *Appl. Opt.*, 19, 482(1980).
138. **Granatstein, V. L., Rhinewine, M., and Fitch, A. H.,** *Appl. Opt.*, 12, 1511(1973).
139. **Kusnowo, A., Ohtsu, M., Kobayashi, N., and Tako, T.,** *Appl. Opt.*, 19, 1227(1980).
140. **Koike, T. and Gardner, W. C.,** *Appl. Spectrosc.*, 34, 81(1980).
141. **Menzies, R. T.,** *Appl. Opt.*, 10, 1532(1971).
142. **Hillman, J. J., Jenning, D. E., and Faris, J. L.,** *Appl. Opt.*, 18, 1808(1979).
143. **Freund, S. M., Sweger, D. M., and Travis, J. C.,** *Anal. Chem.*, 48, 1944(1976).
144. **Freund, S. M. and Sweger, D. M.,** *Anal. Chem.*, 47, 930(1975).
145. **Sweger, D. M. and Travis, J. C.,** *Appl. Spectrosc.*, 33, 46(1979).
146. **Menzies, R. T. and Shumate, M. S.,** *Appl. Opt.*, 15, 2080(1976).
147. **Kanstad, S. W., Bjerkestrand, A., and Lund, T.,** *J. Phys. Sci. Inst.*, 10, 998(1977).
148. **Golden, B. M. and Yeung, E. S.,** *Anal. Chem.*, 47, 2132(1975).
148a. **Green, B. D. and Steinfeld, J. I.,** *3rd Eur. Electroopt. Conf.*, 99, 32(1977).
148b. **Green, B. D. and Steinfeld, J. I.,** *Appl. Opt.*, 15, 1688(1976).
148c. **Green, B. D. and Steinfeld, J. I.,** *Environ. Sci. Technol.*, 10, 1134(1976).
149. **Hoge, F. E. and Kinkaid, J. S.,** *Appl. Opt.*, 19, 1143(1980).

150. Pruiksma, R. and McCreery, R. L., *Anal. Chem.*, 51, 2253(1979).
151. Winefordner, J. D., *New Applications of Lasers to Chemistry*, Hieftje, G. M., Ed., American Chemical Society, Washington, D.C., 1978.
152. Wehry, E. L., *Anal. Chem.*, 52, 75R(1980).
153. Smith, B. W., Plankey, F. W., Omenetto, N., Hart, L. P., and Winefordner, J. D., *Spectrochim. Acta*, 30A, 1459(1974).
154. Vickers, R. S., Chan, P. W., and Johnson, R. E., *Spectrosc. Lett.*, 6, 131(1973).
155. LeBlanc, R. M., Galinger, G., Tessier, A., and Lemieux, L., *Can. J. Chem.*, 52, 3723(1974).
156. Harrington, D. C. and Malmstadt, H. V., *Anal. Chem.*, 47, 271(1975).
157. Van Geel, T. F. and Winefordner, J. D., *Anal. Chem.*, 48, 335(1976).
158. Richardson, J. H., Wallin, B. W., Johnson, D. C., and Hrubesh, L. W., *Anal. Chim. Acta*, 86, 263(1977).
159. Richardson, J. H. and Ando, M. E., *Anal. Chem.*, 49, 955(1977).
160. Richardson, J. H. and George, S. M., *Anal. Chem.*, 50, 616(1978).
161. Bradley, A. B. and Zare, R. N., *J. Am. Chem. Soc.*, 98, 620(1976).
162. Imasaka, T., Kadone, H., Ogawa, T., and Ishibashi, N., *Anal. Chem.*, 49, 667(1977).
163. Imasaka, T., Ogawa, T., and Ishibashi, N., *Anal. Chem.*, 51, 502(1979).
164. Ishibashi, N., Ogawa, T., and Kunitake, M., *Anal. Chem.*, 51, 2096(1979).
165. Campen, W. and Bachmann, K., *Mikrochim. Acta*, 159(1979).
166. Diebold, G. J. and Zare, R. N., *Science*, 196, 1439(1977).
167. Diebold, G. J., Karny, N., Zare, R. N., and Seitz, L. M., *J. Assoc. Off. Anal. Chem.*, 62, 564(1979).
168. Lidofsky, S. D., Imasaka, T., and Zare, R. N., *Anal. Chem.*, 51, 1602(1979).
169. Imasaka, T. and Zare, R. N., *Anal. Chem.*, 51, 2082(1979).
170. Diebold, G. J., Karny, N., and Zare, R. N., *Anal. Chem.*, 51, 67(1979).
171. Maple, J. R., Wehry, E. L., and Mamantov, G., *Anal. Chem.*, 52, 920(1980).
172. Wehry, E. L. and Mamantov, G., *Anal. Chem.*, 51, 643A(1979).
173. Mathews, T. G. and Lytle, F. E., *Anal. Chem.*, 51, 583(1979).
174. Richardson, J. P., Dering, J. P., Johnson, P. C., and Hrubesh, L. W., *Anal. Chem.*, 52, 982(1980).
175. Eastman, J. W., *Spectrochim. Acta*, 36A, 225(1980).
176. Brown, J. C., Edelson, M. C., and Small, G. J., *Anal. Chem.*, 50, 1394(1978).
177. Winefordner, J. D., *Acc. Chem. Res.*, 2, 361(1969).
178. Lytle, F. E. and Kelsey, M. S., *Anal. Chem.*, 46, 85(1974).
179. Sepaniak, M. J. and Yeung, E. S., *Anal. Chem.*, 49, 1554(1977).
180a. Wirth, M. J. and Lytle, F. E., *Anal. Chem.*, 49, 1554(1977).
180b. Harris, R. B., *Am. Lab.*, May, 93(1973).
181. Hirschfeld, T., *Appl. Opt.*, 15, 3135(1976).
182. Hirschfeld, T., *Appl. Opt.*, 15, 3135(1976).
183. Hirschfeld, T., Block, M. J., and Mueller, W., *J. Histochem. Cytochem.*, 25, 719(1977).
184. Hirschfeld, T. and Block, M. J., *Opt. Eng.*, 16, 406(1977).
185. Wright, J. C., *Appl. Spectrosc.*, 34, 151(1980).
186. Ehrlich, D. J. and Wilson, J., *J. Chem. Phys.*, 67, 5391(1977).
187. Gatterman, H. and Stockburger, M., *Chem. Phys.*, 24, 327(1977).
188. Fujiwara, K., Omenetto, N., Bradshaw, J., Bower, J., Nikdel, S., and Winefordner, J. D., *Spectrochim. Acta*, 34B, 317(1979).
189. Fujiwara, K., Omenetto, N., Bradshaw, J., Bower, J., and Winefordner, J. D., *Appl. Spectrosc.*, 34, 85(1980).
189a. D'Alessio, A., Di Lorenzo, A., Sarofim, A. F., Beretta, F., Masi, S., and Venitozzi, C., 15th Symp. Combust., The Combustion Institute, Pittsburgh, 1975.
189b. Coe, D. S. and Steinfeld, J. I., Laser Probes for Combustion Chemistry, Crosley, D. R., Ed., ACS Ser. 134, 1980, 159.
189c. Coe, D. S. and Steinfeld, J. I., *Chem. Phys. Lett.*, 76, 485(1980).
190. Haraguchi, H., Weeks, S. J., and Winefordner, J. D., *Spectrochim. Acta*, 35A, 391(1979).
191. Chan, C. and Daily, J. W., West. States Sect./Combust. Inst. Paper No. 79-20, Provo, Utah, Spring 1979.
192. Chan, C. and Daily, J. W., *Appl. Opt.*, 19, 1357(1980).
193. Daily, J. W., 6th Bienn. Turbulence Symp., University of Missouri, Rolla, October 8, 1979.
194. Bonczyk, P. A. and Shirley, J. R., *Combust. Flame*, 34, 253(1979).
195. Lucht, R. P. and Laurendeau, N. M., *Appl. Opt.*, 18, 856(1979).
196. Berg, J. O. and Shackleford, W. L., *Appl. Opt.*, 18, 2093(1979).
197. Crosby, D. R. and Smith, G. P., *Appl. Opt.*, 19, 517(1980).
198. Baronawski, A. P. and McDonald, J. R., *Appl. Opt.*, 16, 1897(1977).

199. Baronawski, A. P. and McDonald, J. R., *J. Chem. Phys.*, 66, 3300(1977).
200. Griesser, D. R. and Barnes, R. H., *Appl. Opt.*, 19, 741(1980).
201. Bechtel, J. H. and Teets, R. E., *Appl. Opt.*, 18, 4138(1979).
202. Barnes, R. H. and Kircher, J. F., *Appl. Opt.*, 17, 1099(1978).
203. Gelbwachs, J. A. and Birnbaum, M., *Appl. Opt.*, 12, 2442(1973).
204. Allegrini, I. and Omenetto, N., *Environ. Sci. Tech.*, 13, 349(1979).
205. Tucker, A. W., Peterson, A. B., and Birnbaum, M., *Appl. Opt.*, 12, 2036(1973).
206. Clyne, M. A. A., McDermind, I. S., and Curran, A. H., *J. Photochem.*, 5, 201(1976).
207. Imasaka, T., Ogawa, T., and Ishibashi, N., *Bunseki Kagaku*, 26, 96(1977).
208. Heaps, W. S., *Appl. Opt.*, 19, 243(1980).
209. Measures, R. M., Houston, W. R., and Stephenson, D. G., *Opt. Eng.*, 13, 494(1974).
210. Measures, R. M., Houston, W., and Bristow, M., *Can. Aeronaut. Space J.*, 19, 501(1973).
211. O'Neil, R. A., Baja-Bijunas, L., and Raynes, D. M., *Appl. Opt.*, 19, 863(1980).
212. Visser, H., *Appl. Opt.*, 18, 1746(1979).
213. Capelle, G. A. and Francks, L. A., *Appl. Opt.*, 18, 3579(1979).
214. Boutilier, G. D. and Winefordner, J. D., *Anal. Chem.*, 51, 1384(1979).
215. Boutilier, G. D. and Winefordner, J. D., *Anal. Chem.*, 51, 1391(1979).
216. Boutilier, G. D., Ph.D. thesis, University of Florida, Gainesville, 1978.
216a. Crosley, D. R., Ed., Laser Probes for Combustion Chemistry, American Chemical Society Ser. 134(1980).
217. Tobin, M. C., *Laser Raman Spectroscopy*, John Wiley & Sons, New York, 1971.
218. Anderson, A., Ed., *The Raman Effect*, Marcel Dekker, New York, 1971.
219. Konigstein, J. A., *Introduction to the Theory of the Raman Effect*, Reidel, Dordrecht, Holland, 1972.
220. Harvey, A. B., McDonald, J. R., and Tolles, W. M., *Progress in Analytical Chemistry, Vol. 8*, Simmons, I. L. and Ewing, G. W., Ed., Plenum Press, New York, 1976.
221. Eesley, G. L., *J. Quant. Spectrosc. Radiat. Transfer*, 22, 507(1979).
222. McNice, G. T., *Appl. Opt.*, 11, 699(1972).
223. Cunningham, K. M., Goldberg, M. C., and Weiner, E. R., *Anal. Chem.*, 49, 70(1977).
224. Bell, M. I. and Tyte, R. N., *Appl. Opt.*, 13, 1610(1974).
225. Kato, D., *J. Appl. Phys.*, 47, 1072(1976).
226. Hoskins, L. C. and Alexander, V., *Anal. Chem.*, 49, 695(1977).
227. Van Haverbeke, L., Lynch, P. F., and Brown, C. W., *Anal. Chem.*, 50, 315(1978).
228. Van Haverbeke, L. and Hernian, M. A., *Anal. Chem.*, 51, 932(1979).
229. Morris, M. D., *Anal. Lett.*, 9, 469(1976).
230. Rahman, M. S. and Morris, M. D., *Talanta*, 23, 65(1976).
231. Suchanski, M. R. and Van Duyne, R. P., *J. Am. Chem. Soc.*, 98, 250(1976).
232. Harris, J. M., Chrisman, R. W., Lytle, F. E., and Tobias, R. S., *Anal. Chem.*, 48, 1937(1976).
233. Woodruff, W. H. and Farquharson, *Anal. Chem.*, 50, 1391(1978).
234. Funfschilling, J. and Williams, D. F., *Appl. Spectrosc.*, 30, 443(1976).
235. Barrett, J. J. and Adams, N. I., *J. Opt. Soc. Am.*, 58, 311(1968).
236. Barrett, J. J. and Myers, L., *J. Opt. Soc. Am.*, 61, 1246(1971).
237. Hercher, M., Mueller, W., Klainer, S., Adamowicz, R. F., Myers, R. E., and Schwartz, S. E., *Appl. Spectrosc.*, 32, 298(1978).
238. Jones, W. J. and Stoicheff, B. P., *Phys. Rev. Lett.*, 13, 657(1964).
239. Yeung, E. S., *J. Mol. Spectrosc.*, 53, 379(1974).
240. Owyoung, A., *Opt. Commun.*, 22, 323(1977).
241. Owyoung, A. and Jones, E. D., *Opt. Lett.*, 1, 152(1977).
242. Owyoung, A., *IEEE J. Quantum Electron.*, 14, 192(1978).
243. Morris, M. D., Wallen, D. T., Ritz, G. P., and Haushalter, J. P., *Anal. Chem.*, 50, 1796(1978).
244. Haushalter, J. P., Ritz, G. P., Wallen, D. J., Dien, K., and Morris, M. P., *Appl. Spectrosc.*, 34, 144(1980).
245. Levine, B. F. and Bethea, C. G., *IEEE J. Quant. Electron.*, QE-16, 85(1980).
246. Eckbreth, A. C., Bonczyk, P. A., and Verdieck, J. F., Review of Laser Raman and Fluorescence Techniques for Practical Combustion Diagnostics, Technical Report R77-952665-6, United Technologies Research Center, East Hartford, Conn., 1977.
247. Eckbreth, A. C., Bonczyk, P. A., and Shirley, J. A., Investigation of Saturated Laser Fluorescence and CARS Spectroscopic Techniques for Combustion Diagnostics, EPA-600/7/78-104, June 1978.
248. Eckbreth, A. C., Bonczyk, P. Z., and Verdieck, J. F., *Appl. Spectrosc. Rev.*, 13, 15(1978).
249. Eckbreth, A. C., AIAA Paper No. 76-27, 1976.
250. Harvey, A. B. and Nibler, J. W., *Appl. Spectrosc. Rev.*, 14, 101(1978).
250a. Regnier, P. R. and Taran, J. P. E., *Appl. Phys. Lett.*, 23, 240(1973).

251. Regnier, P. R., Moya, F., and Taran, J. P. E., *AIAA J.*, 12, 826(1974).
252. Tolles, W. M., Nibler, J. W., McDonald, J. R., and Harvey, A. B., *Appl. Spectrosc.*, 31, 253(1977).
253. Roh, W. B., Schreiber, P. W., and Taran, J. P. E., *Appl. Phys. Lett.*, 28, 174(1976).
254. Barrett, J. J. and Begley, R. F., *Appl. Phys. Lett.*, 27, 129(1975).
255. Rogers, L. B., Stuart, J. D., Goss, L. P., Malloy, T. B., and Carreira, L. A., *Anal. Chem.*, 49, 959(1977).
256. Hudson, B., Hetherington, W., Cramer, S., Chabay, I., and Klauminzer, G. K., *Proc. Natl. Acad. Sci. U.S.A.*, 73, 3798(1976).
257. Tolles, W. M. and Turner, R. D., *Appl. Spectrosc.*, 31, 96(1977).
258. Chabay, I., Klauminzer, G. K., and Hudson, B. S., *Appl. Phys. Lett.*, 28, 27(1976).
259. Delhaye, M. and Dhamelincourt, P., *J. Raman Spectrosc.*, 29, 396(1975).
260. Delhaye, M. et al., Proc. 5th Int. Conf. Raman Spectrosc., Freiburg, Germany, 1976.
261. Delhaye, M., DeSilva, E., and Hayat, G. S., *Am. Lab.*, April, 83(1977).
262. Dhamelincourt, P., Wallart, F., Leclercq, M., N'Guyen, A. T., and Landon, D. O., *Anal. Chem.*, 51, 414A(1979).
263. *L'Actualité Chimique*. April, (1980).
264. Blaha, J. J., Rosasco, G. J., and Etz, E. S., *Appl. Spectrosc.*, 32, 292(1978).
265. Rosasco, G. J. and Etz, E. S., *Res. Dev.*, June, 20(1977).
266. Rosasco, G. J., Etz, E. S., and Cassatt, W. A., *Appl. Spectrosc.*, 29, 396(1975).
267. Leonard, D. A., Caputs, B., and Hoge, F. E., *Appl. Opt.*, 18, 1732(1979).
268. Patel, C. K. N., *Philos. Trans. R. Soc. London Ser. A*, 293, 257(1979).
268a. Lapp, M. and Penney, C. M., *Laser Raman Gas Diagnostics*, Plenum Press, New York, 1974.
269. Chabay, I., Rosasco, G. J., and Kashiwaji, T., *J. Chem. Phys.*, 70, 4149(1979).
270. Blint, R. J., Bechtel, J. H., and Stephensen, D. A., *J. Quant. Spectrosc. Radiat. Transfer*, 23, 89(1980).
271. Eckbreth, A. C., *Appl. Opt.*, 18, 3215(1979).
272. D'Orazio, M., *Appl. Spectrosc.*, 33, 278(1979).
273. Gober, B. P., *Am. Lab.*, March, 15 (1977).
274. Datta, P. K., Nester, J. R., and Spiro, T. G., *Proc. Natl. Acad. Sci. U.S.A.*, 74, 4146(1977).
275. Ahmadjian, M. and Brown, C. W., *Anal. Chem.*, 48, 1257(1976).
276. Webster, C., *New Sci.*, February, 383(1977).
277. Patel, C. K. N. and Shaw, E. D., *Phys. Rev. Lett.*, 24, 451(1970).
278. Kreuzer, L. B. and Patel, C. K. N., *Science*, 173, 45(1971).
279. Patel, C. K. N., Burkhardt, E. G., and Lambert, C. A., *Science*, 184, 1173(1974).
280. Burkhardt, E. G., Lambert, C. A., and Patel, C. K. N., *Science*, 188, 1111(1975).
281. Patel, C. K. N., *Opt. Quantum Electron.*, 8, 145(1976).
282. Shtrickman, S. and Slatkine, M., *Appl. Phys. Lett.*, 31, 830(1977).
283. Kritchman, E., Shtrickman, S., and Slatkine, M., *Bull. IPS*, 23, 97(1977).
284. Schnell, W. and Fisher, G., *Opt. Lett.*, 2, 67(1978).
285. Kerr, E. L. and Atwood, J. G., *Appl. Opt.*, 7, 915(1968).
286. Kamm, R. D., *J. Appl. Phys.*, 47, 3550(1976).
287. Deavey, C. F., Kamm, R. D., and Hackett, C. E., *Appl. Phys. Lett.*, 23, 633(1973).
288. Konjevic, N. and Jovicevic, S., *Spectrosc. Lett.*, 12, 259(1979).
289. Claspy, P. C., Ha, C., and Pao, Y. H., *Appl. Opt.*, 16, 2972(1977).
290. Siebert, D. R., West, G. A., and Barrett, J. J., *Appl. Opt.*, 19, 53(1980).
291. Lahmann, W., Ludewig, H. J., and Welling, H., *Anal. Chem.*, 49, 549(1977).
292. Patel, C. K. N. and Tam, A. C., *Appl. Phys. Lett.*, 34, 467(1979).
293. Tam, A. C., Patel, C. K. N., and Kerl, R. J., *Opt. Lett.*, 4, 81(1979).
294. Patel, C. K. N. and Tam, A. C., *Nature*, 280, 302(1979).
295. Tam, A. C. and Patel, C. K. N., *Nature*, 280, 5720(1979).
296. Patel, C. K. N. and Tam, A. C., *Appl. Phys. Lett.*, 34, 760(1979).
297. Tam, A. C. and Patel, C. K. N., *Appl. Opt.*, 18, 3348(1979).
298. Oda, S., Sawada, T., Moriguchi, T., and Kamada, H., *Anal. Chem.*, 52, 650(1980).
299. Sawada, T., Oda, S., Shimizu, H., and Kamada, H., *Anal. Chem.*, 51, 688(1979).
300. Oda, S., Sawada, T., Nomura, M., and Kamada, H., *Anal. Chem.*, 51, 686(1979).
301. Hurst, G. S., Payne, M. P., Nayfeh, M. H., Judish, J. P., and Wagner, E. B., *Phys. Rev. Lett.*, 35, 82(1975).
302. Frueholz, R., Wessel, J., and Wheatley, E., *Anal. Chem.*, 52, 281(1980).
303. Brophy, J. H. and Rettner, C. T., *Opt. Lett.*, 4, 337(1979).
304. Feldman, D., *Opt. Commun.*, 29, 67(1979).
305. Hurst, G. S., Nayfeh, M. H., Young, J. P., *Appl. Phys. Lett.*, 30, 229(1977).

306. Hurst, G. S., Nayfeh, M. H., and Young, J. P., *Phys. Rev. A*, 15, 2283(1977).
307. Hurst, G. S., Payne, M. G., Kramer, S. D., and Young, J. P., *Rev. Mod. Phys.*, 51, 767(1979).
308. Hurst, G. S., Payne, M. G., Kramer, S. D., and Chen, C. H., *Phys. Today*, September, (1980).
309. Fairbank, W. M., Jr. and She, C. Y., *Opt. News*, Spring, 4(1979).
310. Falk, H., *Prog. Anal. At. Spectr.*, 3, 181(1980).
311. IUPAC, Nomenclature, Symbols and Units, II, Analytical Chemistry Division, IUPAC, 1975.
312. Morgan, C. G., *Chem. Soc. Rev.*, 8, 367(1979).
313. Alkemade, C. Th. J., To Catch a Single Atom, Plenary Lecture, 6th FACSS Meet., Philadelphia, 1979.
314. Winefordner, J. D., Svoboda, V., and Cline, L. J., *CRC Crit. Rev. Anal. Chem.*, 1, 233(1970).
315. L'vov, B. V., *Spectrochim. Acta*, 33B, 153(1978).

Offprints from:
Analytical Applications of Lasers
Edited by Edward H. Piepmeier

CHAPTER

4

DETECTION OF SMALL NUMBERS OF ATOMS AND MOLECULES

C. TH. J. ALKEMADE

Physical Laboratory of the State University
Princetonplein 5,
Utrecht, The Netherlands

1. INTRODUCTION AND SCOPE

1.1. Selectivity and Detectability

Free atoms, ions, molecules, or radicals (all of which will usually be referred to as *atoms* for simplicity) of a given chemical species can interact with an optical radiation field at certain wavelengths that are characteristic for that species (Chapter 1). By selecting radiation at a characteristic wavelength, we can thus tag these atoms and distinguish them from other species. The signal produced by the interaction is then a measure for the number of atoms of the selected species. This is the very basis of quantitative analytical spectroscopy. Tunable optical lasers (Chapter 1) are beneficial for improving the selectivity of analysis (because of their small spectral bandwidth) as well as the detectability (because of their high radiant power). Especially in diagnostic applications their directionality is an extra bonus for obtaining high spatial resolution, whereas high temporal resolution can be achieved with pulsed lasers of extremely short duration. In this chapter we shall be mainly interested in the capability of lasers to push the detectability toward the ultimate limit set by the discrete nature of matter. The improvement of the spectral selectivity as such will not be considered, unless detectability is intimately connected with selectivity, as in the detection of rare isotopes in a mixture.

The detectability is characterized by the analytical *limit of detection* (*LOD*), which is defined as that concentration, c_m, or quantity of substance, q_m, in the sample, which produces a mean signal equal to k times the root-mean-square (rms) random error (1). A LOD expressed in concentration units (e.g., mol/L, μg/mL) is called a *concentrational limit of detection*, whereas in the other case we shall speak of the *absolute limit of detection* (e.g., in pg). The *statistical confidence factor* k is usually 3. We distinguish here between two categories of random errors. On the one hand, there are errors arising from extrinsic sources of fluctuations, such as fluctuations in the background (produced by concomitants in the sample, by the atomizer, or by scattering of laser radiation), fluctuations in the laser power or in the efficiency of atomization, and detector or amplifier noise. On the other hand, there is an intrinsic error in the signal itself, arising from the discrete nature of matter: First, the number of analyte atoms found in the sample or atomizer will fluctuate around a mean (or expectation) value in a manner described by Poisson statistics. Second, the detection process (e.g., the absorption of a discrete photon and the subsequent release of a photoelectron) is a chance process. The resulting error, which becomes relatively more important for smaller numbers of atoms and detected photons, determines the *intrinsic limit of detection*. This is the ultimate LOD obtainable with a given setup if all extrinsic fluctuations are suppressed. We are, technically, still far from the ideal of complete *atomization* (= conversion of analyte in the sample to free atoms) and complete *probing* (= counting of free atoms). Therefore, we shall define the intrinsic LOD as related to the statistical fluctuation in the number of free atoms being *probed* and *not* in the number of analyte atoms in the *sample*.

1.2. Single-Atom Detection (SAD)

Even under favorable measuring conditions, "conventional" atomic spectrometers (with or without lasers) yield LODs that are set by extrinsic errors. The best absolute LOD, as reported in Table 2.14 and in Omenetto and Winefordner (2) for laser-excited atomic fluorescence (AFS) and atomic absorption spectrometers (AAS) with electrothermal atomizers, are about 0.1 and 1 pg, respectively. If we assume complete atomization, these quantities correspond to a total number of about 10^9–10^{10} free atoms (of median relative atomic mass) in the atomizer. Even if we assume a probe volume, V_p, as small as 1 mm^3 and an (effective) atomizer volume, V_a, as large as 10^4 mm^3, the number of free atoms being probed (counted) at the LOD level is still 10^5 or higher. According to theoretical estimates this number is even expected to be at least 10^7 when conventional AAS is applied with a tube atomizer of 1 mm diameter (3).

The best experimental concentrational LODs found in AFS with flames or inductively coupled plasmas (ICP), using conventional as well as laser sources, are typically 0.1 ng/mL in aqueous solutions [Table 2.13 and (2, 4)]. Assuming V_p to be as small as 1 mm^3 in the flame, this LOD value would still correspond to at least 10^3 free atoms being probed. The best experimental concentrational LODs found in laser-enhanced ionization spectroscopy (LEIS) using flames combined with a premixed or total consumption burner are typically 0.01 ng/mL (Tables 3.1 and 2.13). Assuming $V_p = 10^2$ mm^3, the number of free atoms being probed at the LOD level is then estimated to exceed 10^4.

These rough estimates demonstrate clearly that the number of analyte atoms, N_p, probed in conventional laser-based spectrometers at the LOD level is still so high that its relative statistical fluctuation ($1/\sqrt{N_p}$) is irrelevant. The situation is typically different if we apply special laser-based spectrometers that are capable of probing *small numbers* of free atoms. This requires the signal produced by an individual atom or small group of atoms to become detectable above background and detector noise. In the former case we shall speak of *single-atom detection* (*SAD*) [occasionally also called one-atom detection, OAD (5)]. Although such techniques have been developed mostly for atoms in the strict sense of the word, we shall use the term *SAD* more generally to relate to free ions, molecules, or radicals as well. Similar generalizations will be made as to the meaning of terms like *atomizer* and *atomic spectroscopy*. When we want to refer specifically to free molecules, the term *single-molecule detection (SMD)* will be used.

An SAD technique meets, ideally, the following demands:

1. *Each* (not just *a*!) free analyte atom present in or crossing the probe volume V_p during probing time T is detected and registered as one, and only one count with 100% statistical confidence.
2. The detection is *selective* as to the atomic species sought. Other species in the sample (concomitants) are not detected and do not interfere with the probability of detecting a given free analyte atom. Interferences caused by other species that can be compensated in the calibration procedure are allowed, such as ionization interference and interference with the atomization of the analyte.
3. *No false signals* (counts) are produced by the background originating from the atomizer (e.g., flame background, thermal radiation from furnace walls, scattering of laser radiation) or by the detector and amplifier (e.g., dark current, spurious electric pulses).
4. The *LOD* and *precision* of the analysis are solely determined by the Poisson statistics of the free analyte atoms present in or crossing V_p during T.

This concept of SAD thus relates to the free atoms appearing *in the probing region*, where they can interact with the laser beam and be observed by the detector. With a given atomizer, the realization of SAD will depend upon the region selected. We should distinguish this restrictive SAD concept from the general SAD concept relating to the detection of a single analyte atom present *in the sample* (usually in a bound state). The latter is the ultimate goal (and absolute limit!) in chemical analysis as far as detectability is concerned. This goal is still so unrealistic that we will confine ourselves to SAD in the restricted sense.

Sophisticated, laser-based techniques have been developed during the last decade to detect smaller and smaller numbers of atoms in the gas phase. Species investigated were most often metallic atoms or ions such as the alkalis, Pb, Yb, Ba, Ba^+, and Mg^+ (with Na as "topper"; see also Section 3) and occasionally noble-gas atoms (6–8). However, the ideal experimental conditions under which SAD conditions have been (approximately) attained were mostly aimed at special applications, with "pure" samples, in physics and chemistry. These conditions are quite different from those encountered in analytical spectroscopy dealing with real-world samples.

Applications in fundamental as well as applied physics and chemistry are connected, for example, with the search for rare or short-lived species (produced, e.g., by nuclear reactions) or for rare events induced by solar neutrinos captured in radiochemical detectors (5, 9–14). SAD techniques have also been proposed (15) for demonstrating the possible existence of Na-quark atoms (having a fractionally charged quark attached to the nucleus) amidst 10^{14} normal Na atoms per cubic centimeter. Another example is the measurement of saturated vapor pressures at low temperatures (15). Other applications concern the ultra high-resolution spectroscopy of rare isotopes (16, 17) and the kinetic or statistical behavior of individual atoms in a gas (5, 18, 19). SAD techniques were also applied in the diagnostics, with high spatial and temporal resolution, of plasmas or reaction systems containing ultratrace concentrations of atoms of given species or in specific excited states (12). SAD was further applied in the experimental verification of the antibunching statistics of the photons that are spontaneously emitted by a single atom excited by a strong radiation field (20–23). In Section 3 a few of these applications will be described in more detail.

1.3. Scope of Chapter

For the analytical spectroscopist who wants to detect smaller and smaller numbers of atoms, the development of these SAD techniques is both a challenge and an opportunity. We shall therefore review in this chapter the main streams of UV-visible laser-based spectroscopies that are most promising to detect small numbers of atoms in the gas phase. Techniques that are (primarily) aimed at ultra high-resolution spectroscopy, isotope separation, or remote sensing will not be considered. The use of high-powered lasers to vaporize, atomize and, possibly, excite or ionize analytical samples will not be discussed either (Chapter 19).

For completeness' sake we note that there exist also nonoptical techniques that can be applied, with special arrangements, to detect, localize, and/or identify individual atoms or ions in the solid or gas phase. Examples are the scanning transmission electron microscope, the field ion microscope ("imaging atom probe") and the accelerator mass spectrometer (which combines a nuclear accelerator with a mass spectrometer).

A good question is, how small is "a small number" in the title of this chapter. No sharp borderline can be drawn. Broadly speaking, we shall focus on those techniques that do allow us to count atoms (not just photons or electrons!) or the results of which are best discussed in terms of atom numbers. However, we shall generously include, for comparison, more conventional laser-based techniques that have successfully been applied in spectrochemistry to yield very low LODs. We shall also bring out some of the best LODs that have been obtained for molecular species with laser-based techniques. This will be done to underline how much farther we still are away from SMD (13, 24–28) than from SAD.

In the following we shall often borrow, by analogy, terms from analytical atomic spectroscopy, when we describe techniques that were not aimed at chemical analysis proper. The meaning of such terms (such as analyte, analysis, atomizer, sample, limit of detection) when applied, for example, to diagnostic techniques, may be evident from the context.

Several laser-based techniques and laser-induced processes are dealt with in other chapters too. We shall occasionally refer to them for a more detailed discussion. LODs are also discussed or tabulated in these other chapters. Our interest, however, is focused on the lower end of the LOD range. In several respects this chapter is thus a cross section through other chapters: repetition could not always be avoided.

With regard to the fast development and great variety of laser-based detection

techniques in widespread areas of physics and chemistry, this review can by no means be exhaustive or profound. We shall rather concentrate on simple basic concepts, with only a few, oversimplified formulas, and on general detection schemes (Sections 2 and 3.1). These will be illustrated in Sections 3.2–4 by concrete examples and by experimental data in tabular form.

For further information and more extensive references to the literature, the reader may consult a blend of review papers or book chapters: (2, 27, 29) (mainly fluorescence techniques), (5, 14, 30–33) (mainly ionization techniques), and (3, 13, 26, 34–39) (general).

Terms, definitions, and symbols of the main quantities used are collected in Table 4.1.

2. FROM SAMPLE TO SIGNAL: GENERAL CONSIDERATIONS

2.1. Schematic Layout of Laser-Based Spectrometer

The "atoms" of the species to be detected are produced from a *sample* (Fig. 4.1). The liquid, solid, or gaseous sample may contain these atoms in any chemical state or state of ionization. Their conversion to *free* atoms in the gas phase (*atomization*) takes place in the *atomizer*. The atomizer includes the "atom reservoir" containing the free atoms available for probing.

We distinguish between *continuous-flow atomizers* and *closed atomizers*. Examples of the former class in analytical atomic spectroscopy are the flame and the inductively coupled plasma (ICP), in combination with a pneumatic nebulizer for converting a liquid sample into an aerosol (Fig. 4.2a). Volatilization of the aerosol particles and subsequent dissociation of the analyte compounds occur in the carrier gas heated by combustion or the electric discharge. The

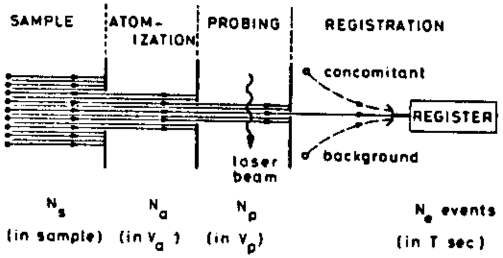

Fig. 4.1. Schematic layout of laser-based spectrometer.

Table 4.1. Symbols, Terms, and Definitions

Symbol	Term and Definition[a]
c_s (c_m)	(Minimum detectable) sample concentration
k	Statistical confidence factor
N_a	Number of free atoms in atomizer
n_a	Number density (= number per unit volume) of free atoms in atomizer
N_e	Number of events at detector during T
N_p	Number of free atoms in V_p
N_s	Number of analyte entities in consumed sample (one free atom derives from one entity)
R	Number of repeated probings
T	Probing time (= duration of a single probing by laser)
t	Time (general)
t_a	Atomization time (= duration of atomization needed for a single probing with a continuous-flow atomizer)
t_m	Total time of measurement for R repeated probings
V_a	Atomizer volume (= volume of closed atomizer or fictitious volume of continuous-flow atomizer; see Section 2.4)
V_p	Probe volume [= (effective) volume irradiated by laser and "observed" by detector]
ϵ_a	Atomization efficiency (= N_a/N_s)
ϵ_d[b]	Detection efficiency (= probability that a given free atom appearing in V_p produces an event during T)
ϵ_o	Overall efficiency (= N_e/N_s)
ϵ_p	Probing efficiency ($\epsilon_p \cdot N_a$ = number of free atoms present in or passing through V_p during T)
ϕ	Flux (= number per second) of detected photons or ions (electrons) produced by N_p atoms, divided by N_p
τ	Transit or residence time
$\bar{x}$	Mean (or expectation) value of x
$(x)_m$	Value of x at limit of detection
s	Standard deviation of x [= $\sqrt{\overline{(\Delta x)^2}}$]
	General Abbreviations
LIBDS	Laser-induced beam deflection spectroscopy
LIFS	Laser-induced fluorescence spectroscopy
LIIS	Laser-induced ionization spectroscopy
LOD	Limit of detection
SAD	Single-atom detection
SMD	Single-molecule detection

[a] By generalization, *atom* is the selected chemical species of any kind (atom, ion, molecule, or radical) that interacts with the laser radiation. As a result of this interaction, an *event* may be produced at the detector. *Atomizer* is any device that produces these "atoms" in the gas phase (so-called *free* atoms) from the sample.

[b] In (39) symbol ϵ was used for ϵ_d. This definition of ϵ_d should not be confused with the efficiency of detecting a (fluorescence) *photon*.

---

open-ended graphite tube and the carbon-rod and carbon-filament atomizers (with pulsed atomization of minute samples), operating with a carrier gas flow, belong to this class, too. A quite different type of continuous-flow atomizer, especially suited for SAD, is the atomic beam (Fig. 4.2b). Here atoms produced, for example, in a furnace containing a metallic sample, effuse through a small hole into a vacuum chamber. Collimation of the atomic beam is achieved by means of a diaphragm placed downstream from the effusive flow.

An example of a closed atomizer is a cuvette filled with a gaseous sample or a cell containing a solid or liquid sample (Fig. 4.2c). The sample may be atomized by thermal or Langmuir evaporation, by atom sputtering in a glow discharge, or by bombardment with a fast-ion beam (in vacuo). In order to simplify our later discussions we shall assume that probing takes place after the sample has been atomized and the atoms have spread more or less uniformly over the atomizer volume. The cuvette or cell is equipped with windows for admitting the laser beam (and for observation in LIFS). The cell may or may not contain a buffer gas. Another example, especially suited for SAD, is the more recently developed *ion* or (neutral) *atom trap* (Fig. 4.2d). Here a few ionized or neutral atoms are trapped in a small confinement in vacuo and stored. This may be realized by means of a rf quadrupole field, an electromagnetic field

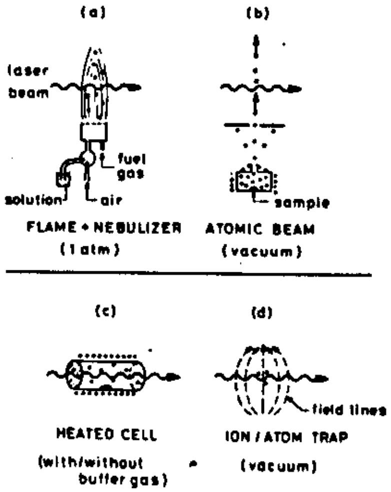

Fig. 4.2. Examples of a continuous-flow atomizer (a and b) and a closed atomizer (c and d).

with appropriate gradients, and/or optical trapping by laser radiation pressure (40–49).

An example of a Ba^+ trap will be described in Section 3.2. The "translational temperature" of the trapped atoms or ions can be reduced to below 10 K by laser cooling. This cooling is brought about by repetitive exchange of linear momentum between the atom and the photons absorbed from a monochromatic laser beam. The atom suffers a net loss of linear momentum after each excitation-emission cycle, if the laser frequency is tuned slightly below the atomic resonance frequency. The resulting reduction of the Doppler broadening of the atomic line and the absence of collision broadening make these traps an attractive atom reservoir for ultra high-resolution spectroscopy and for achieving high spectral selectivity in analysis. A well-collimated atomic beam, if directed perpendicular to the laser beam, offers similar advantages. In this respect, atomic beams and traps are far superior to atom reservoirs filled with a buffer gas at atmospheric pressure at or above room temperature.

It is not always possible to draw a sharp borderline between closed and continuous-flow atomizers. An open-ended tube furnace may be an intermediate case, depending on the chance the atoms have to flow out after being atomized.

The next stage in any laser-based spectrometer is the *probing* of the atoms by one or more laser beam(s) crossing the atomizer and their final *registration* (Fig. 4.1). The advantages and disadvantages of using continuous-wave (cw) or pulsed lasers depend strongly on the detection scheme chosen, the species to be detected, and the need for suppressing interferences from concomitants or background (Section 3).

2.2. Laser Probing of Atoms

The presence of a free atom of a given species is probed by the absorption of one or more photons from the laser beam(s), resulting in the production of a photophysical or photochemical effect.

The *photophysical effect* may be *optical*, *electrical*, or *mechanical* (Fig. 4.3). Here we present a few examples for introduction only. (A more detailed classification and description, especially with regard to SAD, will be given in Section 3.1.) The spontaneous emission of a secondary photon by the atom after laser excitation (fluorescence) is an obvious example of an optical effect (Fig. 4.3a). Any detection technique based on this effect is called here *laser-induced fluorescence spectroscopy* (*LIFS*). (Note that in Chapter 2 it is called laser-excited fluorescence.) The frequency of the fluorescence photons may be the same as that of the laser photons (ν) or different (ν'). We distinguish accordingly between *resonance* and *nonresonance fluorescence* (for a finer distinction, see Fig. 2.1).

The fluorescence photons are emitted in all directions (but not necessarily

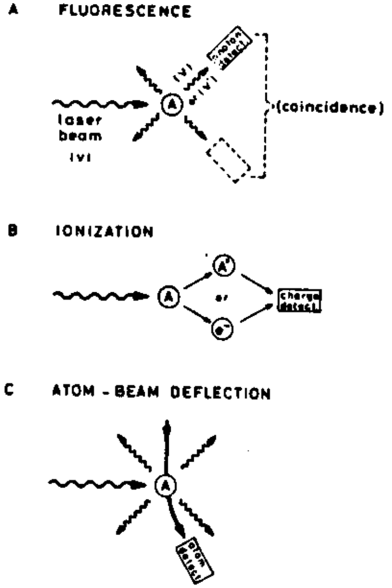

Fig. 4.3. Examples of optical (A), electrical (B), and mechanical (C) laser probing. Ⓐ is the free atom or molecule probed.

isotropically if a polarized laser beam is used). So the photodetector may be positioned at an arbitrary direction of observation, preferably with a large solid angle of acceptance. Since often a monochromator is not needed (a spectral filter may suffice to select one of the few fluorescence lines or to reject laser scattering if $\nu \neq \nu'$), the angle of acceptance can be made quite large by suitable optical arrangements (Section 3.2). A weak resonance fluorescence signal can be discriminated from laser scattering by application of a photon coincidence technique with the aid of a second photodetector (Fig. 4.3a, Section 3.2). If optical saturation (Chapter 1) is attained, a given atom may produce, on the average, at least one photoelectron in each detector during its (short) passage through the laser beam. If the coincidence interval is matched to the passage time, fluorescence photons, occurring in bunches, will have a greater probability of causing a coincidence signal than the randomly received scattered photons.

In the case of Fig. 4.3b, absorption of one or more photons from one or more laser beams results in the production (directly or indirectly; Section 3.1) of an ion and a free electron. These can be directed by an electric or magnetic field to a charge or particle detector. This type of atom detection technique will here be generally called *laser-induced ionization spectroscopy* (*LIIS*).

In the case of Fig. 4.3c, an atom moving in a direction perpendicular to the laser beam acquires transversal linear momentum by absorbing a laser photon. The net recoil effect resulting from multiple absorption-spontaneous emission cycles in the atom deflects its trajectory from the atomic beam axis, in the direction of travel of the laser beam. A particle detector placed off-axis and downstream of the atomic beam counts the atoms that are selectively deflected by the laser. This example of *laser-induced beam deflection spectroscopy* (*LIBDS*) is thus typically based on a mechanical effect produced by atom–laser interaction; LIBDS has not yet been exploited for SAD, but it may have good potentialities in special applications (13, 34). It has until now been mainly considered as a selective separation technique. We have included LIBDS in this review to stress that SAD might be realized by other than optical or electrical techniques, too.

Neutral atoms of low ionization energy can be detected by surface ionization when they impinge on a hot metal wire. The positive ions leaving the surface are accelerated and directed to an ion multiplier tube, where they produce pulses of secondary electrons.

Photochemical effects have so far but seldom been considered for use in SAD or SMD, in contrast to their exploitation in isotope separation. The feasibility of detecting single alkali–halide molecules by laser-induced photodissociation and LIIS detection of the alkali product has been suggested (5, 50).

As a result of its interaction with laser radiation, the atom undergoes a "process," that is, a change or series of changes in its state or motion. A *general characterization of a laser-induced process* is presented in Table 4.2. A process can be characterized as to (I) the final state of the atom, (II) the type of cyclic process, and (III) the multiplicity of recycling. In LIFS, case Ia may apply, for example, when one of the Na-*D* doublet components is excited by the laser. After excitation the atom returns, directly or indirectly, to the initial (ground) state, thus completing a cycle. An *intraatomic* cycle (case IIa) can take place via different routes: by spontaneous or stimulated emission, and by inelastic collisions leading to "quenching" of the excited state or "population mixing" of the doublet states (51) (Table 2.1). A *regenerative* cycle (case IIb) takes place when, for example, in a flame the laser-excited Na atom becomes first ionized or bound in a molecule before it returns to the initial state by recombination with a free electron or by dissociation. If the probing time (Table 4.1) is long enough, the atom may undergo more than one excitation–deexcitation cycle (case IIIa). We may distinguish between the multiplicities of recycling via different routes.

Case Ib applies, for example, when Na atoms in a beam are excited by a narrow-band laser tuned to a particular hyperfine structure (hfs) transition and directed perpendicular to the atomic beam to avoid Doppler broadening. Optical selection rules permitting, the excited Na atom may return to a hyperfine (hf) component of the gound state different from the initial one. As long as it stays there, it cannot be excited again (unless the spectral wing of the associated hf line overlaps with the spectral laser profile). By this "consumptive" process the atom is taken out of circulation. Case Ib is also found when the excited atom becomes trapped by making a spontaneous transition to a metastable level. The atom is then "consumed," unless it is released from the trap by an inelastic collision or by a second excitation step to a higher lying nonmetastable level, using an additional laser. A more general discussion of atom trapping to inaccessible levels is presented in (13, 34, 36, 52). In LIIS, atom consumption naturally occurs, as the ionized atom is removed from the laser interaction region, being captured by an electrode. In principle, it is feasible to release the atom again from the electrode, so that it can return in time to the laser interaction region (case IIb) (34).

When a flame is used as atomizer, this "regeneration" could be realized by immersing the cathode in the flame, near to the laser beam. Regenerative recycling could also be achieved in LIIS when the ionized analyte atom A^+ transfers its charge, by collision, to a different particle M whose ionization

Table 4.2. General Characterization of a Laser-Induced Process[a]

I. As to *final state of the atom*:	
a. *Cyclic process* Atom returns directly or indirectly to initial state in the probe volume within probing time	b. *Consumptive process* Atom does not return to initial state and/or is removed from probe volume
II. As to *type of cyclic process*:	
a. *Intraatomic cycle* Atom returns to initial state in the probe volume without changing its chemical state or state of ionization	b. *Regenerative cycle* Atom returns to initial state and to probe volume after a transitory change in chemical state or state of ionization or in position
III. As to *multiplicity of recycling*:	
a. *Multiple recycling* Atom undergoes more than one interaction cycle during probing time	b. *Single cycling* Atom undergoes no more than one interaction cycle during probing time

[a] We consider here processes that take place in one and the same atom interacting with laser radiation during a single probing. "Initial state" is here defined as the state in which the atom can interact with laser radiation.

energy is lower than that of A. These particles are supposed to have been admixed at a sufficiently large concentration to ensure efficient charge transfer. The M^+ ions and/or free electrons are detected, whereas A is again available for laser ionization. If this recycling process is repeated many times during the probing time (case IIIa), one obtains a considerable amplification of the electric signal produced by one atom A. This is the basis of the resonance ionization spectroscopy with amplification (RISA) proposed in (12); it would be attractive for SAD.

Consumptive interaction processes (case Ib) may have the advantage of preventing a given atom from being counted twice. In the analytical application of laser-enhanced ionization in flames they may have the additional advantage that the resulting depletion of free atoms, such as Li, brings about a shift in the partial equilibrium between atomic Li and LiOH (51, 53). This shift replenishes (partly) the Li atoms consumed in the laser ionization process. This holds at least if the probing time is long enough compared to the equilibration time of the Li ↔ LiOH reaction. This replenishment might be retarded, however, by the enhanced tendency of laser-excited alkali atoms to form monohydroxides (54–56). (Laser excitation of alkali atoms is an intermediate step in LEIS.)

2.3. Counting of Atoms in the Probe Volume; Detection Efficiency

An atom interacting with the laser beam(s) may produce an *event* in the detector that carries one-bit information about its appearance in the probe volume. In LIFS the event may be the emission of just a single photoelectron or a burst of photoelectrons in one photodetector, or it may be the coincidence between such emissions in two photodetectors (Fig. 4.3a). In LIIS the event may be the capture of an ion (or primary electron) by the collector plate or the ion (electron) multiplier.

After internal and/or external amplification the event is registered as a count or current pulse. The *total number of events*, N_e, occurring in a single probing with probing time T can be found by accumulating the counts, or by integrating the current pulses. If T is long, one can also record the count rate or detector output current as a function of time, smoothed by the recorder time constant. Integration over T then yields a measure for N_e. The statistical error can be improved if one repeats the probing R times (Section 2.6). The total time taken for R repeated probings is here called the (*total*) *time of measurement* t_m.

With a pulsed laser, the *probing time* T is determined by the pulse duration or the width of the time gate in case a time-gating circuit is applied, whichever is the shorter. Multiple probings are obtained by firing laser shots at *repetition frequency* f_{rep}. By means of a boxcar integrator and a smoothing circuit, the count rate or output current can then be recorded as a function of time and averaged or integrated over t_m. With a cw laser (whether or not intensity modulated) T is determined by the duration of one uninterrupted observation run. When time gating is applied with a cw laser, T is the width of the time gate. With repetitively pulsed lasers the statistics of measuring depend on the *duty cycle* ($T \cdot f_{rep}$), which is usually very small compared to unity. In this respect pulsed lasers are disadvantageous in comparison with cw lasers operated in either the dc or the ac mode, at a given t_m and with the same (peak) power (3). There are, of course, benefits in other respects when working with pulsed lasers (higher peak power, permitting multiphoton excitation or ionization, frequency doubling, and enlargement of the probe volume while maintaining optical saturation (2, 57) (Chapters 2 and 3).

The *probe volume* V_p is determined by the geometry of the (intersecting) laser beam(s) and by the part of the irradiated region that is "seen" by the detector. When the radiant energy density in the laser beam or the efficiency of detecting a fluorescence photon or charge carrier varies with position inside V_p, we should rather speak of the *effective* probe volume. The latter depends on whether a one- or multiphoton process is involved and on whether saturation is attained or not. For a given laser beam geometry, the saturation volume may be a function of laser power P_L when a focused beam is used or when the beam irradiance drops gradually with off-axis distance (3, 36). In these cases the saturation curve (fluorescence intensity versus P_L) will not show a proper "plateau" in the limit of high P_L (51, 58).

Before establishing the relationship between N_e and the number, N_p, of atoms in V_p, we have to distinguish between two extreme probing conditions: the (*quasi-*)*stationary* and the *nonstationary case* (Fig. 4.4a and b, respectively). Usually V_p is a small part of the atomizer volume V_a and atoms move in and out of V_p freely and independently. Let τ be the (mean) *residence* or *transit time* of an atom in V_p. Following (39) we distinguish between (i) the *flow-controlled case* and (ii) the *diffusion-controlled case*. In case (i), which can occur only with continuous-flow atomizers, τ depends on the *flow velocity*, v_f, and on the linear dimension of V_p in the flow direction. In case (ii), τ is determined by the random motion of the atoms and the (smallest) linear dimension of V_p. If this dimension is less than the mean free path, the thermal velocity distribution of the atoms is decisive; in the opposite case, their diffusional motion should be considered. In a closed atomizer with a uniform atom distribution, only case (ii) can apply. In a continuous-flow atomizer with a carrier gas, transport of atoms takes place by diffusion as well as convection. Case (i) or case (ii) can then apply, depending on whether the one or the other yields the shorter τ value, for given dimensions of V_p.

The (quasi-)stationary case (a) is found if τ is much larger than the probing time T; the nonstationary case (b) occurs if $\tau << T$. In the former case, the number, N_p, of atoms in V_p does, virtually, not vary in a time interval of length T, whereas N_p varies stochastically in the latter case. (Of couse, when atoms

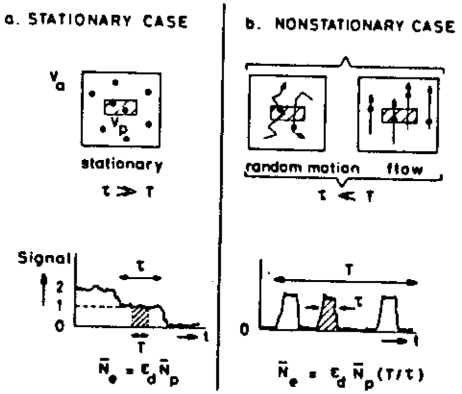

Fig. 4.4. Stationary (a) and nonstationary (b) laser probing. Dots in upper figures denote free atoms. Hatched areas in the bottom figures constitute an "event" produced by an individual atom at the detector. Left upper figure under b represents the diffusion-controlled case (ii) and right upper figure the flow-controlled case (i).

are ionized and captured by a detector as in LIIS, N_p will decrease, by depletion, during probing; but this is not at stake here.) Both with a closed and a continuous-flow atomizer, case (a) can go over to case (b) if T is increased, and conversely.

At the bottom of Fig. 4.4 it is schematically shown how in LIFS the number of events occurring in probing time T could be determined. We suppose that each atom, as long as it stays in V_p and is irradiated by the laser, produces a train of photoelectrons due to multiple recycling. In Fig. 4.4a the signal (photocurrent) is plotted as a function of time t, assuming continuous irradiation. The signal varies by a unit step each time an atom leaves or enters V_p; the mean interval between two consecutive steps is just τ. When time gating is applied with $T \ll \tau$, the signal produced by one atom, integrated over T, counts as *one* event (hatched area in Fig. 4.4a). Alternatively, one could count the photoelectrons released during T. Then the mean number of photoelectrons counted per atom constitutes one event.

At the bottom of Fig. 4.4b the photocurrent is again plotted as a function of t, but now in the nonstationary case. Every time an atom crosses V_p, a pulse of mean duration τ is observed. The mean charge contained in one such pulse constitutes again *one* event (see hatched area). The number of events occurring in T ($\gg \tau$) is then found by dividing the photocurrent, integrated over T, by

the pulse charge. Alternatively, one could count the time-resolved pulses during T, each individual pulse corresponding to one event.—The variable magnitude of the events is, as such, irrelevant, as long as we can clearly distinguish them from background and electronic noise. When two events may be recorded simultaneously, as in Fig. 4.4a, we only require that their spread is sufficiently small to discern them from the recording of one or three events, etc.

The distinction between the stationary and nonstationary probing case parallels that made in (59) between the usage of LIF as a density and as a flux detector, respectively.

The *relationship between N_e and N_p* depends on whether the (a) stationary or (b) nonstationary case applies. In the former case we have straightforwardly:

$$\bar{N}_e = \epsilon_d \cdot \bar{N}_p \tag{4.1a}$$

where ϵ_d is the *detection efficiency* ($0 \leqslant \epsilon_d \leqslant 1$; see Table 4.1). In LIFS ϵ_d depends on the rate of photoexcitation, the solid angle of observation, the quantum efficiency of the photocathode, and so on. The probability that an event remains unobserved because it is obscured by background or electronic noise is *not* included in ϵ_d. ("Detection" thus refers here to the physical process in the photodetector, not to the actual registration of this process.) Similarly, in LIIS ϵ_d depends, for example, on the collection efficiency of the charge carrier(s) and the efficiency of the particle multiplier.

If $\bar{N}_e \ll 1$, it should be interpreted as the *probability* that one event occurs during T. Similarly, if $\bar{N}_p \ll 1$, it represents the probability of finding one atom in V_p at an arbitrary moment. The probability of finding two atoms in V_p is then $(\bar{N}_p)^2$, and so on. For a statistically stationary stochastic system the overbar on N_e or N_p relates to the average over an ensemble of similar systems at any moment as well as to the time average for one system.

In the nonstationary case (b) we have instead of Eq. (4.1a):

$$\bar{N}_e = \epsilon_d \cdot \bar{N}_p \cdot \frac{T}{\tau} \tag{4.1b}$$

This equation holds because the number of atoms that pass through V_p within T is, on the average, equal to $\bar{N}_p \cdot (T/\tau)$. Even when $\bar{N}_p \ll 1$, its value can be assessed in a *single* probing if (T/τ) is known and sufficiently large to make $\bar{N}_e > 1$.

In the diffusion-controlled case, an atom that has just left V_p and lingers near its boundary has an enhanced chance to reenter V_p and to cause a second event. The time sequence of the pulses in Fig. 4.4b is then not fully random ("bunching" effect) and Eq. (4.1b) ceases to be strictly valid.

2.4. Overall Efficiency of Counting Atoms in a Sample

Fig. 4.1 illustrates, in the form of a flowchart, that usually but a small fraction of the N_s atoms present in the sample "survive" to become detected. There is a waste of atoms at the atomization and probing stages, whereas not all atoms under probing will produce an event. (We leave out of consideration here that, in addition, only a fraction of the events may be actually observed because of background and electronic noises.) We define the *overall efficiency* ϵ_o of a laser spectrometer to count atoms in the sample as the probability that a given atom in the sample produces an event in a single probing or

$$\epsilon_o = \frac{N_e}{N_s} \quad . \tag{4.2}$$

We can decompose ϵ_o into a product of partial efficiencies, namely the *atomization efficiency* ϵ_a, the *probing efficiency* ϵ_p and the *detection efficiency* ϵ_d (for definitions, see Table 4.1):

$$\epsilon_o = \epsilon_a \cdot \epsilon_p \cdot \epsilon_d \tag{4.3}$$

In order to derive an expression for ϵ_p, we shall first consider the relation between N_a and N_p.

The number density, n_a, of free atoms in a *closed* atomizer with volume V_a containing N_a free atoms is determined by

$$N_a = n_a \cdot V_a \tag{4.4}$$

With the assumed uniform atom distribution (Section 2.1), we immediately get for the mean number, $\overline{N}_p$, of atoms in the probe volume V_p:

$$\overline{N}_p = n_a \cdot V_p = N_a \frac{V_p}{V_a} \tag{4.5}$$

In the case of stationary probing (Fig. 4.4a), we obtain from Eq. (4.5) and the definition of ϵ_p:

$$\epsilon_p = \frac{\overline{N}_p}{N_a} = \frac{V_p}{V_a} \tag{4.6a}$$

In the nonstationary case (Fig. 4.4b), we have instead

$$\epsilon_p = \frac{\overline{N}_p}{N_a} \cdot \frac{T}{\tau} = \frac{V_p}{V_a} \cdot \frac{T}{\tau} \tag{4.6b}$$

as $\overline{N}_p \cdot (T/\tau)$ is the mean number of atoms that have passed through V_p within probing time T [cf. Eq. (4.1b) and annex discussion]. We note that Eq. (4.6b) ceases to hold when $T/\tau \geq V_a/V_p$. For, at $T/\tau = V_a/V_p$, a given atom that is initially found anywhere inside V_a, will turn up sometime during T in V_p with a probability close to unity. Then ϵ_p will be close to unity, too.

Expressions (4.6a) and (4.6b) are also applicable for a *continuous-flow* atomizer if we define here N_a as the total number of free atoms produced during *atomization time* t_a (Table 4.1). Accordingly, we introduce formally a (*fictitious*) *atomizer volume* V_a that obeys Eqs. (4.4) and (4.5) where n_a relates to the probe region. In other words, V_a is the volume that would be occupied by all N_a free atoms produced during t_a, if we could keep their density uniform and equal to its value in V_p.

Using Eqs. (4.1a) and (4.6a) in the stationary case and Eqs. (4.1b) and (4.6b) in the nonstationary case, we easily check the validity of expression (4.3) in either case. The idealizations made implicitly in the derivation of these equations should be kept in mind. Nevertheless, in these simplified equations the basic role of the parameters involved stands out more clearly.

In the *stationary* case, where Eq. (4.6a) applies, and with a closed atomizer, ϵ_p would approach unity if we make V_p as large as V_a. For a continuous-flow atomizer, this limit is hard to realize, especially so when working with a flame or ICP. Here n_a will be small and thus the (fictitious) volume V_a large, at given N_a [Eq. (4.4)], in comparison with open electrothermal atomizers. This holds because of the larger carrier gas flow and thermal expansion in the former case (2). With a given continuous-flow atomizer and a given c_s, n_a is fixed. V_a may then be reduced by shortening t_a, resulting in a smaller N_a value, so that fewer sample atoms are wasted before and after probing takes place. Ideally, t_a should match T. A carbon rod or filament atomizer with pulsed atomization of minute samples is attractive in this respect.

In the *nonstationary* case, where Eq. (4.6b) applies, an unfavorable (V_p/V_a) ratio can be compensated by a large (T/τ) ratio. Under flow-controlled measuring conditions, the cross-sectional area (O_a) of the flowing gas stream should match the area (O_p) of V_p, so that each atom passes through V_p. When, for example, atoms are vaporized from a sample deposited on a (hot) filament, this may be obtained by gas-dynamic focusing using a sheathing gas jet (57, 60). In a particular case the gas jet could be constricted to a diameter of about 0.1 mm.

Suppose the gas stream is cylindrical, with a uniform flow velocity v_f. Then the (fictitious) analyzer volume V_a equals $O_a \cdot v_f \cdot t_a$, whereas $V_p = O_p \cdot v_f \cdot \tau$ if τ is flow controlled (Section 2.3). Applying Eq. (4.6b), under nonstationary measuring conditions, we find $\epsilon_p = (O_p/O_a) \cdot (T/t_a)$. Here v_f and τ drop out. At given (O_p/O_a) and T, ϵ_p can then be improved only by reducing t_a.

When we try to maximize ϵ_p by changing the instrumental parameters or measuring conditions, we should be aware that ϵ_a and ϵ_d may be changed, too. A change of T, τ, or V_p (which may also depend on laser power; Section 2.3) could influence ϵ_d because, for example, the number of fluorescence photons emitted per atom in a single probing may depend on these parameters. Also, a change in V_a might affect ϵ_a if the latter depends on the flow velocity or the dimensions of the atomizer. Furthermore, some of these parameters cannot be changed independently of each other. For example, a change of the linear dimension of the probe volume in the flow direction also affects the transit time τ. An increase of τ, in turn, could ensue a changeover from nonstationary to stationary measuring conditions (if T is held constant).

In practice the best way to maximize ϵ_o or ϵ_d will depend strongly on the particular application and detection technique at hand. So we had to content ourselves with a few general guidelines only.

With regard to the distinction made in Section 1.2 between the restricted and the general concept of SAD, we conclude that a necessary (but not sufficient!) condition for the former is $\epsilon_d = 1$, whereas the latter concept implies $\epsilon_o = \epsilon_a \cdot \epsilon_p \cdot \epsilon_d = 1$. Usually we have $\epsilon_a \cdot \epsilon_p << 1$, so that a large number of analyte atoms in the sample is wasted for each atom counted in the probe volume.

2.5. Calibration Procedure and Conversion Factors

The *calibration procedure* in (chemical or diagnostic) analysis depends primarily on the kind of quantity sought and on the state of sample to be analyzed. We may, for example, want to measure the concentration or absolute quantity of analyte in a solution, the saturated vapor pressure of an atomic or molecular species, isotope ratios in a solid sample, the absolute rate at which a rare event takes place, or the absolute number of daughter atoms produced by radioactive decay. Calibration would, in general, be straightforward if we would be able to count the events produced by individual atoms, knowing ϵ_o (Sections 2.4 and 4.2). Usually, ϵ_o is hard to measure or to calculate from instrumental parameters, atomic properties, and laser beam characteristics, especially so if atomization of solid or liquid samples is involved. However, ϵ_o drops out when we are only interested in isotope ratios of the same element. In diagnostic applications where one is only interested in the number density, n_a, of atoms in the gas phase, the atomization efficiency plays no role. If the detection efficiency ϵ_d is known, one derives N_p from measured N_e through Eq. (4.1a) under stationary probing conditions. Then n_a follows from N_p through Eq. (4.5), if we know also V_p (the latter might be hard to assess, however; see Section 2.3). In LIFS, ϵ_d can be determined by means of an additional scattering experiment if, for example, a noble gas is present and its pressure and Rayleigh scattering cross section are known (19, 61, 62). In LIIS one can occasionally eliminate one of the factors that determine ϵ_d (such as the ion collection efficiency) by plotting the signal strength versus some suitably chosen instrumental parameter (collector voltage). One works then at the plateau where "saturation," if any, is reached.

In most spectrochemical applications, calibration is obtained in an indirect way by means of a series of reference samples. These samples contain a known amount or concentration of analyte in a chemical environment that closely resembles that of the unknown samples. Interferences by concomitants or matrix effects are thus accounted for. In this way one bypasses the various (unknown) partial efficiencies contained in ϵ_o.

A quite different type of indirect calibration can be applied, for example, when we want to measure absolute vapor pressures at very low temperatures. Calibration can here be obtained by repeating the measurements, under the same experimental conditions, at higher temperatures at which the absolute vapor pressure is already known. This procedure was applied in LIFS, under (near-) SAD conditions, to pure atomic Na and Pb vapors (15, 63–65) (Section 3.2). Interestingly, in one of these experiments with Na this procedure was combined with a direct, absolute calibration using the known vapor cell dimensions and atomic absorption coefficient (15). The latter procedure utilized in an ingeneous way the effect on the fluorescence signal caused by preabsorption of the laser beam before entering the probe volume. This procedure could therefore be followed only at sufficiently high vapor pressures.

The *conversion factor* ψ relates the concentration c_s (or quantity q_s) of analyte in the sample to the number density n_a (or number N_a) of free atoms in the atomizer:

$$\psi = \frac{n_a}{c_s} \quad (\text{or} = N_a/q_s) \tag{4.7}$$

Expressions for ψ have been given, for example, in (2, 35, 51, 64). These expressions involve ϵ_a, which can thus be derived from ψ if we do know the other instrumental factors involved. These factors include the flow rate (mol/s) and thermal expansion of the carrier gas or the velocity and cross section of the carrier gas stream in a continuous-flow atomizer. They can often be readily measured, whereas ψ can be determined by an absolute measurement of n_a at given c_s (51).

We note that ψ differs by a factor $(\beta_v \cdot \beta_a)$ from the "conversion factor" K as defined in (51). β_v accounts for incomplete volatilization of the aerosol particles, whereas β_a accounts for losses of free analyte atoms due to molecule formation or ionization in the gas phase (1). Typical values of ψ (or K) for a flame with pneumatic nebulizer are in the 10^{10}–10^{11} (atoms/cm^3)/(μg/mL) range if $\beta_a \cdot \beta_v = 1$. (The usage of parts per million, etc., as a unit for concentration is discouraged, as it could relate to relative numbers as well as relative masses, in the gas phase or in the sample.) Remarkably, a similar ψ value (3×10^{10}) was found when a Pb solution was evaporated in a graphite-cup continuous-flow atomizer used for analysis by LIFS (64). One would here expect a comparatively much higher value (Section 2.4). This discrepancy might be explained by the low ϵ_a ($\approx 1\%$) and rather high velocity of the carrier gas (≈ 10 cm/s) reported in the same paper.

Although ψ is usually not known accurately enough to calibrate chemical analyses, it may be an interesting quantity for the following reasons:

1. The atomization efficiency can be assessed from ψ (see preceding discussion).
2. ψ enables us to convert LODs reported in the analytical literature to atomic densities in the atomizer, and conversely. This conversion is especially useful when we want to compare analytical LODs with the intrinsic values (Section 2.6).
3. Through ψ we can intercompare different types of atomizers as to their analytical performance for various analytes.

2.6. Statistical Expressions

The intrinsic LOD as defined in Section 1.1 relates to the inherent error in the signal, caused by statistical fluctuations in the number of atoms probed and in the detection process. The minimum detectable signal was defined as k times its intrinsic rms error. When small numbers of atoms are to be counted, it is appropriate to consider the number of events, N_e, counted in a single probing interval T, as *the* signal. The minimum detectable signal is therefore

$$(\overline{N}_e)_m = k \cdot \tilde{N}_e \tag{4.8}$$

where $\tilde{N}_e \equiv \sqrt{\overline{(\Delta N_e)^2}}$ is the rms intrinsic error in N_e. The relation between $\overline{N}_e$ and $\overline{N}_p$ is given by Eq. (4.1a) or (4.1b) in the stationary or nonstationary case, respectively. Through this relation we can express $(\overline{N}_p)_m$ in $(\overline{N}_e)_m$, whereas we derive $(n_a)_m$ from $(\overline{N}_p)_m$ by using Eq. (4.5). The minimum detectable sample concentraton c_m follows, in turn, from $(n_a)_m$ through the conversion factor ψ [Eq. (4.7)]. Alternatively, we can directly relate $(\overline{N}_e)_m$ to the minimum detectable number of analyte atoms in the sample, $(\overline{N}_s)_m$, by using ϵ_o [Eq. (4.2)].

In the following we present *statistical expressions* for the *mean signal*, the *precision* [$\equiv$ relative standard deviation (1)], the *detection efficiency*, and the *limit of detection* relating to the number (density) of atoms in the probe volume, for single as well as repeated probings. We disregard again extrinsic errors.

Numerous expressions for the precision or LOD involving extrinsic errors have been presented in the spectrochemical literature [see, e.g., (2, 3, 35, 66–68)]. Only rarely was the contribution of the fluctuation in N_p included (3), and then only for the stationary probing case. A detailed study of the effect of particle fluctuations on the scattered light intensity has been made in (69). The possibility of verifying statistical-mechanical expressions for atom number fluctuations by SAD techniques was discussed in (5).

Let us first consider the *stationary case* where $\overline{N}_e = \epsilon_d \cdot \overline{N}_p$ [Eq. (4.1a)]. If $\epsilon_d = 1$, we have $\tilde{N}_e = \tilde{N}_p$ and $\tilde{N}_e = \sqrt{\overline{N}_e}$ if N_p and thus N_e obey Poisson statistics. However, if $\epsilon_d < 1$, N_e will fluctuate even if N_p is fixed, as the occurrence of an event is now a chance process, described by a Bernoulli (or binomial) distribution. (We assume that events produced by different atoms are statistically uncorrelated.) The relative spread of N_e, at fixed N_p, will be the smaller, the closer ϵ_d approaches unity. If N_p obeys Poisson statistics and N_e, at *fixed* N_p, obeys Bernoulli statistics, we obtain exactly for any ϵ_d

$$\tilde{N}_e = \sqrt{\overline{N}_e} \quad (= \sqrt{\epsilon_d \cdot \overline{N}_p}) \tag{4.9}$$

In other words, N_e obeys Poisson statistics, too. This outcome is the same as that obtained in the theory of partition shot noise in electronic devices (70).

One should be careful in deriving expressions for the fluctuations in the photocurrent when the number of emitting atoms fluctuates. One must not, in general, add the variance ($\equiv$ squared standard deviation) induced by the atom number fluctuations to that associated with the photocurrent shot noise. This is seen most clearly in the simple case when each atom produces just one photoelectron ($\epsilon_d = 1$). Adding up these variances would then make the standard deviation in the photocurrent $\sqrt{2}$ times too high!

The assumption that the production of an event (in casu: the emission of a photoelectron) by one atom is statistically uncorrelated with the events produced by other atoms implies the condition of *incoherent* radiation detection. This means that the intensities, *not* the amplitudes, of the radiation fields produced by each atom at the photocathode are additive. Then also the probabilities of photoelectron emission—which are proportional to the corresponding radiation intensities—are additive (69). This condition is surely fulfilled in the experimental situations considered here. The fluorescence radiation emitted by the atom is not coherent with the exciting laser field nor with the radiations emitted by other atoms (34).

Equation (4.9) holds also in the *nonstationary case*, if the transient appearance of an atom in V_p during T ($\gg \tau$) is purely random. We have only to replace in the second part of this equation $\epsilon_d \cdot \overline{N}_p$ by the expression given in Eq. (4.1b).

We now derive a statistical expression for ϵ_d, being the probability of an event occurring in a single probing when one atom is present in, or passes through V_p. Let ϕ be the constant probability per second that a photoelectron is generated (in LIFS) or an ion (or primary electron) is detected (in LIIS) as long as there is one atom in V_p. If the atom will generate at most one photoelectron during its whole stay in V_p, each photoelectron generated counts as one event. We then have in the stationary case ($\tau >> T$)

$$\epsilon_d = \phi \cdot T \quad (\text{if } \phi \cdot T << 1) \tag{4.10a}$$

and in the nonstationary case ($\tau << T$)

$$\epsilon_d = \phi \cdot \tau \quad (\text{if } \phi \cdot \tau << 1) \tag{4.10b}$$

[The probability, $(\phi \cdot T)^2$ or $(\phi \cdot \tau)^2$, that two photoelectrons are generated per atom is then much less than $\phi \cdot T$ or $\phi \cdot \tau$ and thus negligible, indeed.]

When in LIFS $\phi \cdot T$ or $\phi \cdot \tau$ is arbitrarily large and multiple recycling occurs, we have to consider the *Poisson distribution* for the number, m, of photoelectrons generated per atom during T or τ:

$$p(m) = \frac{1}{m!} \cdot \exp[-\bar{m}] \cdot \bar{m}^m \tag{4.11}$$

Here we have to substitute $\phi \cdot T$ or $\phi \cdot \tau$ for $\bar{m}$. Since the generation of any number ($m \geq 1$) of photoelectrons by a given atom is, by definition, one event, we arrive at the following general expression for ϵ_d in LIFS:

$$\epsilon_d = \sum_{m=1}^{\infty} p(m) \tag{4.12}$$

(The special case when a pulse-height discriminator is applied will be considered in Section 3.2.)

When in LIIS or LIFS $\phi \cdot T$ or $\phi \cdot \tau$ are arbitrarily large and no recycling takes place, we generally find for ϵ_d

$$\epsilon_d = 1 - \exp[-\phi \cdot T] \quad (\text{stationary case}) \tag{4.13a}$$

$$\epsilon_d = 1 - \exp[-\phi \cdot \tau] \quad (\text{nonstationary case}) \tag{4.13b}$$

Here the probing is a consumptive process, so that each atom produces no more than one ion (or primary electron) or one photon. One easily checks that expressions (4.10a) and (4.10b) follow from expressions (4.12) or (4.13a) and (4.13b), respectively, in the limit $\epsilon_d \to 0$.

The Poisson distribution law applies also to the total number of events, N_e, produced by all atoms present in or passing through V_p during probing time T:

$$p(N_e) = \frac{1}{N_e!} \cdot \exp[-\bar{N}_e] \cdot \bar{N}_e^{N_e} \tag{4.14}$$

The mean value, $\bar{N}_e$, is again given by Eq. (4.1a) or (4.1b). The validity of Eq. (4.14) was verified in a particular LIIS experiment under nonstationary probing conditions with an Yb and a Na beam (63). In this experiment ϵ_d was close to unity, whereas $\bar{N}_p$ and $\bar{N}_e$ ranged from 0.003 to 0.03 and from 0.35 to 3, respectively. The probing time T was 20 s.

Table 4.3 collects statistical expressions for the mean signal, precision and

Table 4.3. Statistical Expressions[a]

Quantity	Stationary Case (a) ($\tau >> T$)	Nonstationary Case (b) ($\tau << T$)
Mean signal	$\bar{N}_e = \epsilon_d \bar{N}_p$ (4.15) [$\bar{N}_e = \phi T \bar{N}_p$ (4.17)]^b	$\bar{N}_e = \epsilon_d \bar{N}_p (T/\tau)$ (4.16)
Precision		
1 probing	$\tilde{N}_e/\bar{N}_e = 1/\sqrt{\bar{N}_e}$ (4.18a)	
R probings	$\tilde{N}_e/\bar{N}_e = 1/\sqrt{R\,\bar{N}_e}$ (4.18b)	
Intrinsic LOD[c]		
N_e {1 probing	$(\bar{N}_e)_m = k\,\tilde{N}_e = k\sqrt{(\bar{N}_e)_m}$ or: $(\bar{N}_e)_m = k^2$ (4.19a)	
N_e {R probings	$(\bar{N}_e)_m = k^2/R$ (4.19b)	
N_p: R probings	$(\bar{N}_p)_m = k^2/\epsilon_d R$ (4.20) [$(\bar{N}_p)_m = k^2/\phi T R$ (4.22)]^b	$(\bar{N}_p)_m = (k^2/\epsilon_d R)(\tau/T)$ (4.21)
n_a: R probings	$(n_a)_m = k^2/\epsilon_d V_p R$ (4.23) [$(n_a)_m = k^2/\phi T V_p R$ (4.25)]^b	$(n_a)_m = (k^2/\epsilon_d V_p R)(\tau/T)$ (4.24)

[a] N_e is number of events *per probing*; for explanation of other symbols, see Table 4.1. For statistical expressions for ϵ_d, see text.

[b] Equations within square brackets refer to the limiting case when the probability of one atom in V_p producing a photoelectron (in LIFS) or an ion (in LIIS) during probing time T (case a) or transit time τ (case b) is small. These equations are placed between the two column headings, because they hold in both cases.

[c] LOD relates here to number (density) of atoms in V_p or number of events at detector (not to sample concentration).

[Reproduced, with slight modifications, from (39) by permission of the Society for Applied Spectroscopy, USA.]

intrinsic LOD in the case of stationary (a) and nonstationary (b) probing. A Poisson distribution is assumed for N_c and N_p, and extrinsic errors are disregarded, as before. Some expressions have already been dealt with; the others follow straightforwardly from them, if we assume that repeated probings are statistically uncorrelated. This assumption need not necessarily hold in case (a), if $f_{rep} > 1/\tau$ *and* $\epsilon_d \approx 1$. If $\epsilon_d << 1$, the relative spread in N_e largely exceeds that in N_p, so that consecutive probings are statistically uncorrelated, irrespective of $f_{rep} \cdot \tau$. A few remarks are to be made:

1. At the limiting condition underlying Eq. (4.17) (see footnote *b* of Table 4.3), the mean signal appears to be the same in case (a) as in case (b), although the general expressions (4.15) and (4.16) differ from each other by a factor (T/τ) (>1). This factor is, however, canceled in Eq. (4.17) because ϵ_d for case (a) exceeds that for case (b) by the same factor [Eqs. (4.10a) and (4.10b)]. This cancellation also occurs in Eqs. (4.22) and (4.25), which hold for the same condition that underlies Eq. (4.17).

2. Equation (4.18a) for the precision holds formally also when $\overline{N}_e << 1$. We can still determine such low $\overline{N}_e$ values at any precision by repeating the probings a sufficiently large number of times [Eq. (4.18b)]. The mean total number of events observed in R probings, $\overline{N}_e \cdot R$, should exceed unity for obtaining a statistically significant measurement.

3. Expressions for the intrinsic LOD relating to n_a follow from those relating to N_p by dividing the latter ones by the probe volume V_p. We recall that ϵ_d, τ, or ϕ may depend on the extent and shape of V_p. So an enlargement of V_p need not necessarily lead to an improvement of $(n_a)_m$. Much depends on the particular experimental conditions at hand. The expressions for $(n_a)_m$ are of direct interest in diagnostic studies. They are of indirect interest in chemical analysis because c_m follows from $(n_a)_m/\psi$ (Section 2.5).

4. Remarkably, R appears in the denominator of expressions (4.19b)–(4.25) to the *first* power. This contrasts with the conventional, extrinsic LOD, which varies in direct proportion to $1/\sqrt{R}$ if the background and detector noise spectrum is "white" (51, 71). The dependence of the intrinsic LOD on probing time T is less evident, as ϵ_d occurring in Eqs. (4.20), (4.21), (4.23), and (4.24) may vary with T, too. Only in the particular situation where Eqs. (4.22) and (4.25) apply can we generally state that the intrinsic LOD improves in direct proportion to T. This is again in obvious contrast with the conventional LOD, which improves in direct proportion to $\sqrt{T}$ (2, 51, 71).

5. Expressions that hold under SAD conditions are obtained by taking $\epsilon_d = 1$. Expressions (4.17), (4.22), and (4.25) are then no longer applicable.

6. One should not extrapolate the usual expressions for the analytical (extrinsic) LOD to such low c_s or q_s values that the mean number of atoms probed becomes of the order of unity or less.

3. SPECIFIC DETECTION TECHNIQUES AND EXPERIMENTAL RESULTS

3.1. Classification of Detection Techniques

The broad classification of laser beam detection techniques in Section 2.2 will here be refined, and some examples of experimental realizations and results obtained will be described in the following sections. We shall focus our attention on techniques that enable us, with special arrangements, to detect small numbers of atoms (and molecules) or even single atoms. Figure 4.5 summarizes the basic schemes of those techniques that have proved to be most successful in this respect.—With regard to the existing, wildly flowering, and confusing terminology, we have tried to use a more consistent set of descriptive terms.

Optical Detection Techniques. This category encompasses techniques based on any optical effect—such as fluorescence, absorption, stimulated emission (3,

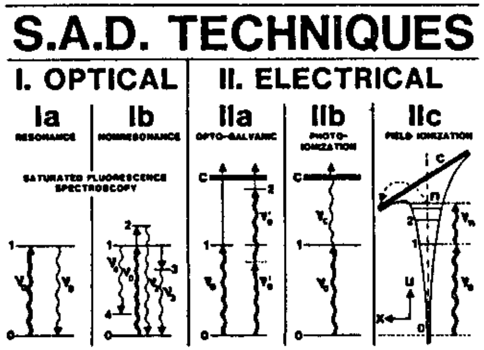

Fig. 4.5. Classification of main types of laser-based single-atom detection (SAD) techniques. Simplified energy level schemes are given with the relevant atomic transitions. A double, upward pointing, wavy arrow denotes a saturated transition induced by a laser tuned to an atomic resonance. Single wavy arrows denote nonsaturated transitions by photon absorption or spontaneous photon emission. Straight lines denote collisional transitions. Energy levels are denoted by 0 (for the ground state), 1, 2, . . . , *n*; the continuum state is denoted by c. Optical frequencies are indicated by *ν*. Under IIc the distortion of the potential energy function *U*(*x*) of the valence electron, caused by an external dc electric field in the *x* direction, is schematically shown. Here horizontal bars represent discrete energy levels, whereas the sloping line represents the continuum state. A spontaneous transition from a high-lying bound state *n* to the continuum state c may occur by quantum mechanical tunneling through a potential barrier. [Reproduced from (39) by permission of the Society for Applied Spectroscopy, USA.]

72), polarization*, Raman scattering (incoherent or coherent) (Chapter 10) (73), birefringence (74), anomalous dispersion (75), and anomalous refraction—that can be induced or detected by laser radiation [for a survey see (27, 35, 76)]. We restrict ourselves to fluorescence and absorption techniques, which are the more promising ones as regards detectability.

Techniques based on *laser-induced fluorescence spectroscopy* (*LIFS*) can be subdivided into *resonance* (*RF*) and *nonresonance fluorescence* (*NF*) techniques (Section 2.2 and Chapter 2). Their basic operation schemes are shown in Fig. 4.5, Ia and Ib. The main advantage of using a laser is that optical saturation (Chapter 1) can be achieved. [The term *saturated optical nonresonance emission spectroscopy* (*SONRES*) has therefore come into use.] The main practical advantage of using NF, instead of RF, is that laser background scattering can be simply rejected. If an optical transition is allowed from the laser-excited level 1 in Fig. 4.5, Ib, to a lower lying excitation level 4, NF can be applied without requiring inelastic collisions in a buffer gas.

Since the emission of a fluorescence photon is preceded by the absorption of a laser photon, the fluorescence excitation spectrum (≡ fluorescence intensity versus laser detuning) is essentially an absorption spectrum. This holds at least if saturation broadening (51) (Chapter 1) is avoided and if the probability that an excited atom reemits a photon is independent of the detuning (77).

The use of lasers in conventional *atomic* (*AAS*) or *molecular absorption spectroscopy* (*MAS*) may not bring about a substantial gain in LOD as long as the latter is determined by fluctuations in the laser power (3). Then, only the directionality of the laser beam can be an advantage in obtaining a long absorption pathlength l_{abs} by multiple folding of the beam inside the cell. However, the minimum detectable absorption factor α_m ($= k_m \cdot l_{abs}$; $k \equiv$ napierian absorptivity, proportional to number density) can be greatly improved by special laser-based variants of AAS or MAS. These variants include: intracavity absorption spectroscopy (*ICAS*), low frequency and rf laser wavelength modulation spectroscopy, laser Zeeman or Stark modulation spectroscopy (where the absorption line frequency is modulated) and saturated absorption spectroscopy (where the saturation induced by a pump laser is monitored by AS with a relatively weak probe laser). We will discuss here only two of these variants, which have the prospect of obtaining low LODs [for a survey see (26, 27, 35, 76)].

In *ICAS*, where the absorption cell is placed inside the laser cavity (Chapter 12) (26, 27), laser photons pass a large number of times through the atomic vapor before they are coupled out. In this way l_{abs} may be enhanced by a factor of 100–1000 (3). Due to the nonlinear interaction between laser field and atoms,

---

*A LOD of 0.05 ng/mL has recently been attained for sodium in an air-acetylene flame by laser-induced polarization spectroscopy [W. G. Tong and E. S. Yeung, *Anal. Chem.*, 57, 70 (1985)].

a small ($k \cdot l_{abs}$) value may already drastically change the laser output if the laser operates close above threshold. With multimode (broadband) lasers an extra enhancement of absorption sensitivity occurs, that is proportional to the number of oscillating modes (78). (Mode competition may affect the spectral laser characteristics too.) With long pathlengths, k_m values ranging from 10^{-8} to 10^{-9} cm^{-1} have been attained with standing-wave lasers (35, 79). A value of 10^{-10} cm^{-1} has been attained with a ring traveling-wave laser (79) for an unidentified species in air contained in a cuvette of nearly 150 cm length. For the Na-*D* doublet lines a value $k \approx 10^{-8}$ cm^{-1} corresponds to $n_a = 4 \times 10^3$ cm^{-3} if the Na atoms are present in a gas at 1 atm pressure and 2000 K and a narrow-band line source is used (51). This illustrates the feasibility of detecting small numbers of atoms by ICAAS in an absorption cell of small internal cross section (≈ 1 mm^2) at reduced gas temperature and pressure. For molecular species the prospects are much less good (27, 35). This is because their ground-state population is distributed over a manifold of rovibrational levels, and the oscillator strength of a rotation line is much smaller than that of the Na-*D* lines. For similar reasons the detectability of LIFS for molecules is much worse than for atoms.

We note that k_m varies $\sim (l_{abs})^{-1}$, when α_m is fixed for a given detection technique. Since α correlates with the number of atoms per centimeter squared (i.e., $n_a \cdot l_{abs}$), and $N_p = n_a \cdot V_p = n_a \cdot l_{abs} \cdot O_p$ [Eq. (4.5); $O_p \equiv$ laser beam cross section], the minimum detectable *number* of atoms $(\bar{N}_p)_m$ is $\sim O_p$ but independent of l_{abs}. The minimum detectable *number density* $(n_a)_m$, however, is independent of O_p, but $\sim (l_{abs})^{-1}$.

In contrast with conventional wavelength modulation techniques, *rf laser-wavelength modulation spectroscopy* (usually called frequency modulation spectroscopy) operates at modulation frequencies f_m in the megahertz-gigahertz ranges (80). The wavelength of a single-mode laser is here modulated by an external electro-optical phase modulator. The intensity remains constant but the laser spectrum now contains sidebands mutually separated by f_m hertz. When the laser beam is sent through an (external) absorption cell, while one sideband is tuned at, or near to the absorption line center, the amplitude and relative phase of this sideband will be altered. This results in an *amplitude* modulation of the transmitted laser beam, which can be heterodyne detected. One thus obtains a signal that is a measure of the absorption factor. Apart from being a null method, this technique has the advantage that electronic detection takes place outside of the frequency band of the excess laser power fluctuations. Preliminary experiments with an I_2 vapor cell (80) and a Na-seeded flame (81) did not yield impressive α_m values, as these were determined by absorption background noise. But this noise is not characteristic of the detection capability of this technique as such.

Since measuring stimulated Raman gain is equivalent to measuring *negative* absorption, rf modulation spectroscopy can be applied here, too. This was demonstrated by an experiment with a deuterium gas cell, where the detectability appeared to be shot-noise limited (82).

Electrical Detection Techniques (LIIS). They can be subdivided into *optogalvanic* (IIa), *photoionization* (IIb) and *field ionization* (IIc) *techniques* (Fig. 4.5). This distinction is based on the different ways in which ionization from the laser-excited level is accomplished. In all cases species selectivity is obtained, as before, by tuning the laser frequency into resonance with one or more successive transitions between discrete atomic levels. (For this reason the term *resonance ionization spectroscopy, RIS*, has come into use for technique IIb; this term could, however, also refer to other techniques.)

Following (53), we define the *optogalvanic effect* as a perturbation of the state of ionization in a plasma in response to the absorption of optical radiation, which changes the relative level populations of atomic or molecular constituents of the plasma. Ionization from the laser-excited state is brought about by inelastic collisions with electrons or other particles in the plasma. This may occur in one step or in several steps involving higher-lying excitation levels. Since the collisional ionization and intermediate excitation steps are endoergic (requiring activation energy), a sufficiently high gas or electron temperature is needed. Inelastic collisions may then also produce background ionization in the absence of laser excitation. (In work with flames the term *laser-enhanced ionization spectroscopy, LEIS*, has therefore come into use—although background ionization is not essential.) For a more detailed description we refer to Chapter 3 and (32, 33, 53, 83). Two variants based on one- and two-photon excitation, respectively, are shown in Fig. 4.5, IIa.

Since endoergic collisions are involved in the ionization step, the laser-excited level should preferably lie close to the ionization continuum. Levels with excitation energies E_{exc} exceeding the laser photon energy can be populated by choosing a nonresonance absorption line. It is often more efficient to excite (even saturate) a high-lying level from the ground state by a *multistep process* using multiple laser beams tuned at consecutive atomic transitions. In a *multiphoton (MP) process* several photons of the same frequency are absorbed simultaneously. Apart from the energy matching condition ($E_{exc} = 2 \times$ photon energy), the probability of a two-photon process is considerably enhanced when there happens to exist a suitable intermediate level with $E_{exc} \approx$ photon energy. MP processes (including photodissociation and photoionization) are therefore, in general, more probable in molecules than in atoms. Two-photon excitation is to be distinguished from one-photon excitation by a frequency-doubled laser beam because of the different optical selection rules involved.

With the *photoionization technique*, the atoms after being excited by absorption of one or more laser photons, with the same or different frequencies, are transferred to the ionization continuum by nonresonant absorption of another laser photon (Fig. 4.5, IIb). This transfer may, occasionally, also proceed via an unstable autoionizing state excited by resonant photon absorption from a level below the ionization continuum. With this technique collisions are not needed, and the presence of a buffer gas is not essential. In flames processes IIa and IIb may both occur. For a more detailed treatment we refer to (5, 30, 31, 34) (see also Chapters 3 and 18). The potentialities of these techniques for SAD have, in particular, been considered in (5, 34).

With the *field ionization technique* the atoms are first raised by a multistep or a MP process to a Rydberg level lying close under the ionization continuum (Fig. 4.5, IIc). Atoms in Rydberg levels have a long lifetime in the absence of quenching collisions. By applying a pulsed electric dc field shortly after the excitation pulse, the "Rydberg atom" can spontaneously ionize before it has a chance to decay to a lower-lying level. No additional energy is needed here in the ionization step. This autoionization process is brought about by the reduction of the potential energy, U, experienced by the excited valence electron when moving in a direction opposite to the electric field vector (Fig. 4.5, IIc). In this direction the bottom of the continuum state is bent below the Rydberg level energy. Even when there exists a potential barrier for the transition to the continuum state (as depicted in Fig. 4.5, IIc), a spontaneous transition is still possible by quantum mechanical tunneling. The reason that the electric field is switched on *after* the excitation pulse is that otherwise the accompanying Stark effect would blur the Rydberg levels, which are closely packed near the ionization limit. This blurring effect would spoil the selectivity of the (last) excitation step to the Rydberg level. This technique works best with atomic beams in vacuo. For a further discussion, with special emphasis on SAD, the reader is referred to (13, 31, 34, 84).

Mechanical Detection Techniques. This category encompasses the *laser-induced beam deflection technique*, of which one variant based on *radiation pressure* was, exemplarily, described in Section 2.2. Beam deflection can also be brought about in an external electric or magnetic field when, as a result of laser excitation, the *atomic polarizability* or *magnetic moment* is changed (13, 34).

Optoacoustic spectroscopy (OAS) (also called photoacoustic spectroscopy) falls within the same category, as it exploits a mechanical effect, in casu an increase in gas pressure. This increase results from the heating effect of selective (laser) absorption in a closed cell containing the gaseous sample. The resulting (periodic or pulselike) pressure increase is detected by means of a sensitive microphone (Chapter 5) (27, 35). In contrast with the previously discussed techniques, OAS requires conversion of excitation energy into heat through quenching collisions. OAS is usually applied to detect molecules or to study their absorption spectra in the gaseous or condensed phase. It is a complement to reflection and transmission spectroscopy. Detection limits k_m as low as 10^{-10} cm^{-1} have occasionally been reached with lasers in NO pollution analysis. When comparing this achievement with those attainable by optical MAS, it should be realized that in OAS the absorption pathlength is usually restricted to typically 10 cm. However, intracavity arrangements can be applied in OAS too. Analytical detection limits expressed in *relative* particle densities are impressive ($1:10^{11}$). But when they are expressed in *absolute* numbers of molecules probed, this technique appears to be much less sensitive than the others. The typically low absorption cross section of molecular spectral lines is mainly to be blamed for that (as we saw earlier in this section).

3.2. Experimental Results by Fluorescence and Absorption Techniques

Some laser-based fluorescence and absorption experiments will be described that illustrate the foregoing, rather schematic, considerations.

Table 4.4 collects data that relate to the experimental conditions and the LODs obtained in experiments using resonance fluorescence (1–4), nonresonance fluorescence (5–10), and intracavity absorption (11) spectroscopy. For comparison, a nonresonance fluorescence experiment (19) dealing with rhodamine 6G molecules in the liquid phase has also been included. The numerical data listed will enable us to judge how close the experimental LODs relating to numbers, $(\bar{N}_p)_m$, or number densities, $(n_a)_m$, of atoms in the *gas* phase approach the intrinsic values or even the SAD limit. Values of V_p are inserted to convert $(\bar{N}_p)_m$ into $(n_a)_m$, or conversely. The ratio τ/T is of interest in helping to select the appropriate formulas in Table 4.3 that hold in the stationary or nonstationary case.

The figures entered are often correct as to order of magnitude only because of insufficient or ambiguous specifications in the literature. In some instances they had to be deduced indirectly from other data reported or to be estimated from analogous situations. (The specifications in experiment 19 are exemplary in their completeness and detail.) It should be admitted that the primary aim of some experiments was not to achieve low detection limits per se. Also, in some analytical applications one was rather interested in LODs pertaining to the sample before atomization. In some of these cases a conversion factor ψ had to be assumed in order to estimate $(n_a)_m$.

The *goals* of application and consequently the atomizer designs used vary largely. Experiments 6–10 and 19 were aimed at lowering the analytical detection limit. It is therefore interesting to compare the result obtained in experiment 9, where a cell with pure, saturated Pb vapor was used to investigate the optimum measuring conditions, with that obtained in experiment 10. In the latter, a real sample (here: a liquid Pb solution) was evaporated in a graphite cup

---

Table 4.4.

Experiment	Reference	Atomizer[b]	Technique[c]	Species	Laser[d]	Saturation
1	(52)	Be	RF	Na	c	Yes
2	(16, 17)	Be	RF	^{138}Ba	c	Yes
3	(61)	Ce(Ne)[i]	RF[j]	^{20}Na	c	No
4	(19)	Ce(He)	RF[j]	Na	c	Yes
5[j]	(85, 86)	Fl	NF[j]	Na	p	Yes
6	(87)	ETA	NF[j]	Na	c	No
7	(88–90)	Ce(Ar)	NF[j]	Na	c	Yes
8[j]	(88, 90)	Fl	NF[j]	Na	p	Yes
9	(65)	Ce	NF	Pb	p	Yes
10[e]	(64)	ETA	NF	Pb	p	Yes
11	(91)	Ce(Ne)	ICA	Na	c	Yes
12	(92)	Fl	OG	Cs	p	[Yes]
13	(93)	Fl	OG	Li	p	(No)
14	(11, 94)	Ce(Ar)[f]	PI	Cs	p	Yes
15	(28)	Ce(Ar)[f]	PI	Naphthalene	p	(Yes)
16	(84, 95, 96)	Be	FI	Na	p	Yes
17	(9, 84, 97)	Be	FI	^{173}Yb	p	Yes
18	(98, 99)	Fl *Sample cell*	OA	Na	p	Yes
19	(24, 25)	LFC	NF	Rhodamine 6G	c	No

[a] For explanation of symbols see Table 4.1. Numbers in parentheses are highly uncertain. Numbers within brackets were indirectly *derived* from data in the original paper(s) or *assumed*. Many of these numbers are reliable as to order of magnitude only.

[b] Be = atomic beam (usually combined with oven); Ce(G) = closed cell (possibly with buffer gas G; usually in oven); ETA = electrothermal atomizer (as used in AAS); Fl = flame with nebulizer; LFC = liquid flow cytometer.

[c] RF = resonance fluorescence; NF = nonresonance fluorescence; ICA = intracavity absorption; OG = optogalvanic; PI = photoionization; FI = field ionization; OA = optoacoustic.

[d] c = continuous wave; p = pulsed.

[e] Relating or converted to statistical confidence factor $k = 3$.

[f] Taken from (100).

[g] Derived from specified dark count rate and dark count number.

[h] At assumed threshold $m_{th} = 6$ and 2 for photoelectrons in one burst in case 2 and 1, respectively.

[i] ^{20}Na atoms were produced by reaction of a proton beam with Ne atoms.

[j] Fluorescence of Na-*D* doublet was observed, while only one of its lines was excited by the laser in cases 3 and 4; in cases 5–8 fluorescence was observed at the other doublet line only.

Experimental Results[a]

V_p (cm^3)	τ (s)	T (s)	ϵ_d	$(\bar{N}_p)_m$[e]	$(n_a)_m$[e] (cm^{-3})	R
10^{-3}	10^{-5}	[10][l]	0.4[h]	10^{-4}	0.1	[1][l]
5×10^{-4}	1×10^{-6}	(100)[g]	1×10^{-2}[h]	(5×10^{-5})[h]	(0.1)[h]	1
2×10^{-4}	3×10^{-4}	4×10^{-3}	0.1	0.1	5×10^2	100
[3×10^{-4}]	3×10^{-4}	2×10^{-3}	1	2×10^{-3}	10	[10^3][k]
10^{-5}	2×10^{-7}	1×10^{-6}	2×10^{-3}	[10^3]	[10^8]	1
(1)	?	(1)	?	(10^6)	10^6	100
10^{-3}	?	(15)	?	10^{-2}	10	1
10^{-2}	[10^{-4}]	5×10^{-7}	[5×10^{-3}]	[50]	[5×10^3]	[≥30]
0.1	10^{-5}	5×10^{-9}	[10^{-3}][m]	30	3×10^2	5×10^3
0.1	$>10^{-5}$[o]	5×10^{-9}	[10^{-3}]	150	1.5×10^3	150
7×10^{-3}	[10^{-5}]	60[p]	—	(4×10^3)	(6×10^5)	1
(10^{-2})	[3×10^{-4}]	1×10^{-8}	?	[4×10^3]	[4×10^3][q]	10
0.5	[10^{-3}]	1×10^{-6}	?	[5×10^4]	[1×10^5][q]	20
5×10^{-3}	10^{-3}	2×10^{-6}	1	5	100	1
10^{-3}	?	1×10^{-6}	[s]	(10^4)	(10^7)	[t]
5×10^{-3}	(3×10^{-6})	1×10^{-8}	0.5	15	3×10^3	1
5×10^{-4}	(10^{-6})	1×10^{-8}	0.3	0.15	3×10^2	120
2	[10^{-3}]	1×10^{-6}	—	(2×10^7)	(10^7)	?[u]
1×10^{-8}	4×10^{-5}	1	7×10^{-2}	1	1×10^8	10

[k] Minimum value required to obtain the reported $(\bar{N}_p)_m$ value under assumed SAD conditions.

[l] See (39) for a discussion of assumed values within brackets.

[m] Assuming a quantum efficiency of 10% of photodetector.

[n] Some data were taken from (65).

[o] The actual τ may exceed the reported value of 10^{-5} s because motion of atoms is limited by diffusion in buffer gas.

[p] Duration of one spectral scan across the laser profile (personal communication by authors).

[q] Derived from reported LOD in sample solution, assuming conversion factor $\psi = 10^{11}$ cm^{-3}/(μg/mL) [see also (101) for case 13].

[r] A minor component was admixed to the gas for operation as a gas-proportional counter.

[s] ϵ_d relating only to a molecule in the specific level(s) from which laser excitation takes place, is close to 1; $\epsilon_d \ll 1$ if it relates to a molecule in any level.

[t] Registration occurs by recording the two-photon laser excitation spectrum from the $v = 0$ level in the ground state. The number of laser shots required for one registration was not reported.

[u] Only the value $f_{rep} = 10$ Hz was reported.

atomizer and a concentrational LOD of 0.05 pg/mL and an absolute LOD of 10^{-15} g were achieved. In both experiments single-step excitation by one frequency-doubled laser beam was applied.

A similar absolute detection limit for Pb was obtained in a graphite rod atomizer by using NF with two-step excitation by two lasers (102). Remarkably, $(n_a)_m$ was several orders of magnitude larger in the latter experiment than in experiment 10. This clearly demonstrates that not only $(n_a)_m$ is decisive for obtaining good analytical LODs but also the atomizer design.

Experiment 5 was designed as a diagnostic tool for measuring temporally and spatially resolved trace concentrations in gas flows of engineering interest. Experiment 1 was especially set up to detect single atoms, whereas experiment 2 demonstrated the possibility of high-resolution spectroscopy in situations where only a small number of atoms (here: Ba isotopes) is available. Experiment 3 was aimed at detecting ^{20}Na isotopes produced by a proton beam reacting with ^{20}Ne atoms, and at studying the kinetic behavior of Na atoms in neon gas. The extension of the saturated Na vapor–pressure curve toward lower temperatures was the goal of experiment 6. Finally, experiment 11 was meant as a study of the effect of ICAAS on the spectral features of a narrow-band laser.

Resonance fluorescence (*RF*) *spectroscopy* has to face the problem of reducing *laser background scattering*. When, for example, one Na-*D* level is excited in an atomic beam experiment in vacuo, the other component does not fluoresce. When the laser is tuned at the first resonance line of Ba ($6^1P_1 \leftarrow 6^1S_0$), the NF line ($6^1P_1 \rightarrow 5^1D_2$), emitted from the laser-excited level, is but weak and lies in the infrared region. One has in these cases no other choice than applying RF. There are, however, various means to suppress laser background scattering (and any other background as well) (86). Under saturation conditions one can apply to this end the *photon-burst technique* (13, 16, 17, 19, 36, 52, 103). If the mean number of photoelectrons, $\phi \cdot \tau$, generated by one atom crossing the laser beam exceeds unity (Section 2.6), the atom has a good chance to generate a burst of at least two photoelectrons during its crossing. By applying a pulse-height discriminator and/or a coincidence setup (Fig. 4.3), one can discriminate the temporally bunched fluorescence photons from the randomly scattered laser photons and dark-current electrons. The gate width should match τ, and the chance of more than one atom being present in the probe volume should be negligible. The detection efficiency ϵ_d is then given by Eqs. (4.11) and (4.12) if we replace therein the lower limit of summation by the threshold value m_{thr} (>1). For a given mean number, $\bar{m}$, of photoelectrons per burst, ϵ_d will of course become smaller, the higher the threshold. But this decrease will be overcompensated by a still stronger reduction in the randomly released background electrons.

One can make $\bar{m} > 1$ by increasing ϕ or τ. The latter can be increased by expanding the laser beam cross section, but this should not be done at the cost of saturation. ϕ can be increased by improving the photon collection efficiency or by selecting a photodetector with a larger quantum efficiency η. Since we do not need a monochromator in RF detection, the solid angle of observation Ω_F can be made large.

The feasibility of the photon-burst technique may be simply shown for an (effectively) two-level atom with equal statistical weights. Under saturation conditions each atom will spend half of its life in the excited level (Chapter 1). Given a single atom, the probability per second, ϕ, of detecting a photon is then given by $\phi = \frac{1}{2} A \cdot (\Omega_F/4\pi) \cdot \eta$, where A is the Einstein transition probability. Using the relation $\bar{m} = \phi \cdot \tau$ in the nonstationary case and adopting realistic values $A = 3 \times 10^7\ \mathrm{s}^{-1}$, $\Omega_F/4\pi = 0.5$ and $\eta = 0.1$, one finds $\bar{m} = 0.7 \times 10^6\ \tau$. For $\tau > 1.5\ \mu\mathrm{s}$, $\bar{m}$ will thus exceed unity. (The possible, slight anisotropy of the spontaneous photon emission has here been disregarded.)

Figure 4.6 illustrates how in atomic beam experiment 2 a solid angle of $0.6 \times 4\pi$ sr was realized. The result is an $\bar{m}$ value of 1.3 photoelectrons per ^{138}Ba atom, when its first resonance level was saturated. According to Eq. (4.11) the fractional probability of finding 2 and 6 photoelectrons in one burst is then 0.2 and 0.01, respectively. Figure 4.7 shows for different selected m values or multiplicities the hfs excitation spectrum of Ba with natural isotopic composition, obtained by detuning the laser frequency over a range of 200–400 MHz from the line center of the main ^{138}Ba isotope. It is seen that the line-to-background ratio improves considerably when the multiplicity is enhanced. With $m \geq 6$ the residual background was due to the dark current of the photomultiplier tube (which exhibits some temporal bunching, too). It is also seen that the lines become narrower with increasing multiplicity. This beneficial line narrowing in high-resolution spectroscopy (13) arises because $\bar{m}$ is smaller in the line wings than in the line center. As a consequence, ϵ_d drops more sharply with increasing multiplicity at line wing excitation than at line center excitation. Also, the peak height of the ^{130}Ba line grows relative to that of the ^{135}Ba and ^{137}Ba lines. The first peak becomes even dominant at $m_{thr} = 6$, although the corresponding abundance ratios are 0.1, 6.5, and 11%. The line strengths for the 135 and 137 isotopes are comparatively small and saturation was not reached (17).

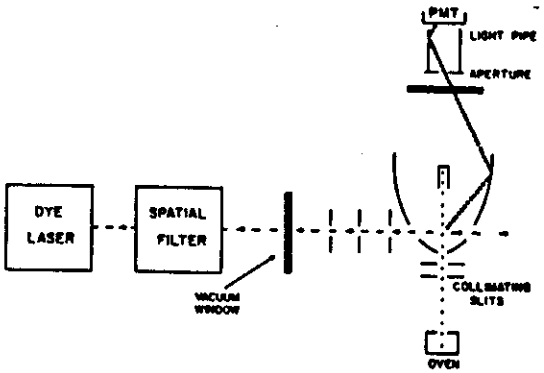

Fig. 4.6. Experimental setup for detection of resonance fluorescence of Ba atoms evaporated in an oven and collimated to form an atomic beam in vacuo. The intersection of this beam and the laser beam is found in the focus of an ellipsoidal mirror, giving a large solid angle of detection. Laser background scattering is suppressed by means of various diaphragms. PMT = photomultiplier tube. [Reproduced from (16) by permission of the American Physical Society.]

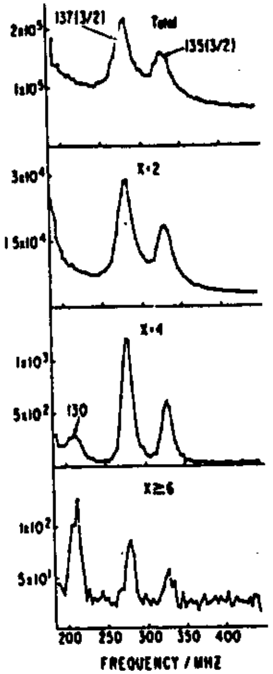

Fig. 4.7. Detail of the hfs excitation spectrum of Ba with natural isotope composition, measured with the setup shown in Fig. 4.6 by application of the photon-burst technique, for various selected multiplicities of x photoelectrons per burst. The top figure was obtained without multiplicity selection. The frequency difference scale refers to the line center of the ^{138}Ba isotope. [Reproduced from (16) by permission of the American Physical Society.]

The photon-burst technique was also applied in Na beam experiment 1, where

$\bar{m}$ was 2 and m_{thr} was chosen equal to 2, yielding $\epsilon_d = 0.4$. The background was dominated by stray light. Pulse-height discrimination was here combined with coincidence measurements with two photodetectors. In experiment 4 the photon-burst technique was realized by measuring the single-clipped autocorrelation function displaying the number of counts in 100 successive time samples. Whenever an atom crossed the laser beam, a bump was seen with a height of about 15 photoelectron counts and a width equal to τ. Since the background (due to stray light and Rayleigh scattering) was relatively low, ϵ_d was, virtually, unity.

The application of the photon-burst technique may be hampered by the occurrence of a consumptive process in the probing (Section 2.2; Table 4.2, case Ib). In beam experiments 1 and 2, where a narrow-band laser was used and collisions did not occur, the Na atom and some of the isotopic Ba species may become trapped in hfs levels of the ground state that are inaccessible to laser excitation. Ba atoms may, moreover, become trapped in the metastable 5^1D_2 level. If the atoms reside long enough in the saturating laser beam, they will all end up in the trap level. The value of $\bar{m}$ as a function of τ then reaches a plateau (16).

Trapping in the $F = 1$ hyperfine (hf) level of the Na ground state can, in principle, be avoided by using a narrow-band laser tuned at the transition from the $F = 2$ level of the ground state to the $F = 3$ level of the $^2P_{3/2}$ state. (Optical selection rules forbid spontaneous transitions from the latter level to the $F = 1$ ground level.) However, saturation broadening may lead to excitation of the nearby $F = 2$ level in the upper state, too. From the latter level spontaneous transitions to the trap level $F = 1$ are allowed. This detrimental effect of saturation broadening was eliminated in experiment 1 by using a circular polarized laser beam. Of course, by using a broadband laser that excites atoms from both hf ground-state levels one could also avoid trapping. But the excitation rate would then also be reduced, at a given laser power.

The loss of atoms due to trapping in a metastable level depends on the branching ratio of the spontaneous transitions to this level and to the ground state. In Ba experiment 2 this branching ratio was small enough to avoid noticeable trapping during $\tau = 1$ μs.

Nonresonance fluorescence (*NF*) *spectroscopy* was applied in experiments 5–8 with sodium, where efficient population mixing of the *D*-doublet levels was brought about by collisions in the buffer or carrier gas. This technique was also applied in experiments 9 and 10 with lead, which emits a strong NF line at 405.8 nm from the saturated 7s $^3P_1^0$ level. The lower level ($6p^2\ ^3P_2$) of the NF transition is, however, metastable and a noticeable fraction of the Pb atoms may eventually become trapped during the probing time T (= pulse duration) of 5 ns, which was here much less than τ (stationary case). According to (104) the optimum pulse duration would have been 7 ns under saturation conditions. In this case an increase in T would thus have had little effect on the LOD, but an increase in f_{rep} could still have been beneficial. This holds at least as long as f_{rep} does not exceed τ^{-1} or the reciprocal of the metastable lifetime. Since in the experiments f_{rep} was 50 Hz, a considerable gain in LOD, at given t_m, is still feasible. In experiment 9 the extrinsic LOD was determined by fluorescence from the quartz windows at the wavelength of the NF line used.

ICAAS experiments in chemical analysis have not been entered in the table because their LOD performance was rather disappointing (105). For Na solutions nebulized into a slot-burner flame, placed inside the laser cavity, the LOD was no more than one order below the best LODs obtained in conventional AAS (106). Laser instability was mainly responsible for this meager achievement, but this might be considerably remedied.

The listed *limits of detection* $(\bar{N}_p)_m$ may be compared with the intrinsic values calculated from Eqs. (4.20) and (4.21) in the stationary and nonstationary case, respectively, or from Eq. (4.22) (Table 4.3). This cannot be done, however, for experiments 6 and 7, where ϵ_d is unknown, and for experiment 11, where ϵ_d is not well definable.

With the proviso that the listed data are correct within one order of magnitude, we find that the LODs in experiments 1, 2, 3, 9, and 10 exceed their intrinsic values by no more than one order of magnitude. The LOD found in experiment 4 is intrinsic and determined by atom number fluctuations because $\epsilon_d = 1$. In experiments 5 and 8 $(\bar{N}_p)_m$ comes close to the intrinsic value calculated from Eq. (4.22), but the experimental values were derived indirectly and are thus rather uncertain. Anyway, since here $\epsilon_d << 1$, the intrinsic LOD is determined mainly by shot noise in fluorescence detection, not by atom number fluctuations.

Flame experiments 5 and 8 yielded $(n_a)_m$ values that differed by more than 4 orders of magnitude, although both come close to their intrinsic values at similar T and ϵ_d. This large difference is connected with the difference in product $V_p \cdot R$ occurring in Eq. (4.25). This product was very small in experiment 5, which was aimed at flame diagnostics with high spatial (small V_p) and temporal ($R = 1$) resolution. [Note that in Eq. (4.25) τ has dropped out.] The other experiment was aimed at obtaining good analytical LODs (approximately 1 pg/mL for Na).—The detrimental effect of laser-enhanced NaOH formation on the LOD might not have been negligible in these experiments, done with a laser pulse duration of about 1 μs (Section 2.2). Laser background scattering was reported to play no role in both NF experiments, as expected.—Experiment 5 was erroneously listed in (39) as RF.

Single-atom detection exists only if $\epsilon_d = 1$ *and* the intrinsic LOD is attained. Only experiment 4 meets these conditions, whereas experiment 1 approaches SAD capability within one order of magnitude.

SAD has also been realized by applying RF in combination with a saturating cw laser beam and an ion trap, which allows observation of single ions over a protracted period of time (47, 48). Figure 4.8 illustrates the application of a rf

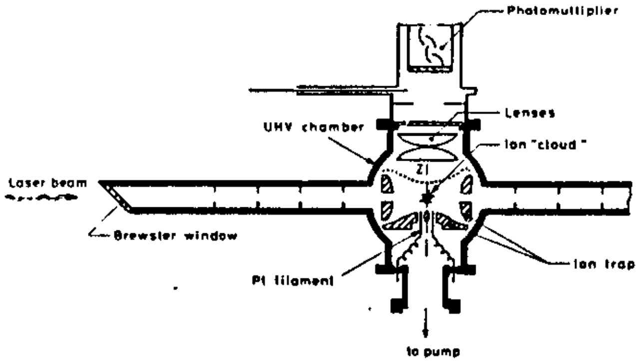

Fig. 4.8. Experimental setup for detection of resonance fluorescence of Ba^+ ions trapped in a rf quadrupole field. The Ba^+ ions were produced by evaporation from a metallic Ba sample deposited on a hot Pt filament. [Reproduced, with slight modifications, from (47) by permission of Springer Verlag, Berlin.]

quadrupole trap for Ba^+ ions that were evaporated, after surface ionization, from a Ba sample deposited on a hot platinum filament (47). Figure 4.9 displays the photon count rate, Z, as a function of t. The clearly distinguishable steplike structures in the latter figure correspond to consecutive escapes of single ions from the trap (compare Fig. 4.4a). The mean residence time, τ, of an ion in the trap appears to be about 2 min. The probe volume, V_p, is about 5% of the trap volume, V_a. But each ion oscillates rapidly inside V_a, thereby crossing frequently V_p. The count rate Z measured was actually an average over many repeated crossings. Therefore, we can effectively equalize V_p and V_a, which makes $\epsilon_p = 1$ [Eq. (4.6a)]. Since the time T (≈ 1 s) taken for a single probing in Fig. 4.9 is obviously less than τ, we should apply Eq. (4.20), holding in the stationary case, to calculate the intrinsic LOD. Because ϵ_d is obviously 1, we get $(\bar{N}_p)_m = 3^2/R$ if repeated probings are separated in time by at least τ seconds. [Equation (4.20) holds only for statistically *un*correlated probings.) Another condition is that the mean number of atoms, $\bar{N}_a$, should not decay (as in Fig. 4.9) because of uncompensated escape losses during t_m. Upon closer inspection of the scatter in the individual points in Fig. 4.9, we conclude that the rms error due to background counts is small relative to the mean step height. So extrinsic measurement errors were negligible indeed.—Since V_p was not specified in (47) we could not calculate $(n_a)_m$. An absolute LOD in the sample of 10^5 Ba atoms has been attained, which was restricted by the ionization and trapping efficiencies. This result implies an overall efficiency $\epsilon_\eta \approx 10^{-5}$. (Personal communication by Dr. W. Ruster, 1985.)

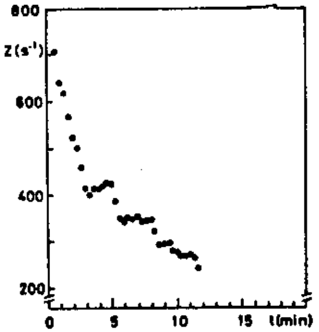

Fig. 4.9. Photon count rate Z of stored Ba^+ ions, measured as a function of t with the setup shown in Fig. 4.8. [Reproduced from (47) by permission of Springer Verlag, Berlin.]

In contrast with the photon-burst technique combined with pulse-height discrimination, the described ion trap technique does not require that at most one atom is present at a time in the probe volume.

There exists also in Ba^+ a metastable doublet level ($5d^2\ {}^2D$) between the laser-excited ($6p^2\ {}^2P_{3/2}$) level and the ground state ($6s^2\ {}^2S$). In the reported experiment, accumulation of Ba^+ ions in the metastable level was prevented by adding a low-pressure buffer gas (H_2) to quench this level.

In experiment 19 with a rhodamine 6G solution the intrinsic LOD as calculated from Eq. (4.21) is about 4 orders of magnitude lower than the experimental value. Raman scattering in the solvent was mainly responsible for that. The detection efficiency ϵ_d is remarkably high (≈ 0.1). The probing efficiency ϵ_p may also be high, as every molecule was forced to pass through V_p. This was achieved by hydrodynamic focusing, that is, by constricting the capillary diameter to the waist of the laser beam. Nevertheless, SMD has by far not been reached here.

3.3. Experimental Results by Ionization and Optoacoustic Techniques

Table 4.4 lists the experimental conditions and results obtained for a few optogalvanic (OG), photoionization (PI), and field ionization (FI) experiments with lasers. Data are also listed for a single optoacoustic (OA) experiment with Na in a flame.

The *goal* of OG and PI experiments 12, 13, and 15 was the improvement of analytical LODs. PI experiment 14 demonstrated the utility of a gas-proportional counter as an electron detector for realizing SAD of rare gaseous species. By applying a pulsed laser the statistical and kinetic behavior of a small ensemble of atoms was studied here, too. FI experiments 16 and 17 demonstrated the potentialities of this technique in SAD and in high-resolution spectroscopy of rare or short-lived species.

The best analytical LOD in *optogalvanic spectroscopy* up to now has been obtained in experiment 13 with Li excited to its first resonance level by a flashlamp-pumped dye laser in an acetylene-air flame. The reported analytical LOD of 1 pg/mL holds for $k = 3$ and was converted to $(n_a)_m$ by using the reported conversion factor ψ. This result is more remarkable as Li has a pronounced tendency to form LiOH in flames (Section 2.2). It is relevant to note here the use of a relatively long laser pulse (see ibidem). LODs of the same order of magnitude were realized for Co, Cs (experiment 12), In, Tl, and Mg (Fig. 3.7) (53, 107). In the case of Co, having a relatively high ionization energy, two-step laser excitation was applied. Cs atoms were directly excited to their second resonance level. Most LODs were set by shot noise in the current induced by flame background ionization. The use of hydrocarbon flames having a high natural ionization level (51) is thus unfortunate in this respect.

The problem of atom trapping in inaccessible levels does not arise in flames at 1 atm pressure because of the generally high rates of inelastic collisions (51).

A classic example of the *photoionization technique* is experiment 14. The experimental setup used in the detection of single Cs atoms by two-photon ionization via the 7P state is shown in Fig. 4.10. Cs vapor is produced by evaporation from a pure Cs sample contained in the side arm of a gas-proportional counter with quartz windows, filled with Ar at a typical pressure of 100 torr and a small admixture (10%) of methane. The secondary electrons were collected on a central wire at a high positive voltage. Background ionization was suppressed by time gating. The authors reported that nearly every atom appearing in the laser beam produced an observed event, in this case a burst of secondary electrons. The intermediate 7P state was saturated so that the depletion of this state by photoionization was instantaneously supplemented by atoms from the ground state, whose population was in quasiequilibrium with the 7P population. The photoionization rate was large enough to attain "saturation" in the production of ion–electron pairs, too. Trapping of Cs atoms in a lower, metastable state, populated by radiative decay from the 7P state, turned out not to be a limiting factor, as the photoionization rate from this metastable state was also large enough.

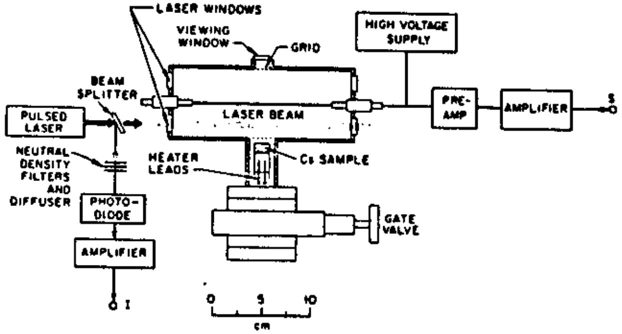

Fig. 4.10. Experimental setup used in the detection of single Cs atoms by the photoionization technique with the help of a gas-proportional electron counter. [Reproduced from (94) by permission of Springer Verlag, Berlin.]

A similar setup was used in experiment 15 for the detection of naphthalene molecules in the vapor phase. The $(n_a)_m$ value listed corresponds to the detection of about 1 molecule per 10^{12} buffer gas atoms. Similarly good results have been obtained by this technique for aniline (108).

The PI technique with various excitation schemes can, in principle, be applied to most elements of the periodic table, including, for example, ^{85}Kr (5, 109). Resonantly enhanced multiphoton ionization (MPI) is also coming more and more into use in chemical analysis and gas diagnostics for the detection of simple as well as complex molecules or radicals. This technique is then often combined with other methods such as gas chromatography and mass spectrometry (109). On the other hand, MPI of molecular constituents of the buffer gas or concomitants in the sample could contribute to background ionization in intense laser fields (5). PI preceded by laser-induced photodissociation might be used to detect, for example, CsI at SMD level (Section 2.2).

Selectivity is a greater problem with molecules, which have more closely spaced absorption lines, than with atoms. However, the selectivity (and detectability) for molecules can be improved by using supersonic jet expansion, which effectively "cools" the internal degrees of freedom (Chapter 7) and reduces Doppler broadening (just as in the case of atomic beams; Section 2.2).

The usage of a gas-proportional counter could be a problem when real samples are to be introduced or atomized in the proportional counter. In experiment 15 with a sample of pure naphthalene vapor this problem did not arise. The usage of ion or electron particle multipliers poses another problem, as they require vacuum conditions. It is also possible to collect the primary ions or electrons, without internal amplification, on two parallel-plane electrodes or on an electric probe. Interestingly, using a graphite furnace atomizer provided with a tungsten rod electrode, an absolute analytical LOD of 10^{-15} g has been obtained for Na by a multistep PI technique (110) (Chapter 3).

The application of the *field ionization technique* is exemplified by experiments 16 and 17. In experiment 16, a Na beam was produced from an oven containing the metallic element. Na atoms were raised to their 13D Rydberg level via the

3P level in a two-step photoexcitation process with two pulsed dye lasers. Saturation of the Rydberg level was attained so that about $\frac{3}{5}$ of all available atoms were brought into this level, according to the ratio of the statistical weight factors involved. In experiment 17, Yb isotopes were produced by irradiating a hot tantalum target by an intense beam of energetic protons. The ionized Yb isotopes were spatially separated by a mass separator and implanted, after acceleration, into different regions of a tantalum foil. Heating of this foil and proper collimation of the released atoms by means of a narrow cylindrical tube produced the atomic beam required for high-resolution spectroscopy. Because of the high ionization energy, a three-step excitation process was required to saturate the high-lying 17^3P_2 level, in which $\frac{5}{12}$ of the selected isotopic species was found.

The experimental setup used to detect the resonantly excited Yb atoms by field ionization is schematically shown in Fig. 4.11. The atomic beam, which is crossed at right angles by the triple laser beams, passes in between two parallel-plane electrodes to which a high-voltage pulse with a rectangular shape is applied about 20–30 ns after termination of the laser pulses. "Saturation" of the ion current was obtained with an electric field strength of about 12 kV/cm. The Yb^+ ions passing through a slit in the cathode were registered by means of a secondary-emission multiplier with an efficiency close to unity. A reference

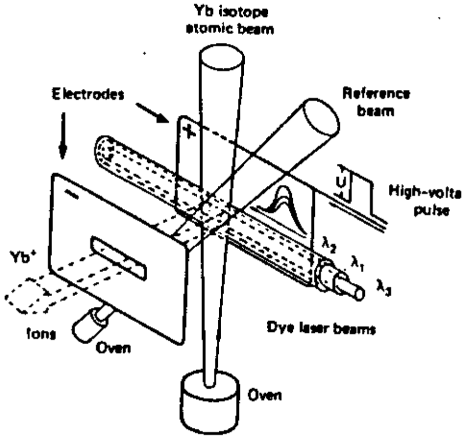

Fig. 4.11. Arrangement of coaxial dye laser beams, particle beams, and electrodes used in the detection of single Yb atoms by the field ionization technique. [Reproduced from (9) by permission of Springer Verlag, Berlin.]

beam effusing from an oven containing metallic Yb with natural abundance ratios was used for tuning the laser frequencies to the atomic transitions.

In experiments 16 and 17 ϵ_d was limited only by the fractional quasiequilibrium population of the saturated Rydberg level and was, therefore, on the order of unity (Table 4.4). Since collisions were absent, the lifetime of this level was sufficiently long to ensure that its population did not markedly change during the delay time of the high-voltage pulse.

In (96) it was claimed that the FI technique is more universally applicable to other elements than the LIFS techniques, as Rydberg levels exist for every element. Also, the laser power required is much less than in the PI technique because of the relatively low photoionization cross sections. On the other hand, the simultaneous tuning of two or more laser beams to consecutive atomic transitions may be a disadvantage. Since the laser pulse duration is short (less than 10 ns), the application of stationary saturation formulas might be questioned. The applicability of the FI technique is, however, restricted to atomizers where inelastic collisions are absent and no discharge occurs as a consequence of the applied electric field.

The *detection limits* listed in Table 4.4 are extrinsic in OG experiments 12 and 13, as they were determined by noise in the flame background signal or in the electronic circuit. In PI experiment 15 the reported LOD was determined by (unspecified) background noise and should thus be classified as extrinsic, too. In PI and FI experiments 14, 16, and 17 the intrinsic LOD, calculated from Eq. (4.20) or (4.23), was attained, whereas ϵ_d was on the order of unity.* In these cases the ideal of SAD was therefore closely approached. We note that in the stationary case, the value of τ drops out in the calculation of the intrinsic LOD.

As to LIIS techniques in general we can state that they usually require pulsed lasers for efficient ionization (Chapter 3) (5, 13, 53). Pulsed lasers are indispensable anyway, here as in LIFS, when a MP process or frequency doubling or mixing is involved. Since cross sections for photoionization from an excited level are comparatively small, highest demands are made on the irradiance of the ionizing laser beam in PI. On the other hand, the spectral bandwidth of this beam is not as critical as that used for resonant excitation of discrete atomic levels. The laser power requirements depend also on the competition between photoexcitation and collisional quenching. However, once full optical saturation has been reached, neither quenching nor the laser irradiance play a role anymore (Chapter 1).

When multiple, pulsed laser beams are to be used, their temporal and spatial

---

*In a recent PI experiment [A. T. Tursunov and N. B. Eshkabilov, *Sov. Phys. Tech. Phys.*, 29, 93 (1984)] the intrinsic LOD was also attained for gallium atoms in an atomic beam with $\epsilon_d = 0.3$, $V_p = 6 \times 10^{-4}$ cm^3, laser pulse duration $T = 8 \times 10^{-9}$ s and $\tau \gg T$.

overlap in the probe volume as well as their simultaneous tuning need careful attention. This holds especially so when focused laser beams (diameter ≤ 0.1 mm) and/or short pulses (≤ 1 ns) are applied (Chapter 3). Multistep excitation by multiple, resonantly tuned laser beams gives the gratification of enhancing the overall selectivity (13).

The degree of focusing, which anyway is limited by diffraction and possibly also by the laser mode structure, should not be pushed too far because of saturation broadening. This broadening of the excitation line profile may cause the spectral selectivity to deteriorate. As a general rule, one should rather try to enlarge the saturated probe volume, at a given laser power, unless high spatial resolution is wanted, as in diagnostic applications.

The LOD, at given measuring time t_m, may be improved by increasing f_{rep} and thus the duty cycle. The existence of an optimum value for f_{rep} should be kept in mind, however (Section 3.2).—These general considerations are equally valid in LIFS.

The potentiality of PI and FI techniques to detect small numbers of atoms (Table 4.4) implies (nearly) unit ionization efficiency in V_p as well as efficient collection of the charge carriers. Unit collection efficiency is easy to attain (13). Such favorable measuring conditions may also be found in OGS if the effective ionization rate constant times the duration of the saturating laser pulse significantly exceeds unity and the electrode voltage surpasses its "saturation" value (53) (Chapter 3). However, background ionization in the flame is likely to prevent the attainment of intrinsic LODs. This is probably the cost to be paid for the usage of this versatile atomizer in chemical analysis. The atomizers applicable in PI and FI spectroscopy are less suited for handling real-world samples. But here the effect of residual background ionization may be suppressed by applying a coincidence technique in the detection of electron–ion pairs (13).

Optoacoustic detection has only incidentally been applied to free atoms (experiment 18). Efficient conversion of absorbed photon energy into heat by quenching collisions is expected in the acetylene–air flame used (51). By applying a pulsed laser, acoustic pulses were generated that were detected by a microphone placed close to the flame. The reported LOD value is still large when compared to the best results obtained by fluorescence and optogalvanic techniques with flames. But this preliminary LOD value could probably be improved.

3.4. Combined Detection Techniques

In recent years efforts have been made not so much in inventing new laser-based detection techniques as in combining existing techniques with each other or with other methods of analysis such as mass spectrometry and chromatography. This hybridization can lead to improved sensitivity, selectivity, and background suppression in chemical analysis. It can also enlarge the coverage of atomic and molecular analyte species and the kinds of samples amenable to analysis. Many of these combinations are still in a stage of development or were ventilated merely as possibilities. Although some combinations are good prospects for the detection of small numbers of atoms and molecules or even for SAD/SMD, hard facts and experimental data are still lacking. We mention here only a few combinations [see also (38, 109)].

The combination of the PI technique with a mass spectrometer is a most obvious one, as it bypasses the need of a separate ionization chamber (Chapter 18). This combination was first applied in fundamental and diagnostic studies. In chemical analysis the technique called resonance ionization mass spectrometry (RIMS) is now reaching maturity (57, 111–115). The versatility of this technique depends on atomizing the analyte from a solid sample under vacuum conditions. Briefly, RIMS provides selectivity as to mass number A (by mass analysis) as well as to atom number Z (by resonance ionization). It is therefore especially useful in eliminating isobaric interferences in mass spectrometry when isotope ratios are to be determined. (Note that this elimination can also be achieved by accelerator–mass spectrometry, if a nuclear accelerator happens to be available; Section 1.3.) RIMS has worked in the intracavity mode too (57). The addition of a (simple) mass spectrometer has been considered for rejection of background ions in photoionization spectroscopy (6). The prospects of this combination for SAD have been theoretically considered in (37).

Whereas in the preceding combination PI comes first, it comes last when used as an element-specific detector in LIFS or ICAAS (116, 117). This detector is an auxiliary cell (or flame) that contains free atoms of the same species as the analyte at sufficiently high concentration. Resonance line radiation from the analytical cell, absorbed in the detector, acts as the first step in a multistep laser-assisted photoionization process (or OG process in the flame). The ion current produced is then a measure for the incident radiation intensity. The quantum efficiency of the detector is improved by making the ionization and ion collection efficiencies as large as possible (Section 3.3.). Theoretically this combinational technique might have SAD capability (116).

Combinations of laser-induced beam deflection with LIFS or LIIS have been suggested for improving the overall detection selectivity and for suppressing background (13, 34). The latter goal might be achieved by measuring the deflected beam signal and fluorescence signal in coincidence.

An interesting combination of magnetic-state selection by beam deflection and mass spectrometry has been described for the study of optical resonances in short-lived Na isotopes produced by nuclear spallation of Al by 150 MeV protons (118). This technique is based on the orientation of the electron spin in the Na($^2S_{1/2}$) ground state brought about by optical pumping of one of its Zeeman sublevels $m_J = \pm\frac{1}{2}$. Optical pumping is accomplished by tuning a saturating laser beam at one of the hfs lines of the *D* doublet. A magnetic filter focuses atoms in the pumped sublevel onto a hot rhenium surface and defocuses atoms in the other sublevel. The ions produced by surface ionization on the hot rhenium are finally analyzed according to their mass. This technique has been developed for high-resolution spectroscopy, but could be useful also in ultrasensitive detection of short-lived species.

4. CONCLUSIONS AND RECOMMENDATIONS

4.1. Conclusions

Selective detection of small numbers of atoms in the gas phase has been experimentally proven to be possible for a large variety of elements by applying laser-based fluorescence, photoionization (PI), and field ionization (FI) techniques. Results have been obtained in atomic beams, vapor cells, and electromagnetic ion traps, working under ideal conditions and with sophisticated measuring arrangements. In a few experiments the SAD limit has even been attained. With more conventional analytical atomizers such as the flame and electrothermal atomizer, free atom numbers as low as 100 have been detected by the use of nonresonance fluorescence (NF) techniques.—Good detectability and high selectivity often appear to go hand in hand.

Most of these experiments were not aimed at chemical analysis. Low limits of detection (LOD) relating to free atoms in the atomizer do not imply, per se, low absolute or concentrational LODs in the analytical sample. The efficiencies of atomization (ϵ_a) and probing (ϵ_p) play an important role here, too.

Apart from the special case of the alkali halides (Section 2.2), SMD lies beyond the horizon of present experimental possibilities. The reason why molecules are much more difficult to detect by laser probing than atoms is theoretically clear. In trace analysis of gas mixtures, however, it is often the *relative* concentration that matters. Relative LODs as low as $1:10^{11}$ are attainable for molecular species by laser-based detection techniques.

Intrinsic LODs have been obtained not only in the SAD experiments proper but also in some others. However, in most of the latter experiments ϵ_d was small compared to unity. This implies that shot noise in the detection process and not atom number fluctuations determined the intrinsic signal fluctuations.

The minimum number, $(\bar{N}_p)_m$, of free atoms detectable in probe volume V_p can be much lower than just 1 atom (Section 2.3). Of course, a statistically meaningful assessment of $(\bar{N}_p)_m$ $(<< 1)$ is possible only if during the total measurement time (t_m) at least some atoms have actually been observed. Under stationary probing conditions (Fig. 4.4) this requires that statistically uncorrelated probings be repeated a sufficiently large number of times (R). Under nonstationary probing conditions a single probing of duration T may suffice, if enough atoms pass through V_p during T ($>>$ transit time τ) (Section 2.3).

Apart from the widely varying goals pursued in the experiments entered in Table 4.4, the listed LOD values should not be used, as such, for merit rating. These values were obtained under largely different measuring conditions (R, T, V_p, t_m). Some normalization of these parameters would be appropriate, while allowing for the different dependencies of the intrinsic and the extrinsic LODs on R and T (Section 2.6).

One handicap to a more quantitative evaluation of the experimental results is the often insufficient specification of the experimental conditions in the literature. Another handicap is that the theoretical expressions presented hold only for strongly idealized situations. No account was taken, for example, of the nonuniform spatial distribution of the atoms in the atomizer and the nonuniform spatial, spectral, or temporal distributions of the (pulsed) laser irradiance. Also, statistical correlations between repeated probings or between successive atom crossings through V_p were disregarded.

4.2. Recommendations for Spectrochemical Analysis

The spectrochemist who wants to use gas-phase detection for smaller and smaller numbers of analyte atoms or molecules in condensed-phase samples is faced with the following problems:

(i) Improvement of the detection efficiency ϵ_d for atoms or molecules in the gas phase,
(ii) Suppression of background noise,
(iii) Improvement of the atomization efficiency ϵ_a,
(iv) Improvement of the probing efficiency ϵ_p.

In solving problems (i) and (ii) the spectrochemist should take notice of the special laser-based techniques described, possibly in combination with other methods of analysis or separation existing in analytical chemistry. Some of these laser-based techniques operate under vacuum conditions. The analytical atomic spectroscopist should therefore overcome any possible *horror vacui* in designing atomizers that produce free analyte atoms from real-world samples in an evacuated compartment. The "atomizers" used in the described FI and ion trap experiments with Yb and Ba^+ are especially instructive.

The PI technique is certainly a good candidate for chemical analysis at SAD levels. But here we are confronted with the extra problem of achieving efficient and versatile sample atomization without disturbing, by contamination, the performance of the ion or electron detector present inside of the atomizer confinement.

Atomizers handling real-world samples are expected to produce higher background levels. Ample attention should therefore be given to the special methods of improving the signal-to-background ratio that were occasionally mentioned in Section 3.

Problem (iii) is, of course, not new in analytical atomic spectroscopy. But special care should be taken that the atomization does not affect the laser–atom interaction, and to the avoidance of analyte contamination. There is a great variety of means to produce free atoms or ions from a (minute) solid sample deposited or collected on a filament or foil, and from a solid sample surface under vacuum or low-pressure conditions (Section 3). In ultratrace analysis, especially when measuring isotope ratios, one may consider the feasibility of multistage atomization. Here the analyte is preselected by a laser-assisted separation technique and/or mass separator and accumulated on a foil—in one or more cycles—before final atomization for laser probing takes place (36). In this way concomitant interferences and matrix effects may be suppressed, while preconcentration of the analyte species is achieved.

Problem (iv) is specific for laser-based techniques. The possible expansion of the laser beam by optical means is limited by the high irradiance required for efficient probing and detection. The atomizer design should thus be matched to the optimal shape and extent of the probe volume, which depend also on the photon or ion collection system used. Under stationary probing conditions and in a closed atomizer this means, ideally, that V_a should be made equal to V_p [Eq. (4.6a)], or that the probings should be repeated so often that each free atom present in V_a appears in V_p during at least one of the probings. Under nonstationary probing conditions, it is not necessary that all free atoms are confined inside V_p during probing. It suffices that they all pass through V_p during T at a transit time τ ($< T$) long enough to ensure their efficient detection. If in a closed atomizer $V_p/V_a << \tau/T$ [Eq. (4.6b)], the optimum number of repeated probings is $R = (V_a/V_p) \cdot (\tau/T)$. With continuous-flow atomizers the atomization time t_a should match the total measurement time t_m, in order to reduce analyte losses when working with microsamples. When pulsed lasers are to be used, due consideration should be given to analyte losses resulting from a bad duty cycle. The laser repetition frequency should then be raised close to its optimum value (Section 3.2) or pulsed atomization, synchronized with the laser pulses, may be attempted.

Some of these matching problems are discussed in Chapter 3 in relation to optogalvanic spectroscopy (OGS) with flames. Flames seem, in general, not to be suited for realizing SAD because of their high background levels, limited atomization efficiencies, unfavorable conversion factors, analyte contamination in the combustion gases and difficulties with handling ultramicrosamples. But OGS combined with a quadrupole ion mass spectrometer might improve the LODs in flames that are limited by flame background ions (39). Ion counting techniques would then be applicable, too.

Space-charge amplification, already applied in research on Rydberg atoms in combination with PI and OG detection (119), might be considered for chemical analysis by LIIS (39). It can easily lead to a 100-fold enhancement of the electric pulse generated by an individual analyte ion. But it requires the presence of a hot cathode filament, acting as an electron emitter, close to the (narrow) laser beam. This may put special demands on the atomizer and the filament material. For example, the use of an oxygen-lean flame would be mandatory.

In general, the spectrochemist pursuing extremely low LODs, should have an open mind to tricks and techniques developed in other areas of physical and chemical research or chemical analysis. We mention, for example, the advanced ion trap technology developed for detection in gas chromatography. The technique of accumulating analyte species by trapping them in the lower part of a flame on a cooled silica tube may be borrowed from flame AAS (120) to enhance the sensitivity.

For advancing the detectability of *molecules* other than alkali halides toward SMD levels, resonantly enhanced multiphoton ionization in combination with supersonic jet expansion and a conventional mass spectrometer is promising (121) (Section 3.3). Nevertheless, there is still a long way to go before molecular LODs will be realized that are comparable to the best ones obtained for atoms. There is ample opportunity here for surprising innovations. The utilization of laser-induced selective photochemical effects might be considered for probing complex molecules. Also, the suggestions made in (25) for improving the LOD of molecules probed in the liquid phase by LIFS should be taken to heart in the analysis of gaseous molecules, too.

Calibration by reference samples could pose an extra problem when working at SAD levels, because of analyte contamination. Linear extrapolation of the calibration curve toward the lower end of the concentration scale is one possible solution. It requires, however, that contamination levels are reproducible and not too high. If SAD conditions are realized in the gas phase, atom counting combined with knowledge of ϵ_a and ϵ_p may provide absolute calibration. The value of ϵ_p may be calculated using expressions given in Section 2.4 or more refined expressions, depending on the probing conditions at hand. The value of ϵ_a can be determined by measuring the conversion factor (Section 2.5) using higher concentration reference samples. The ϵ_a value thus measured allows also for interferences by concomitants and matrix effects, if these are constant in the relevant concentration range.

Since effort and effect are, unfortunately, always balanced, a high price tag is attached to the application of any of the described ultrasensitive detection techniques to chemical analysis. Besides, the handling and maintenance of lasers working at the top of their performance requires an expert's skill (and patience!). The same may apply to the use of atomizers especially designed for work at SAD levels under vacuum conditions. Most of the techniques reviewed here are therefore not expected to bring about a breakthrough in routine analysis.—As to the cost problem of laser-based analytical techniques, we refer to the enlightening paper (38).

"Small is beautiful" but also difficile, when one tries to detect a small number of atoms or even a single atom in a whole sample. It will remain a thrilling challenge in the years ahead to pursue this noble goal.

REFERENCES

1. "Nomenclature, Symbols, Units and Their Usage in Spectrochemical Analysis—II. Data Interpretation," *Pure Appl. Chem.*, **45**, 99 (1976); "III. Analytical Flame Spectroscopy and Associated Non-flame Procedures," *Pure Appl. Chem.*, **45**, 105 (1976).
2. N. Omenetto and J. D. Winefordner, *Prog. Analyt. Atom. Spectrosc.*, **2**, 1 (1979).
3. H. Falk, *Prog. Analyt. Atom. Spectrosc.*, **3**, 181 (1980).
4. M. L. Parsons, S. Major, and A. R. Forster, *Appl. Spectrosc.*, **37**, 411 (1983).
5. G. S. Hurst, M. G. Payne, S. D. Kramer, and J. P. Young, *Rev. Mod. Phys.*, **51**, 767 (1979).
6. C. H. Chen, G. S. Hurst, and M. G. Payne, *Chem. Phys. Lett.*, **75**, 473 (1980).
7. G. S. Hurst, in *Symposium on Laser-based Ultrasensitive Analysis*, Amer. Chemical Soc., Abstracts of papers, 1984.
8. T. J. Whitaker and B. D. Cannon, in *Symposium on Laser-based Ultrasensitive Analysis*, Amer. Chemical Soc., Abstracts of papers, 1984.
9. G. I. Bekov, E. P. Vidolova-Angelova, V. S. Letokhov, and V. I. Mishin, in H. Walther and K. W. Rothe, Eds., *Laser Spectroscopy IV*, Springer, Berlin, 1979.
10. H. Walther and K. W. Rothe, Eds., *Laser Spectroscopy IV*, Springer, Berlin, 1979.
11. G. S. Hurst, M. H. Nayfeh, and J. P. Young, *Appl. Phys. Lett.*, **30**, 229 (1977); *Phys. Rev.*, **A15**, 2283 (1977).
12. G. S. Hurst, M. G. Payne, S. D. Kramer, and J. P. Young, *Chem. Phys. Lett.*, **63**, 1 (1979).
13. V. S. Letokhov, "Laser Selective Detection of Single Atoms," in C. Bradley-Moore, Ed., *Chemical and Biochemical Applications of Lasers*, Academic Press, New York, 1980.
14. G. S. Hurst, M. G. Payne, S. D. Kramer, and C. H. Chen, *Physics Today*, **33** (9), 24 (1980).
15. W. M. Fairbank, T. W. Hänsch, and A. L. Schawlow, *J. Opt. Soc. Amer.*, **65**, 199 (1975).
16. D. A. Lewis, J. F. Tonn, S. L. Kaufman, and G. W. Greenlees, *Phys. Rev.*, **A19**, 1580 (1979).
17. G. W. Greenlees, D. L. Clark, S. L. Kaufman, D. A. Lewis, J. F. Tonn, and J. H. Broadhurst, *Opt. Commun.*, **23**, 236 (1977).
18. C. Y. She, W. M. Fairbank, and K. W. Billman, *Opt. Lett.*, **2**, 30 (1978).

19. C. L. Pan, J. V. Prodan, W. M. Fairbank, and C. Y. She, *Opt. Lett.*, **5**, 459 (1980).
20. E. Jakeman, E. R. Pike, P. N. Pusey, and J. M. Vaughan, *J. Phys.*, **A10**, L257 (1977).
21. M. Dagenais and L. Mandel, *Phys. Rev.*, **A18**, 2217 (1978).
22. H. Paul, *Rev. Mod. Phys.*, **54**, 1061 (1982).
23. R. Short and L. Mandel, *Phys. Rev. Lett.*, **51**, 384 (1983).
24. M. Trkula, N. J. Dovichi, J. C. Martin, J. H. Jett, and R. A. Keller, "Prospects for Single-Molecule Detection in Liquids by Laser-Induced Fluorescence," in W. S. Lyon, Ed., *Analytical Spectroscopy*, Elsevier Science, Amsterdam, 1984.
25. N. J. Dovichi, J. C. Martin, J. H. Jett, M. Trkula, and R. A. Keller, *Anal. Chem.*, **56**, 348 (1984).
26. R. A. Keller and J. C. Travis, "Recent Advances in Analytical Laser Spectroscopy," in N. Omenetto, Ed., *Analytical Laser Spectroscopy*, Wiley, New York, 1979.
27. W. Demtröder, "Molecular Absorption and Fluorescence Spectroscopy with Lasers," in N. Omenetto, Ed., *Analytical Laser Spectroscopy*, Wiley, New York, 1979.
28. R. Frueholz, J. Wessel, and E. Wheatley, *Anal. Chem.*, **52**, 281 (1980).
29. N. Omenetto and J. D. Winefordner, "Atomic Fluorescence Spectroscopy with Laser Excitation," in N. Omenetto, Ed., *Analytical Laser Spectroscopy*, Wiley, New York, 1979.
30. M. G. Payne, C. H. Chen, G. S. Hurst, and G. W. Foltz, "Applications of Resonance Ionization Spectroscopy in Atomic and Molecular Physics," in D. R. Bates and B. Bederson, Eds., *Advances in Atomic and Molecular Physics*, Vol. 17, Academic Press, New York, 1981.
31. V. S. Letokhov, V. I. Mishin, and A. A. Puretzky, *Prog. Quant. Electr.*, **5**, 139 (1977).
32. J. C. Travis, G. C. Turk, and R. B. Green, *Anal. Chem.*, **54**, 1006A (1982).
33. G. C. Turk, J. C. Travis, and J. R. DeVoe, *J. de Physique*, **44**, Supplém. No. 11, Colloq. C7, 301 (1983).
34. V. I. Balykin, G. I. Bekov, V. S. Letokhov, and V. I. Mishin, *Usp. Fiz. Nauk*, **132**, 293 (1980) [*Sov. Phys. Usp.*, **23**, 651 (1980)].
35. N. Omenetto and J. D. Winefordner, *CRC Critical Reviews in Analytical Chemistry*, (December 1981).
36. R. A. Keller, D. S. Bomse, and D. A. Cremers, *Laser Focus*, p. 75 (October 1981).
37. O. I. Matveev, N. B. Zorov, and Yu. Ya. Kuzyakov, *Izv. Moskwa Univers., Ser. Khim.*, **19**, 537 (1978).
38. A. L. Robinson, *Science*, **199**, 1191 (1978).
39. C. Th. J. Alkemade, *Appl. Spectrosc.*, **35**, 1 (1981).
40. R. E. Drullinger and D. J. Wineland, in H. Walther and K. W. Rothe, Eds., *Laser Spectroscopy IV*, Springer, Berlin, 1979.
41. W. Neuhauser, M. Hohenstatt, and P. E. Toschek, in H. Walther and K. W. Rothe, Eds., *Laser Spectroscopy IV*, Springer, Berlin, 1979.

42. H. A. Schuessler, "Stored Ion Spectroscopy," in W. Hanle and H. Kleinpoppen, Eds., *Progress in Atomic Spectroscopy, Part B*, Plenum, New York, 1979.
43. J. E. Bjorkholm, R. R. Freeman, A. Ashkin, and D. B. Pearson, in H. Walther and K. W. Rothe, Eds., *Laser Spectroscopy IV*, Springer, Berlin, 1979.
44. W. Neuhauser, M. Hohenstatt, P. E. Toschek, and H. Dehmelt, *Phys. Rev.*, **A22**, 1137 (1980).
45. W. D. Phillips, Ed., *Laser-cooled and Trapped Atoms*, Ntl. Bureau of Standards, Spec. Publ. 653, Gaithersburg MD, 1983.
46. A. Ashkin, *Phys. Rev. Lett.*, **4**, 729 (1978).
47. W. Ruster, J. Bonn, P. Peuser, and N. Trautmann, *Appl. Phys.*, **B30**, 83 (1983).
48. D. J. Wineland and W. M. Itano, *Phys. Lett.*, **82A**, 75 (1981).
49. D. J. Wineland, W. M. Itano, J. J. Bollinger, J. C. Bergquist, and H. Hemmati, in R. A. Keller, Ed., *Laser-based Ultrasensitive Spectroscopy and Detection V*, Proc. SPIE, Vol. 426, Bellingham, WA, 1983.
50. L. W. Grossman, G. S. Hurst, M. G. Payne, and S. L. Allman, *Chem. Phys. Lett.*, **50**, 70 (1977).
51. C. Th. J. Alkemade, Tj. Hollander, W. Snelleman, and P. J. Th. Zeegers, *Metal Vapours in Flames*, Pergamon, Oxford, 1982.
52. V. I. Balykin, V. S. Letokhov, and V. I. Mishin, *Zh. Eksp. Teor. Fiz.*, **77**, 2221 (1979) [*Sov. Phys. JETP*, **50**, 1066 (1979)].
53. J. C. Travis, G. C. Turk, J. R. DeVoe, P. K. Schenck, and C. A. van Dijk, *Prog. Analyt. Atom. Spectrosc.*, **7**, 199 (1984).
54. C. H. Muller, K. Schofield, and M. Steinberg, in J. W. Hastie, Ed., *Characterization of High Temperature Vapors and Gases*, Ntl. Bureau of Standards, Spec. Publ. 561, Washington, D.C., 1979.
55. C. H. Muller, K. Schofield, and M. Steinberg, *Chem. Phys. Lett.*, **57**, 364 (1978).
56. C. A. van den Wijngaart, H. A. Dijkerman, Tj. Hollander, and C. Th. J. Alkemade, *Combust. Flame*, **59**, 135 (1985).
57. N. S. Nogar, S. W. Downey, R. A. Keller, and C. M. Miller, "Resonance Ionization Mass Spectrometry at Los Alamos National Laboratory," in W. S. Lyon, Ed., *Analytical Spectroscopy*, Elsevier Science, Amsterdam, 1984.
58. R. A. van Calcar, M. J. M. van de Ven, B. K. van Uitert, K. J. Biewenga, Tj. Hollander, and C. Th. J. Alkemade, *J. Quant. Spectrosc. Radiat. Transfer*, **21**, 11 (1979).
59. R. Altkorn and R. N. Zare, *Ann. Rev. Phys. Chem.*, **35**, 265 (1984).
60. R. A. Keller and N. S. Nogar, *Appl. Opt.*, **23**, 2146 (1984).
61. F. C. M. Coolen and P. Menger, in J. G. A. Hölscher and D. C. Schram, Eds., *Proceedings of the 12th Intern. Conference on Phenomena in Ionized Gases, Part I*, North-Holland, Amsterdam, 1975.
62. V. I. Balykin, V. S. Letokhov, V. I. Mishin, and V. A. Semchishen, *Pis'ma Zh. Eksp. Teor. Fiz.*, **24**, 475 (1976) [*Sov. Phys. JETP Lett.*, **24**, 436 (1976)].
63. F. C. M. Coolen, L. C. J. Baghuis, H. L. Hagedoorn, and J. A. van der Heide, *J. Opt. Soc. Am.*, **64**, 482 (1974).
64. M. A. Bolshov, A. V. Zybin, V. G. Koloshnikov, and M. V. Vasnetsov, *Spectrochim. Acta*, **36B**, 345 (1981).

65. M. A. Bolshov, A. V. Zybin, and V. G. Koloshnikov, *Kvantovaya Elektron. (Moscow)*, **7**, 1808 (1980) [*Sov. J. Quantum Electron.*, **10**, 1042 (1980)].
66. N. Omenetto, L. M. Fraser, and J. D. Winefordner, *Appl. Spectrosc. Revs.*, **7**, 147 (1973).
67. P. W. J. M. Boumans, R. J. McKenna, and M. Bosveld, *Spectrochim. Acta*, **36B**, 1031 (1981).
68. E. D. Prudnikov, *Spectrochim. Acta*, **36B**, 385 (1981).
69. E. O. Schulz-DuBois, H. Koppe, and R. Brummer, *Appl. Phys.*, **21**, 369 (1980).
70. A. van der Ziel, *Noise in Measurements*, Wiley, New York, 1976.
71. C. Th. J. Alkemade, W. Snelleman, G. D. Boutilier, B. D. Pollard, J. D. Winefordner, T. L. Chester, and N. Omenetto, *Spectrochim. Acta*, **33B**, 3831 (1978).
72. P. K. Wittman and J. D. Winefordner, *Appl. Spectrosc.*, **37**, 208 (1983).
73. M. Lapp and C. M. Penney, Eds., *Laser Raman Gas Diagnostics*, Plenum Press, New York, 1974.
74. H. Debus, W. Hanle, A. Scharmann, and P. Wirz, *Spectrochim. Acta*, **36B**, 1015 (1981).
75. M. C. E. Huber, in D. S. Dosanjh, Ed., *Modern Optical Methods in Gas Dynamic Research*, Plenum Press, New York, 1971.
76. C. Th. J. Alkemade, *Spectrochim. Acta*, **38B**, 1395 (1983).
77. M. J. Jongerius, Tj. Hollander, and C. Th. J. Alkemade, *J. Quant. Spectrosc. Radiat. Transfer*, **26**, 285 (1981).
78. T. W. Hänsch, A. L. Schawlow, and P. E. Toschek, *IEEE J. Quantum Electron.*, **QE-8**, 802 (1972).
79. A. A. Kachanov and T. V. Plakhotnik, *Opt. Commun.*, **47**, 257 (1983).
80. G. C. Bjorklund, *Opt. Lett.*, **5**, 15 (1980).
81. E. A. Whittaker, P. Pokrowsky, W. Zapka, K. Roche, and G. C. Bjorklund, *J. Quant. Spectrosc. Radiat. Transfer*, **30**, 289 (1983).
82. M. D. Levenson, W. E. Moerner, and D. E. Horne, *Opt. Lett.*, **8**, 108 (1983).
83. O. Axner, T. Berglind, J. L. Heully, I. Lindgren, and H. Rubinsztein-Dunlop, *J. Appl. Phys.*, **55**, 3215 (1984).
84. G. I. Bekov, V. S. Letokhov, O. I. Matveev, and V. I. Mishin, *Zh. Eksp. Teor. Fiz.*, **75**, 2092 (1978) [*Sov. Phys. JETP*, **48**, 1062 (1978)].
85. J. W. Daily and C. Chan, *Combust. Flame*, **33**, 47 (1978).
86. J. W. Daily, *Appl. Opt.*, **17**, 1610 (1978).
87. S. Mayo, R. A. Keller, J. C. Travis, and R. B. Green, *J. Appl. Phys.*, **47**, 4012 (1976).
88. J. A. Gelbwachs, C. F. Klein, and J. E. Wessel, *IEEE J. Quantum Electron.*, **QE-13**, No. 9, 11D (1977).
89. J. A. Gelbwachs, C. F. Klein, and J. E. Wessel, *IEEE J. Quantum Electron.*, **QE-14**, No. 2, 121 (1978).
90. J. A. Gelbwachs, C. F. Klein, and J. E. Wessel, *Appl. Phys. Lett.*, **30**, 489 (1977).
91. A. Dönszelmann, J. Neijzen, and H. Benschop *Physica*, **83C**, 389 (1976).
92. V. I. Chaplygin, N. B. Zorov, and Yu. Ya. Kuzyakov, *Talanta*, **30**, 505 (1983).

93. G. C. Turk, J. C. Travis, J. R. DeVoe, and T. C. O'Haver, *Anal. Chem.*, **51**, 1890 (1979).
94. G. S. Hurst, M. H. Nayfeh, J. P. Young, M. G. Payne, and L. W. Grossman, in J. L. Hall and J. L. Carlsten, Eds., *Laser Spectroscopy III*, Springer, Berlin, 1977.
95. G. I. Bekov, V. S. Letokhov, and V. I. Mishin, *Zh. Eksp. Teor. Fiz.*, **73**, 157 (1977) [*Sov. Phys. JETP*, **46**, 81 (1977)].
96. G. I. Bekov, V. S. Letokhov, and V. I. Mishin, *Pis'ma Zh. Eksp. Teor. Fiz.*, **27**, 52 (1978) [*Sov. Phys. JETP Lett.*, **27**, 47 (1978)].
97. G. I. Bekov, V. S. Letokhov, O. I. Matveev, and V. I. Mishin, *Opt. Lett.*, **3**, 159 (1978).
98. J. E. Allen, W. R. Anderson, and D. R. Crosley, *Opt. Lett.*, **1**, 118 (1977).
99. W. R. Anderson, J. E. Allen, T. D. Fansler, and D. R. Crosley, in J. W. Hastie, Ed., *Characterization of High Temperature Vapors and Gases*, Ntl. Bureau of Standards, Spec. Publ. 561, Washington, D.C., 1979.
100. V. I. Balykin, V. S. Letokhov, V. I. Mishin, and V. A. Semchishen, *Pis'ma Zh. Eksp. Teor. Fiz.*, **26**, 492 (1977) [*Sov. Phys. JETP Lett.*, **26**, 357 (1977)].
101. J. C. Travis, P. K. Schenck, G. C. Turk, and W. G. Mallard, *Anal. Chem.*, **51**, 1516 (1979).
102. A. W. Miziolek and R. J. Willis, *Opt. Lett.*, **6**, 528 (1981).
103. G. Schatz, in H. Walther and K. W. Rothe, Eds., *Laser Spectroscopy IV*, Springer, Berlin, 1979.
104. M. A. Bolshov, A. V. Zybin, V. G. Koloshnikov, and K. N. Koshelev, *Spectrochim. Acta*, **32B**, 279 (1977).
105. E. H. Piepmeier, "Atomic Absorption Spectroscopy with Laser Primary Sources," in N. Omenetto, Ed., *Analytical Laser Spectroscopy*, Wiley, New York, 1979.
106. M. Maeda, F. Ishitsuka, and Y. Miyazoe, *Opt. Commun.*, **13**, 314 (1975).
107. N. Omenetto, T. Berthoud, P. Cavalli, and G. Rossi, *Anal. Chem.*, **57**, 1256 (1985).
108. J. H. Brophy and C. T. Rettner, *Opt. Lett.*, **4**, 337 (1979).
109. *Symposium on Laser-based Ultrasensitive Analysis*, Amer. Chemical Soc., Abstracts of papers, 1984.
110. A. S. Gonchakov, N. B. Zorov, Yu. Ya. Kuzyakov, and O. I. Matveev, *Zh. Analyt. Khim.*, **34**, 2312 (1979) [*J. Anal. Chem. USSR*, **34**, 1792 (1980)].
111. J. D. Fassett, J. C. Travis, L. J. Moore, and F. E. Lytle, *Anal. Chem.*, **55**, 765 (1983).
112. J. D. Fassett, L. J. Moore, J. C. Travis, and F. E. Lytle, *Int. J. Mass Spectrom. Ion Processes*, **54**, 201 (1983).
113. J. C. Travis, J. D. Fassett, and L. J. Moore, *Proceed. of 2nd Int. Symposium on Resonance Ionization Spectroscopy and its Applications*, Knoxville (Tenn.), 1984, The Institute of Physics, Conference Series No. 71, New York, 1984.
114. N. S. Nogar, S. W. Downey, and C. M. Miller, *Proceed. of 2nd Int. Symposium on Resonance Ionization Spectroscopy and its Applications*, Knoxville (Tenn.), 1984, The Institute of Physics, Conference Series No. 71, New York, 1984.

115. R. A. Keller, Ed., *Laser-based Ultrasensitive Spectroscopy and Detection V*, Proc. SPIE, Vol. 426, Bellingham, WA, 1983, various papers, pp. 1–32.
116. O. I. Matveev, *Zh. Analyt. Khim.*, **38**, 736 (1983) [*J. Anal. Chem. USSR*, **38**, 561 (1983)].
117. O. I. Matveev, N. B. Zorov, and Yu. Ya. Kuzyakov, *Talanta*, **27**, 907 (1980).
118. G. Huber, C. Thibault, R. Klapisch, H. T. Duong, J. L. Vialle, J. Pinard, P. Juncar, and P. Jacquinot, *Phys. Rev. Lett.*, **34**, 1209 (1975).
119. P. Camus, *J. de Physique*, **44**, Supplém. No. 11, Colloq. C7, p. 87 (1983).
120. J. Khalighie, A. M. Ure, and T. S. West, *Anal. Chim. Acta*, **131**, 27 (1981).
121. M. V. Johnston, in *Symposium on Laser-based Ultrasensitive Analysis*, Amer. Chemical Soc., Abstracts of papers, 1984.